2020-08-03

Utility of High-Definition Fiber Tractography and Eye-Tracking for Measuring Outcome in Chronic Mild Traumatic Brain Injury

Hannah M. Lindsey
Brigham Young University

Utility of High-Definition Fiber Tractography and Eye-Tracking for Measuring Outcome in Chronic Mild Traumatic Brain Injury

Hannah Michelle Lindsey

A dissertation submitted to the faculty of
Brigham Young University
in partial fulfillment of the requirements for the degree of

Doctor of Philosophy

Shawn D. Gale, Chair
Erin D. Bigler
Bruce L. Brown
Derin J. Cobia
Steven G. Luke

Department of Psychology

Brigham Young University

ABSTRACT

Utility of High-Definition Fiber Tractography and Eye-Tracking for Measuring Outcome in Chronic Mild Traumatic Brain Injury

Hannah Michelle Lindsey
Department of Psychology, Brigham Young University
Doctor of Philosophy

A complete understanding of the functional and structural impairments driving persistent post-concussive symptom (PCS) expression in approximately one-third of those who suffer from mild traumatic brain injury (mTBI) is essential for the development of effective treatment strategies and improving quality of life. While traditional outcome measures, such as neuropsychological testing and structural magnetic resonance imaging, are sensitive to the severe functional impairments and widespread tissue damage frequently seen after moderate-to-severe injuries, more advanced measures that are sensitive to the subtle changes in cognitive function and tissue microstructure that may underlie persistent PCS are necessary for the assessment of recovery from mTBI. Toward this end, the current study investigates the utility of eye-tracking analysis and high-definition fiber tractography (HDFT) as advanced measures of functional and microstructural outcome in 11 adults with chronic mTBI and varying levels of PCS (ages 20-60; mean time post-injury = 9.53 ± 6.74 years) in comparison to 10 healthy adults (ages 20-54). Performance on neuropsychological and eye-tracking tasks of processing speed, attention, and working memory, and HDFT-derived quantitative measures of the microstructural integrity of the forceps major, inferior fronto-occipital fasciculus, middle longitudinal fasciculus, and superior longitudinal fasciculus were compared between groups, and the results were used to define discriminatory functions for mTBI classification. The relationships between neuropsychological and eye-tracking measures of cognitive function and HDFT-derived measures of tract integrity

were explored, as was the utility of these functional and structural measures for predicting persistent PCS in chronic mTBI. The results suggest that eye-tracking analysis may be more specific to cognitive impairments resulting from mTBI than neuropsychological testing, and HDFT is highly sensitive and specific to the subtle microstructural changes that persist chronically in this population. Furthermore, white matter integrity assessed using HDFT is more strongly associated with impairments in processing speed, attention, and memory indicated through eye-tracking analysis relative to performance on neuropsychological tests. Finally, although the predictive utility of eye-tracking and HDFT for the experience of persistent PCS was not demonstrated in the present sample, the possibility that these data are confounded by symptom exaggeration, comorbid mental health impairment, or lack of self-awareness for functional deficits cannot be ruled out, and future research using large, homogenous sample of mTBI is necessary to validate the present findings.

Keywords: chronic mild traumatic brain injury, high-definition fiber tracking, eye-tracking, post-concussive syndrome

ACKNOWLEDGMENTS

First and foremost, I want to thank my parents and sisters for their unwavering support of me as I have completed my graduate training and continue to pursue my professional career. I am so blessed to have such loving, patient, and selfless family members who want nothing more than to see me succeed in reaching my goals.

I especially want to thank Shawn Gale for serving as my doctoral advisor and dissertation committee chair, along with Erin Bigler, Steven Luke, Derin Cobia, and Bruce Brown for serving as the other members of my dissertation committee. The assistance each of you have provided me with throughout my doctoral candidacy have been insurmountable, and I could not be more grateful for your guidance and wisdom over the past five years. Additionally, I want to acknowledge Elisabeth Wilde for the great lengths you have gone to assist me in this project and in my professional development. Additionally, I am very thankful for the help of Ollie Fegter, Paula Johnson, Brooke Frandsen, Colt Halter, and Aubrey Jun for their generosity in helping me with the data collection, processing, and management.

I also want to thank Gerald Voelbel and Antonio E. Puente for helping me to establish a strong foundation in research and academia as well as for their role in sparking my interests the field that have since developed into my passion.

Finally, I want to thank all of the participants in this study. I appreciate your kindness and willingness to participate, and I cannot express how grateful I am to have worked with each and every one of you.

TABLE OF CONTENTS

LIST OF TABLES

LIST OF FIGURES

Utility of High-Definition Fiber Tractography and Eye-Tracking for Measuring Outcome in Chronic Mild Traumatic Brain Injury

Approximately 2.8 million people sustained traumatic brain injuries (TBIs) in the US in 2013 (Taylor et al., 2017), demonstrating an 80% growth rate over the previous decade (1.5 million in 2003; CDC, 2017). Roughly 50% of those who survive brain injuries experience chronic disability at varying levels of impairment in cognitive, behavioral, physical, and/or emotional functioning as a function of injury severity (Dikmen et al., 2017; Dikmen et al., 2003; Stocchetti & Zanier, 2016). It is estimated that at least 5.3 million US citizens, accounting for approximately 2% of the population, are currently living with long-term or lifelong TBI-related disability (Faul & Coronado, 2015; Frieden et al., 2015). Significant disability is more often the result of neurobehavioral deficits, which can overlap and exacerbate other functional and physical consequences that impact performance in activities of daily living or ability to return to work (Whiteneck et al., 2016). An understanding of the epidemiology, etiology, and outcomes of TBI is critical for developing rehabilitation strategies and improving the quality of life of those suffering from TBI-related disabilities; thus, it is crucial that sensitive outcome measures are used in the assessment of recovery status and the efficacy of rehabilitation.

The relationship between long-term cognitive impairment and acute TBI severity is generally linear (Rabinowitz, 2014), although variability does exist in the presentation and extent of impairment following brain injuries due to other factors such as cognitive reserve, lesion burden, and demographic characteristics (Bigler & Stern, 2015). While the majority of those who suffer from mild TBI (mTBI) make a full recovery within the first weeks to months (Cristofori & Levin, 2015; Iverson et al., 2007), some patients suffer from post-concussive symptoms (PCS) that persist for more than three months post-injury (Iverson, 2006b; Rees, 2003; Satz et al., 1999;

Willer & Leddy, 2006). Although injury severity is related to the development of persistent PCS (Hessen et al., 2006; Sigurdardottir et al., 2009), it is not a strong predictor when considered alone (Bigler, 2008). In fact, the presence of PCS has been found to be more prevalent and reportedly more severe in those with mTBI than in those with moderate-to-severe TBI (Emanuelson et al., 2003; Englander et al., 1992; Iverson & Lange, 2003), where 15%–30% of individuals with mTBI experience persistent symptoms (McKee & Daneshvar, 2015; Shenton et al., 2012).

In a review of the clinical neuroscience of persistent PCS, Bigler (2008) describes four major features: (1) changes in mental activity and speed of processing that occur with a brief alteration in consciousness or neurological function, (2) impairments in attention, concentration, and working memory, (3) physical symptoms, including headache, dizziness/vertigo, and fatigue, and (4) changes in mood and emotional function. In addition to being among the dominant features of persistent PCS, impairments in speed of information processing, attention, and working memory are the most commonly reported cognitive deficits experienced after TBI (Dikmen et al., 2009; Dikmen et al., 2003; Finnanger et al., 2013; Kraus et al., 2007; Stocchetti & Zanier, 2016; Tomaiuolo et al., 2004). The ability to efficiently take in and process new information from the environment is an essential function for successful employment and social engagement (Asikainen et al., 1999; Schulz et al., 2006). Adequate performance on complex cognitive tasks relies on the coordination of distributed brain networks and their ability to quickly and efficiently register and integrate incoming information (Turken et al., 2008). The transmission of information across these distributed networks and the synchronization of the activity across individual brain regions are mediated by the white matter pathways of the brain (Mesulam, 1998, 2000). The interactive configurations among white matter fiber systems are

largely responsible for the patterns of cortical activity that are distributed throughout the brain; thus, the structural integrity of these pathways is crucial for adequate neural signal transmission and the efficient processing of information (Hilgetag et al., 2000; Kotter & Sommer, 2000; Sharp et al., 2011).

Traumatic axonal injury (TAI) is a consequence of widespread deformation to white matter fiber systems that often results from the biomechanics of TBI (Bigler & Maxwell, 2012; Palacios et al., 2011), particularly when rotational forces are present (Fijalkowski et al., 2006; Vander Vorst et al., 2007; Viano et al., 2005). The diffusivity of the damage across these systems may lead to disconnection between tertiary association cortices of the frontal, temporal, and parietal brain regions, restricting functional integration and causing a general slowing of cognitive processes (Levine et al., 2006; Turken et al., 2008). Higher-order cognition arises from the coordinated action of widespread, distributed neural networks between these regions, the integrity of the white matter pathways that make up those networks plays an important role in the proper functioning of attention, working memory, and speed of processing (Jung et al., 2016; Mesulam, 2000).

The five major cortico-cortical association tracts bridging these regions and underlying higher-order cognitive abilities are the cingulum bundle, the inferior fronto-occipital fasciculus, the inferior and superior longitudinal fasciculi, and the uncinate fasciculus (Lazar, 2017; Oishi et al., 2011; Schmahmann et al., 2007). In particular, visual and verbal working memory, attention, and processing speed abilities have been linked to the integrity of the superior longitudinal fasciculus (SLF; Chechlacz et al., 2015; Chung et al., 2019; Golestani et al., 2014) and the inferior fronto-occipital fasciculus (IFO; Chechlacz et al., 2015; Golestani et al., 2014). In addition to these two major association tracts, some literature suggests that the middle

longitudinal fasciculus (MdLF), a less well-understood association pathway, as well as the forceps major (FMa), which consists of the occipital projections of the corpus callosum, may also have a role in these processes. The spatial relationships between the FMa, IFO, MdLF, and SLF are shown in Figure 1.

The SLF is a major association fiber tract located at the dorsolateral regions of the corona radiata (superolateral to the putamen) that trajects along the superior edge of the insular cortex between the frontal and parietal lobes through the centrum semiovale. The SLF forms a large arc that connects the temporoparietal junction area and parietal lobe with the frontal lobe (Makris et al., 2005; Wang et al., 2016); thus, the SLF connects areas associated with visuospatial processing with speech, motor, and cognitive control centers. The SLF is primarily involved in efficient visuo- and audio-spatial processing, language, attention, awareness, and working memory (Chmura et al., 2015; de Schotten et al., 2012; Lazar, 2017). The SLF is also involved in the regulation of motor behavior and the transfer of somatosensory information (Dick & Tremblay, 2012; Ramnani, 2012).

Three separate segments of the SLF were initially identified in a primate brain (Petrides & Pandya, 1984) and later through tractography studies in humans (Catani & de Schotten, 2012; Makris et al., 2005; Thiebaut de Schotten, Dell'Acqua, et al., 2011; Thiebaut de Schotten et al., 2012; Thiebaut de Schotten, Ffytche, et al., 2011): SLF-I, the most dorsal component connecting the superior parietal lobe and precuneus with the superior frontal gyrus and some areas of the anterior cingulate gyrus; SLF-II, a second branch originating in the angular gyrus and the anterior portion of the intraparietal sulcus and terminating in the posterior regions of the superior and middle frontal gyrus; and SLF-III, the most ventral segment connecting the intraparietal sulcus and inferior parietal lobe to the inferior frontal gyrus. Post-mortem dissection studies of

human brains, however, have failed to replicate the patterns described in the tractography studies; rather, the results of classical (Ture et al., 2000) and more recent (Martino et al., 2010) fiber dissection studies suggest that the SLF consists of only two components, which more closely align with the definitions of SLF-II and SLF-III described above. A recent anatomical validation study used high-definition fiber tractography, complemented by fiber microdissection, to confirm the underlying neuroanatomy of the SLF in the human brain (Wang et al., 2016). The results of this study demonstrated that the fibers corresponding to SLF-I were, in fact, part of the cingulum fiber system, and that the true components of the SLF are as follows: a dorsal component, corresponding to the SLF-II, that connects the angular gyrus and superior parietal lobe to the caudal middle frontal and dorsal precentral gyri, and a ventral component, corresponding to SLF-III, which connects the supramarginal gyrus to the ventral precentral and inferior frontal gyri. The results of this study also demonstrated some asymmetry in the connectivity of the SLF (Wang et al., 2016), where connections between the supramarginal gyrus and the dorsal precentral gyrus in the left hemisphere only. In the right hemisphere, some connectivity between the supramarginal gyrus and pars triangularis was observed as well. It is of note that the studies linking SLF integrity to performance on tasks of visual and verbal working memory and attentional ability (Chechlacz et al., 2015; Chung et al., 2019; Golestani et al., 2014), these associations were only seen in the SLF-II and SLF-III.

The IFO is the longest association fiber bundle, and it connects the occipital cortex, temporobasal areas, and superior parietal lobe to the frontal lobe, while passing through the temporal stem of the posterior temporal lobe. Recent tractography and anatomical dissection studies have shed new light on the specific cortical terminations of the IFO, where the posterior terminations include the posterior portions of the superior and inferior occipital gyri and the

inferior portion of the middle occipital gyrus (Martino et al., 2010), and the anterior projections include the middle and inferior frontal gyri, dorsolateral and orbitofronal cortices, and the frontal pole (Sarubbo et al., 2013). The IFO is involved in decision making, visual and verbal working memory and attention, visual information processing, including recognition and conceptualization, and multimodal sensory integration and motor planning (Chmura et al., 2015; Sarubbo et al., 2013; Taoka et al., 2006).

Recently, fiber tractography and post-mortem dissection studies have confirmed the presence of the middle longitudinal fasciculus (MdLF) in humans (Kalyvas et al., 2020; Makris, Preti, Wassermann, et al., 2013; Makris et al., 2017; Maldonado et al., 2013; Wang et al., 2013). The MdLF is a relatively less well-known association fiber bundle that originates in the superior temporal gyrus and projects to the superior parietal lobule and parieto-occipital region through the transverse temporal gyrus and to the posterior occipital lobe through the angular gyrus (Kalyvas et al., 2020). Specifically, posterior terminations occur in the angular gyrus, supramarginal gyrus, superior parietal lobe, precuneus, cuneus, and lateral occipital lobule (Makris et al., 2017; Wang et al., 2013). While the specific functional role of the MdLF has yet to be confirmed, recent studies have convincingly argued for its role in higher-order auditory processing based on its specific anatomical connectivity (Makris, Preti, Asami, et al., 2013). Specifically, the MdLF has been suggested to be the auditory equivalent to the "what" and "where" pathways of the visual system, conveying information related to the spatial perception of sound (Wang et al., 2013). Furthermore, there is some evidence to suggest that the MdLF may play a role in the integration of auditory and visual information (Makris, Preti, Wassermann, et al., 2013; Makris et al., 2017), visuospatial attention (Makris et al., 2009; Makris, Preti, Asami, et al., 2013), and working memory (Cabeza et al., 2008; Conner et al., 2018).

In addition to these association tracts, the efficient processing of incoming information relies largely on the integrity of the corpus callosum, the largest commissural fiber tract in the brain, which is particularly vulnerable to the biomechanics of TBI (Bigler, 2008; Bouix et al., 2013; Dean et al., 2015). The splenium makes up the posterior third of the corpus callosum, connecting the right and left occipital and temporal lobes via the tapetum. Projection fibers extending posteriorly from the splenium toward the occipital cortex form the FMa, which is involved in the efficient processing of visual information and visual attention (Catani & Thiebaut de Schotten, 2008; Chmura et al., 2015; Niogi et al., 2008), and some evidence suggests that the FMa plays a role in the mediation of smooth pursuit eye movements (Maruta et al., 2014; Tusa & Ungerleider, 1988). Deficits in visual processing speed have been shown to relate to the integrity of the splenial projections and the nearby posterior thalamic radiation in other adult neurological populations (Menegaux et al., 2017).

Functional Outcome

Neuropsychological tests are considered to be one of the most important tools for assessment of outcome following brain injury (Maruta, Lee, et al., 2010) as they are very sensitive to TBI-related dysfunction during the chronic recovery phase following moderate-to-severe TBI (Dikmen et al., 2009); however, traditional neuropsychological testing methods appear to be insensitive to the chronic effects of mTBI (Bigler, 2013; Rohling et al., 2011), and a valid biomarker is necessary for effective treatment planning and rehabilitation in those with persistent PCS following mTBI.

Recently, eye-tracking methods have been utilized as sensitive measures of functional outcome following mTBI. The visual system is dispersed throughout thirty regions of the brain and requires functional contributions from eight cranial nerves (Ciuffreda et al., 2014), thus some

visual system damage is to be expected upon the occurrence of diffuse TAI. While moderate and severe injuries often lead to structural lesions that result in ocular motor palsies, optic neuropathies, and orbital pathologies, mTBI tends only to disrupt visual function, resulting in abnormal saccadic, pursuit, and vergence eye movements that persist chronically (Cifu et al., 2015; Ciuffreda et al., 2014; Ventura et al., 2014).

Based on findings of recent research, eye-movement analysis and neuropsychological testing may have different clinical utilities in the chronic post-injury period (i.e., > 3 months) after TBI. For example, Kraus and colleagues (2007) compared oculomotor function and neuropsychological performance between healthy individuals and those with chronic TBI. Their results demonstrated that eye movements were relatively more sensitive and specific for differentiating mTBI from healthy controls, whereas neuropsychological testing was relatively more sensitive and specific in differentiating mTBI from moderate-to-severe TBI. The authors concluded that eye movements are sensitive to the more subtle neurobehavioral deficits that can result from mTBI. This differentiation might be explained by the more selectively prefrontal deficits seen in mTBI versus the more global deficits present across a range of cognitive abilities and their underlying structural systems seen in moderate-to-severe TBI. A later study of the predictive value of anticipatory saccade function for impairment in procedural learning and fronto-striatal circuitry in chronic mild to severe TBI yielded similar findings (Kraus et al., 2010). Abnormal oculomotor performance was observed in relation to injury severity, where more severe injuries were negatively correlated with the proportion of anticipatory saccades. These authors argue that the chronic impairment of fronto-striatal functions that result from brain injuries are proportionate to injury severity and that this finding demonstrates the sensitivity of oculomotor testing to TBI across all levels of severity. Similar findings were also demonstrated

in a study by Maruta, Suh, and colleagues (2010) who hypothesized that the variations in attention that take place on a moment-to-moment basis cannot be detected by measures that are incapable of continuously monitoring attentional status, such as neuropsychological tests; thus, eye-tracking measures may be more sensitive to persistent impairments reported by those with mTBI, because they are capable of monitoring attention over time and capturing momentary lapses in attention. Furthermore, Heitger et al. (2008) found that eye-movement function during the acute post-injury period was more effective in distinguishing those with mTBI who would develop PCS (100% sensitivity and 100% specificity) from those who would not than neuropsychological testing, motor function, and self-reported health condition.

Eye-movement paradigms that have been commonly used to assess attention, working memory, and speed of information processing in TBI include visually-guided saccades (VGS), memory-guided saccade sequences (MGS), and predictive smooth pursuit eye-movement (SPEM) tasks (Table 1; for a review, see Hunt et al., 2015).

Saccadic eye movements require the complex coordination and timing of neural circuitry in various brain areas and are thus likely to be sensitive indicators of diffuse TAI (Cifu et al., 2015). Performance on VGS tasks depends on one's ability to efficiently shift their gaze toward a peripheral target and reflects basic attentional and processing speed capacities. MGS tasks involve sequential saccadic movements toward the locations of previously presented stimuli, reflecting working memory capacity (Funahashi, 2014; Hutton, 2008; Liversedge & Findlay, 2000). The brain regions involved in saccadic eye movements include the frontal eye fields, the dorsolateral prefrontal cortex, the supplementary motor area, the posterior parietal cortex, the middle temporal area, and the occipital lobe with the striate cortex; subcortical structures include

the thalamus, superior colliculus, the brainstem, and the basal ganglia (Heitger et al., 2002; Kraus et al., 2007; McDowell et al., 2008).

Predictive SPEM is controlled by neural circuitry that overlaps the pathways involved in attention and working memory and may be particularly sensitive to disconnection among distributed brain networks from TAI in TBI (Suh, Kolster, et al., 2006). Such tasks that utilize a periodically occluded target that follows a continuous circular trajectory have reliably demonstrated sensitivity to deficient anticipatory control resulting from momentary lapses in attention in mTBI populations (Diwakar et al., 2015; Maruta et al., 2014; Maruta, Suh, et al., 2010; Maruta et al., 2012; Suh, Basu, et al., 2006; Suh, Kolster, et al., 2006). The core regions involved are the frontal, supplementary, and parietal eye fields, the dorsolateral prefrontal cortex, the middle and superior temporal cortices, the extrastriate visual area, and the cerebellum. Furthermore, the integrity of fiber tracts connecting to and from the prefrontal cortex correlates with predictive SPEM performance (Fukushima et al., 2013; Lencer & Trillenberg, 2008; Sharpe, 2008; Thier & Ilg, 2005).

Structural Outcome

Advanced structural imaging techniques provide information for a clearer understanding of the consequences of brain injury in the acute and chronic phases of recovery across the spectrum of injury severity. This allows for an enhanced ability to determine the best way to conduct rehabilitation therapies and assess their effectiveness for the TBI patient (Bigler & Wilde, 2010). Historical methods used to examine the macro- and microstructural properties of the brain have advanced beyond post-mortem procedures and magnetic resonance imaging (MRI) studies toward more sensitive, non-invasive neuroimaging techniques that have substantially increased our knowledge of the structural changes that take place in the brain

during recovery, such as diffusion tensor imaging (DTI). DTI is based on a tensor model that models the diffusion pattern as a Gaussian distribution (Basser et al., 1994). DTI allows for the visualization and direct assessment of white matter pathway integrity by providing estimates of anisotropy and diffusivity, which are used to characterize the structural connections in the brain at the microstructural level through the quantification of water molecule diffusion across various tissues in the brain (Abhinav et al., 2014; Alexander et al., 2007; Mori & Zhang, 2006; Oishi et al., 2011). The most commonly used DTI index of white matter integrity is fractional anisotropy (FA), which is a measure of the asymmetry of diffusion within a voxel (Alexander et al., 2007). Changes in FA have been suggested to reflect changes in fiber organization (Beaulieu et al., 1996), where low FA values are present with isotropic diffusion, which may reflect reduced microstrucral integrity within white matter pathways (Alexander et al., 2007; Pierpaoli & Basser, 1996; Pierpaoli et al., 1996), although FA is largely nonspecific when interpreted alone. For this reason, commonly-used DTI metrics, such as FA, have been suggestive to be insensitive to white matter associations with cognitive function (Lazar, 2017).

Studies relating brain structure to neuropsychological function following brain injury have demonstrated DTI is effectively able to differentiate those with TBI from healthy controls, regardless of severity level or post-injury timeframe (Hulkower et al., 2013). Furthermore, the observable integrity of white matter viewed through DTI is in agreement with that which is seen histologically, thus DTI meets criteria for use as a neuroimaging biomarker of the health of white matter connections in mild, moderate, and severe TBI (Bigler, 2013; Bigler & Maxwell, 2011, 2012). Despite its sensitivity to injury severity, DTI is unable to replicate many basic neuroanatomical features described by means of fiber dissection and histological techniques due to its inability to solve the problem of crossing fibers or to determine the accurate origin and

destination of fibers (Abhinav et al., 2014; Alexander et al., 2001). These limitations commonly result in multiple artifacts and the production of looping or false tracts, and these problems are accentuated in damaged brains (Fernandez-Miranda et al., 2012). Recent studies have further demonstrated that DTI indices may be affected by several factors related to image acquisition, such as the number of gradient directions (Ni et al., 2006), spatial resolution (Oouchi et al., 2007), *b*-value (Hui et al., 2010), field strength (Huisman et al., 2006), partial volume effects (Alexander et al., 2001), and head motion (Yendiki et al., 2014). For reasons such as these, more sensitive approaches toward fiber mapping have emerged over the past 15 years and demonstrate important improvements over the shortcomings of DTI (Jones et al., 2013).

To resolve the major issue of crossing fibers, model-free approaches that use exhaustive sampling to obtain the empirical distribution of water diffusion include non-parametric reconstruction methods that make use of the diffusion orientation distribution function (ODF; Figure 2) to describe the intravoxel heterogeneity of water molecule diffusion as defined on a unit sphere. Relative to that which is resolved by the diffusion tensor model, ODF provides greater angular resolution and allows for the determination of the set of directions of multiple pathways running through each voxel (Wedeen et al., 2005), rather than the average direction of diffusion. Peak ODF orientations can be used with fiber tractography for more accurate reconstructions of complex fiber trajectories. Inherently, signal responses at multiple diffusion sampling directions are required for ODF estimation, and such data can be acquired using non-parametric models that utilize either single-shell or grid sampling techniques.

High angular resolution diffusion imaging (HARDI) is a single-shell sampling scheme that uses a persistent angular structure method (Jansons & Alexander, 2003) and consistent diffusion gradient strength (Tuch et al., 2002). Diffusion spectrum imaging (DSI) is a model-

free, grid sampling approach that estimates diffusion ODF through the application of the probability density function (PDF) by taking the inverse Fourier transform of MR data (Figure 2). DSI models the diffusion spectra across the 3D *q*-space (Wedeen et al., 2005), where the local maxima of diffusion ODF is measured at each radial direction within a voxel using the PDF. The accuracy of DSI fiber mapping is supported by neuroanatomical (Johansen-Berg & Rushworth, 2009) and radiographic (Schmahmann et al., 2007) comparisons in humans; however, disadvantages exist in that a very high rate of sampling is required to achieve a large enough spectral bandwidth (*b*max; recommended at 10,000 s/mm^2) to obtain the accurate PDF for all points across the *q*-space grid (Wedeen et al., 2005). This higher rate of sampling increases scan time and the rate of motion errors substantially, which poses a challenge to the utility of DSI with clinical populations. *Q*-ball image sampling (QBI; Tuch, 2004) is an alternative model-free approach that estimates the ODF directly from spherically-shaped HARDI data in *q*-space through the application of a Funk-Radon transformation and the utilization of a constant *b*-value (Tuch, 2004; Tuch et al., 2003). As a result, the sampling rate in *q*-ball imaging is 2-3 times faster than that of DSI, which is much more feasible for use in clinical populations. Unfortunately, a tradeoff exists with the use of a reduced *b*max values, which degrades the angular resolution in QBI (Kuo et al., 2008; Tuch, 2004).

The necessity to facilitate accuracy of prediction for application in clinical settings led to a systematic investigation toward the optimal *b*max value under constraints of scan time and angular gradient resolution, and a more flexible approach, generalized *q*-sampling imaging (GQI), was developed (Yeh et al., 2010). GQI obtains the spin distribution function (SDF) from QBI's shell-sampling scheme or from DSI's grid-sampling scheme; in doing so, it demonstrates

improved resolution for crossing fibers and increased accuracy in fiber tractography (Wang et al., 2013; Yeh et al., 2013).

Over the last decade, the technique has been further developed into an advanced, high-definition fiber tracking (HDFT) pipeline (Fernandez-Miranda et al., 2012; Guise et al., 2016; Jarbo et al., 2012; Pathak, 2015; Shin, Verstynen, et al., 2012; Verstynen et al., 2011; Wedeen et al., 2005; Yeh et al., 2013; Yeh et al., 2016; Yeh et al., 2010), which involves a unique combination of methods related to data acquisition, preprocessing, reconstruction, and tractography that are built on optimized DSI and GQI sampling methods (Abhinav et al., 2015; Kuo et al., 2008; Sotiropoulos et al., 2013; Verstynen et al., 2011; Yeh et al., 2013; Yeh et al., 2010). This novel combination of methods includes the dense-sampling of region-of-interest-based tractography data, multiple intervoxel sampling, and deterministic tractography aided by quantitative anisotropy (Yeh et al., 2013), using the Euler method for streamline integration (Conturo et al., 1999; Mori et al., 1999). The reliability and validity of HDFT for the accurate reconstruction of white matter fiber tracts has been demonstrated through studies of quality control assurance (Guise et al., 2016) and neuroanatomical validation (Fernandez-Miranda et al., 2012), and evidence for the resolution of the crossing and termination problems has been demonstrated (Fernandez-Miranda et al., 2012; Yeh et al., 2013). The major limitation of scan time typically required for the acquisition of DSI data has recently been overcome through the implementation of multi-band accelerated acquisition (Sotiropoulos et al., 2013), which substantially reduces scanning time to less than 15 minutes.

The advantages of HDFT over DTI have initiated research into the utilization of HDFT as a sensitive measure of the microstructural damage that remains after TAI in chronic TBI, even in those with mild injuries (Presson, Krishnaswamy, et al., 2015; Shin, Okonkwo, et al., 2012; Shin

et al., 2014). In addition to reliably reconstructing known white matter pathways, HDFT utilizes specific methods of quantification that are useful in determining the degree of white matter injury that is present in TBI (Shin, Verstynen, et al., 2012). These methods include advanced measures of diffusion density, including quantitative anisotropy (QA) and restricted diffusion imaging (RDI; Yeh et al., 2017; Yeh et al., 2013), measures of diffusivity, including generalized fractional anisotropy (gFA), as well as shape-based measures, such as tract spread (Presson, Beers, et al., 2015; Presson, Krishnaswamy, et al., 2015; Shin, Okonkwo, et al., 2012). Prior medical imaging techniques, such as DTI, are estimated to detect TBI-related structural damage only 5%–30% of time, and normal structure is detected by MRI in 43%–68% of mTBI, which make up about 80% of the TBIs reported in the US each year (Shin et al., 2014). A more sensitive method of detection of structural damage is necessary, and the findings of studies using HDFT have led researchers to believe that this advanced neuroimaging technique "may one day provide a definitive imaging modality for TBI" (Shin, Okonkwo, et al., 2012, p. 3).

Aims and Hypotheses

The present study examined the functional and microstructural outcomes of adults with chronic mTBI and varying levels of PCS in comparison to healthy adults with the following aims:

1. To examine the sensitivity and specificity of traditional versus advanced measures of cognitive outcome, specifically neuropsychological testing versus eye-tracking analysis, for characterizing chronic functional impairments in adults with mTBI relative to healthy adults.

   Hypothesis: Performance on eye-tracking tasks of attention, working memory, and processing speed will more accurately discriminate between adults with mTBI from those

with no history of TBI than performance on traditional neuropsychological measures of attention, working memory, and processing speed.

2. To examine the sensitivity and specificity of advanced measures of microstructural outcome derived from HDFT for characterizing chronic impairments to the integrity of the white matter pathways underlying cognitive function in adults with mTBI relative to healthy adults.

   Hypothesis: HDFT-derived measures of white matter integrity extracted from the FMA and bilateral IFO, MdLF, and SLF will accurately discriminate between adults with mTBI from those with no history of TBI.

3. To evaluate the strength of the structure-function relationship in mTBI when measured using HDFT and eye-tracking analysis versus HDFT and neuropsychological testing.

   Hypothesis: Reduced microstructural integrity of each pathway, indicated by increased QA and RDI and decreased gFA and tract spread, will relate to impairments in processing speed, attention, and working memory, and this relationship will be stronger between HDFT metrics and measures of cognition obtained through eye-tracking analysis relative to the relationship between HDFT metrics and measures of cognition obtained through neuropsychological testing.

4. To determine the value of eye-tracking analysis versus neuropsychological testing for predicting the frequency and severity of PCS in chronic mTBI.

   Hypothesis: Poor performance on both neuropsychological tests and eye-tracking tasks of attention, working memory, and processing speed will predict a greater frequency and severity of persistent PCS experienced by those with chronic mTBI.

5. To determine the value of HDFT for predicting the frequency and severity of PCS in chronic mTBI.

   Hypothesis: Reduced integrity of the FMa, IFO, MdLF, and SLF, indicated by increased QA and RDI and decreased gFA and tract spread, will predict a greater frequency and severity of persistent PCS experienced by those with chronic mTBI.

Method

Participants

An a priori power analysis, conducted using G*Power v. 3.1 (Faul et al., 2009; Faul et al., 2007), revealed that a total of 40 participants were required in order to achieve adequate power of $1–\beta \geq .80$ (Cohen, 1992) to detect a large proportion of variance ($f^2 = 0.35$) in outcome that is explained by functional or structural measures, with three covariates and statistical significance based on a two-tailed alpha of .05. Participants were recruited using flyers posted around the local community and on social network platforms, or through word-of-mouth. Inclusion criteria for the mTBI group included the following: adults between the ages of 18–69 who have suffered from a non-penetrating mTBI at least 12 months prior to participation in the study. Participants must be fluent in English with 20/40 corrected or uncorrected vision, which was confirmed using a Snellen eye chart prior to enrollment. In accordance with the World Health Organization (Carroll et al., 2004), Department of Defense (The Management of Concussion/mTBI Working Group, 2009), and American Congress of Radiological Medicine (Mild Traumatic Brain Injury Committee of the Head Injury Interdisciplinary Special Interest Group of the American Congress of Rehabilitation Medicine, 1993), injury severity was classified according to a post-resuscitation Glasgow Coma Scale (GCS; Teasdale & Jennett, 1974) score between 13–15, duration of post-traumatic amnesia (PTA) lasting less than 24 hours, and/or duration of loss of consciousness

(LOC) lasting less than 30 minutes. Although GCS is the most commonly-used classification system in brain injury research (Hawryluk & Manley, 2015), it has only demonstrated usefulness in aiding early management and prognosis after TBI (Katz & Alexander, 1994; McDonald et al., 1994; Nakase-Thompson et al., 2004). PTA duration, however, has been shown to have strong utility as a predictor of long-term outcome (Brown et al., 2005; Hart et al., 2016; Katz & Alexander, 1994; Sherer et al., 2008; Wilde et al., 2006), it is considered the most sensitive indicator of TAI (Povlishock & Katz, 2005), and it can be estimated retrospectively using structured interviewing (Hart et al., 2016); therefore duration of PTA was used as the primary method by which injury severity is classified.

Abnormal day-of-injury CT scans in those who would otherwise be classified as having sustained a mTBI have consistently predicted poorer long-term functional outcome relative to those without CT abnormalities (Borgaro et al., 2003; Hessen & Nestvold, 2009; Iverson, 2006a; Kashluba et al., 2008; Lange et al., 2009). The presence of such abnormalities is thus used to differentiate between two mTBI groups, classifying those with abnormal day-of-injury CT scans as having sustained complicated injuries and those without as having sustained uncomplicated injuries. Evidence in support of this distinction is provided in the literature, where complicated mild injuries more often result in neurobehavioral and neuropsychological outcomes similar to that which is seen in moderate TBI (Levin et al., 2008; Taylor et al., 2010; Williams et al., 1990), however little-to-no attention has been given to the issue of whether or not an otherwise mild injury with abnormal neuroimaging findings should be labeled as moderate TBI. For these reasons, only those who met criteria for uncomplicated mTBI were included in the present study.

Exclusion criteria for the mTBI group included the following: abnormal day-of-injury CT if injury is otherwise classified as mild (i.e., complicated mTBI), a history of moderate-to-severe

TBI (i.e., GCS < 13, PTA ≥ 24 hours, or LOC ≥ 30 minutes), ischemia, or diagnosis of other neurological (e.g., Huntington's disease, dementia, brain tumor, etc.) or severe psychiatric (i.e., bipolar disorder, schizophrenia, psychosis, dissociative disorder) condition, current or past drug or alcohol misuse/dependence, severe clinical impairment in vision, hearing, and/or speech that would impact performance on cognitive tasks, MRI contraindication, current or possible pregnancy, and current use of psychostimulant, benzodiazepine, anticonvulsant, or neuroleptic medication, as these have been shown to impair cognitive function and eye-movement control (Reilly et al., 2008). Additionally, exclusion criteria for the healthy control group included any history of TBI. The eligibility of all potential participants was determined initially by the successful completion of an online screening questionnaire and ultimately by telephone interview prior to enrollment in the study. Upon completion of the study, each participant received $30.00 in compensation and a copy of their T1-weighted structural imaging data.

Neuropsychological Assessment

The standardized clinical measures used in this investigation were selected as reliable and valid measures of premorbid intellectual ability, and of auditory and visual processing speed, attention, and/or working memory (Table 2). The domains contributing to successful information processing are particularly relevant to the present investigation as they are amongst the most commonly impaired following TBI. Furthermore, speed of information processing has historically been shown to positively correlate with higher-order perceptual functioning and problem-solving abilities as well as degree of social withdrawal (Prigatano & Fordyce, 1986; Prigatano et al., 1986). More recently, researchers have demonstrated the role information processing speed plays as a significant mediator of the relationship between TBI severity and adaptive functioning in the chronic phase of recovery from TBI (Rassovsky et al., 2015;

Rassovsky et al., 2006). Such findings suggest that the brain's basic capacity to rapidly process information from the environment profoundly affects one's capacity for social adjustment, occupational functioning, and general adaptation. The neuropsychological battery included the following eight measures, which were administered to all participants in the order presented here.

Test of Premorbid Function

The Test of Premorbid Function (TOPF), a component of the Advanced Clinical Solutions package (Pearson, 2009a) for use with the Wechsler Adult Intelligence Scale–Fourth Edition (WAIS-IV; Wechsler, 2008a), was used to provide an estimate of premorbid intellectual ability. Premorbid intelligence estimations were based on demographic information (geographic region, sex, race/ethnicity, highest level of education, and occupation) along with performance on a 70-item word reading test. The TOPF demonstrates good reliability as an estimate of premorbid ability in TBI, for word recognition is generally believed to be relatively resistant to the cerebral damage associated with mTBI (Green et al., 2008; Mathias et al., 2007). Though measures of word-recognition may somewhat underestimate premorbid ability in severe brain injury, word reading performance has proven to be adequately sensitive to varying levels of TBI severity (Strauss et al., 2006). According to the manual (Pearson, 2009b), the TOPF has excellent psychometric properties, with high internal consistency across all age groups in healthy individuals (r = .98) and in those with TBI (r = .98), and good convergent validity with WAIS-IV FSIQ scores (r = .70). According to the manual, when the demographic characteristics are combined with TOPF score, prediction accuracy for FSIQ scores in healthy individuals and in those with TBI increases relative to that of TOPF score alone. Age-corrected normative data for TOPF performance is provided in the administration and scoring manual (Pearson, 2009a), and

the regression equation used presently to predict premorbid Wechsler Abbreviate Scale of Intelligence – Second edition (WASI-II; Wechsler, 2011) 4-subtest FSIQ from simple demographics and TOPF performance can be found in Holdnack et al. (2013).

Socioeconomic Status. Responses to several items that are included in the demographic, personal, and developmental factor questions on the TOPF record form were used to calculate a socioeconomic index (SEI) score for the present sample. Specifically, the following items were scored using the values provided by (Holdnack et al., 2013) and included in the calculation of SEI: highest education level, current employment status, current occupation, and self-reported ratings of the economic status of current and childhood neighborhoods (1 – *poor*, 2 – *somewhat poor*, 3 – *average*, 4 – *well-off*, 5 – *wealthy*), elementary school quality (1 – *poor*, 2 – *somewhat poor*, 3 – *average*, 4 – *above average*, 5 – *superior*), and the Likert-scale rating of level of agreement or disagreement with the statement, "When I change jobs, it is a step up for me" (1 – *strongly disagree* to 5 – *strongly agree*). Current employment status and ratings of the economic status of one's current neighborhood were given the same weight as education level and occupation, which was twice that of the weight of ratings of elementary school quality, childhood neighborhood, and whether changing jobs was typically considered a step up. Weighted values were summed across all seven items, and the total scores were converted into sample-specific *z*-scores.

Digit Span

The Digit Span subtest of the WAIS-IV (Wechsler, 2008a) was designed as a brief assessment of auditory attention and working memory. Digit Span consists of three component trials, Digit Span Forward (DSF), Backward (DSB), and Sequencing (DSS), for which the examinee is instructed to recall strings of numbers presented orally. While the DSF is a better

indicator of auditory attention, the DSB and DSS have been shown to be particularly informative as measures of auditory working memory. Overall, performance on the Digit Span trials is sensitive to cognitive impairment and recovery (Kersel et al., 2001; Millis et al., 2001), TBI severity (Carlozzi et al., 2015) and the subtest has high internal consistency ($r > .89$) across all age groups (Wechsler, 2008b). Raw scores on each component trial were converted to age-corrected scale scores per the normative data provided in the administration and scoring manual (Wechsler, 2008a).

Additionally, the Digit Span subtest of the WAIS-IV includes and embedded measure of effort. A revised version of the Reliable Digit Span (RDS-R) has been suggested for use with the WAIS-IV (Reese et al., 2012), where the longest paired string of digits accurately recalled for each of the three component trials is summed. A cut off score of ≤ 11, has shown to better distinguish good and suspect effort in TBI (sensitivity = 59%, specificity = 94%) relative to the traditional RDS (Young et al., 2012).

Symbol Digit Modalities Test

The Symbol Digit Modalities Test (SDMT; Smith, 2000) is a timed measure of psychomotor processing speed that requires efficient decoding of nine symbol-digit pairs. The SDMT simultaneously draws upon several other cognitive processes, including visual scanning, working memory, and attention. The SDMT has been shown to be extremely sensitive to TBI in adults (Ponsford & Kinsella, 1992). Sensitivity to the cognitive effects and recovery of TAI in severe TBI has also been demonstrated (Felmingham et al., 2004), and performance on the task can differentiate between early versus late stages of recovery (Bate et al., 2001). Morgan and Wheelock (1992) demonstrated that the SDMT has good convergent validity ($r = .91$), and factor analytic studies suggest that it measures similar aspects of attention as the Stroop, the Test of

Everyday Attention, Ruff 2 & 7 (Bate et al., 2001; Chan, 2000; Chan et al., 2003), and the Trail Making Test (McCaffrey et al., 1988; Ponsford & Kinsella, 1992; Shum et al., 1990). Total correct raw scores were converted to age- and education-corrected *z*-scores using the normative data provided in the manual (Smith, 2000).

Trail Making Test

The Trail Making Test (TMT) consists of two parts (A, B), which are used together to measure attention, processing speed, and mental flexibility, and it is part of the Halstead-Reitan Neuropsychological Battery (Reitan & Wolfson, 1985, 1993). Parts A and B are both valid and reliable measures of efficiency of visual search ability (Strauss et al., 2006), and provide additional information regarding skills of attention, visual scanning, eye-hand coordination speed, and information processing speed. TMT part B provides an additional measure of planning ability, visuo-motor speed and concentration, and mental flexibility. Raw scores are determined as the number of seconds required to complete each trial, and demographically-corrected T-scores were determined using the revised comprehensive norms for the expanded Halstead-Reitan Neuropsychological Battery (HRNB; Heaton et al., 2004).

Auditory Consonant Trigrams

The Auditory Consonant Trigrams (ACT) task is an adaptation of the Brown-Peterson Task (Brown, 1958; Peterson & Peterson, 1959) that was developed as a measure of verbal working memory. Stuss et al. (1988) found that the test is sensitive to TBI, and duration of PTA or LOC is predictive of poorer performance on the ACT. The authors further examined the reliability and construct validity of the task, which was found to be adequate. A psychometric update was published by Shura et al. (2016), in which the authors determined that the internal consistency of the ACT trials is adequate ($\alpha = .79$), and a normative sample was developed for

raw scores on the 9-, 18-, and 36-second trials as well as for total raw score. These normative data were used in the present study to convert raw trial and total scores into *z*-scores.

Ruff 2 and 7 Selective Attention Test

The Ruff 2 and 7 Selective Attention Test (2 & 7 test; Ruff & Allen, 1996) is a cancellation task that was developed to assess sustained and selective attention, where Automatic Detection and Controlled Search trials alternate consecutively in 15-second intervals for a total of 20 trials. These two domains are scored in terms of speed and accuracy for each trial type, and the four resulting scores are used as component measures of selective attention; sustained attention is measured through total speed and accuracy across all 20 trials. According to the manual (Ruff & Allen, 1996), internal consistency of the 2 & 7 test is high ($r > .80$), and coefficients for the two trial types are both very strong ($r > .95$). The 2 & 7 test maintains good convergent and divergent validity over a six-month retesting period, and its diagnostic utility for TBI is supported by Cicerone and Azulay (2002). Raw scores for speed, errors, and accuracy [Accuracy = Speed ÷ (Speed – Errors)] were calculated for both trials and converted to T-scores, and Total Speed and Total Accuracy scores were calculated as the sum of T-scores for speed and accuracy across the two trials. T-score conversions were determined by the normative data that is provided in the manual (Cicerone & Azulay, 2002), which is stratified by years of age and education.

Symbol Span

The Symbol Span subtest of the Wechsler Memory Scale – Fourth edition (WMS-IV; Wechsler, 2009a) was developed as a visual analog to the Digit Span subtest of the WAIS-IV. The test involves the use of novel visual stimuli to measure the capacity to temporarily retain a mental image and its spatial location within a sequence in one's working memory. According to

the manual (Wechsler, 2009b), Symbol Span has demonstrated good split-half reliability (r = .88). Furthermore, Carlozzi et al. (2013) analyzed the construct validity of the WMS-IV for use with individuals with TBI and found large effect sizes for poorer performance on the Symbol Span subtest by those with complicated mild/moderate TBI (d = –0.94) and severe TBI (d = –1.58) versus the WMS-IV normative sample; however, this study did not find evidence that Symbol Span performance is able to distinguish between levels of injury severity in those with TBI. Raw scores were converted to age-corrected scaled scores per the normative data provided in the administration and scoring manual (Wechsler, 2009a). Like Digit Span, Symbol Span is also useful for the detection of suboptimal effort. Young et al. (2012) found that an age-corrected scale score cutoff of ≤ 7 (sensitivity = 52%, specificity = 84%) can be used to distinguish between good from suspect effort.

Paced Auditory Serial Addition Task

The Paced Auditory Serial Addition Task (PASAT; Gronwall & Wrightson, 1974, 1981; Gronwall, 1977) was originally developed to assess complex mental manipulation and provide an estimate of auditory information processing speed in those with TBI. According to a study by (Crawford et al., 1998), the PASAT has very high internal consistency (α = .90). The Victoria Computerized Adaptation of the PASAT retains the same psychometric properties as the original version (McInerney, 2004) and was used in the present study. Total correct were obtained for each trial, and raw scores were converted to age-corrected z-scores using the normative data provided by Stuss et al. (1988). Total correct scores were summed across the four trials to generate an overall total correct score, which was converted into demographically corrected T-scores using the revised comprehensive norms for the expanded HRNB (Heaton et al., 2004).

Assessment of Post-Concussive Symptoms

Two self-report measures of PCS that are recommended for use as common outcome measures in TBI research (Wilde et al., 2010) were used to determine the presence and severity of PCS in the present sample. The 22-item Neurobehavioral Symptom Inventory (NSI; Cicerone & Kalmar, 1995) measures symptom frequency and severity using a 5-point scale, where the respondent is asked to indicate the extent to which they were disturbed by each symptom over the course of the past two weeks (0 – *no problem*, 1 – *mild problem*, 2 – *moderate problem*, 3 – *severe problem*, 4 – *very severe problem*). A total score is obtained by summing responses across all items (range = 0–78), although a four-factor model structure has been described, where subscale scores may be derived for Somatosensory (range = 0–28), Cognitive (range = 0–16), Affective (range = 0–24), and Vestibular (range = 0–12) symptoms (Meterko et al., 2012; Vanderploeg et al., 2015). In a psychometric validation study, King et al. (2012) established that the NSI has high internal consistency overall (Cronbach's $\alpha = 0.95$) and among the subscales ($\alpha =$ 0.88-0.92). Furthermore, sensitivity analysis indicated a large effect size for the NSI total score when distinguishing between TBI and non-TBI samples (King et al., 2012). The NSI was administered to all participants in the present study.

The 16-item Rivermead Post Concussion Symptoms Questionnaire (RPQ; King et al., 1995; Potter et al., 2006) is used to measure the presence and severity of the 16 most commonly reported post-concussive symptoms found in the literature. Respondents are asked to rate the severity of several symptoms currently experienced (i.e., within the last 24 hours) in relation to their experience of such symptoms prior to the injury on a 5-point scale (0 – *not experienced*, 1 – *no more of a problem*, 2 – *mild problem*, 3 – *moderate problem*, 4 – *severe problem*). The total score for the RPQ (range = 0–64) is determined by summing the scores across all symptoms rated as at least a mild problem (i.e., with a score of 2 or higher), as a rating of 1 indicates that

the symptom was present before the injury and has not worsened since the injury. The RPQ has well established internal consistency (Eyres et al., 2005), test-retest reliability (King et al., 1995), and internal construct validity (Eyres et al., 2005; Lannsjo et al., 2011) as a measure of PCS in mild TBI. Due to the absence of a history of TBI for the healthy control group to use as a reference point, the RPQ was only administered to patients in the mTBI group.

Eye-Tracking Analysis

Apparatus

Eye movement recordings were obtained using a SR Research EyeLink 1000 Plus eye tracker (SR Research, Ottawa, ON, Canada) with a 25 mm lens. Pupil position and corneal reflectance were monitored with a spatial resolution of 0.01° and sampling at 1000 Hz. SR Research Experiment Builder software (version 2.1.512) was used to design and control the experimental protocol, and all data was extracted from the recordings using SR Research Data Viewer software (version 4.1.63). A 24-inch (diagonal) stimulus monitor was positioned in front of the participant at a distance of 45 cm, and spatial resolution was set to 1920 × 1080 pixels, such that the monitor subtends 66° × 38° of visual angle. A chin and head rest was used to minimize head movement. Recordings of monocular viewing were obtained from the dominant eye, whenever possible. A 19-, 13-, and 9-point calibration of gaze on the monitor was performed prior to the VGS, MGS, and SPEM tasks, respectively. For calibration to be accepted, the average error must not have fallen below .49° and the maximum error must not have exceeded .99°. Saccades were detected based on velocity and acceleration threshold criteria of 100°/s and 1500°/s, respectively. Prior to beginning the eye-tracking analysis, visual acuity was tested for each participant using a Snellen eye-chart, and right or left eye dominance was determined using the method described by Miles (1929).

Paradigms

Visually-Guided Saccades. A green fixation cross with a diameter of 1° of visual angle (28 pixels) was centered on a dark gray screen at intervals alternating pseudo randomly for 1000-2000 ms after the participant fixated on the cross for 500 ms. A round, white, 28 × 28 pixel target stimulus then randomly appeared for 1000 ms at one of 30 possible locations along 8 radial directions (0°, 45°, 90°, 135°, 180°, 225°, 270°, 315°) around the central fixation cross. Targets appeared at eccentricities of 5°, 10°, 15°, 20°, 25°, or 30° horizontally, 5°, 10°, or 15° vertically, or 10°, 15°, or 20° diagonally (see Figure 3a). The fixation cross was extinguished at the same time that the target stimulus appeared on the screen, and participants were instructed to look directly at the target as quickly and accurately as possible (Figure 4). Each trial was followed by a 200 ms gap, during which time no stimuli was presented on the screen. Following 6 practice trials, a total of 60 trials occurred across two separate blocks of 30 iterations each. The participant were given a short break between the two blocks. Each trial required 2.2 s, thus a total of approximately 198 s (3.3 minutes) was required for the entire VGS task.

Following the removal of blink saccades, the following outcome measures were investigated as a function of eccentricity: primary saccade latency (the time required to initiate a saccade in ms), primary saccade velocity (°/s), time to peak velocity (ms) of the primary saccade, and duration (ms) of the primary saccade. Additionally, mean absolute position error (PE), quantified as the absolute difference in distance between the target position (TP) and the final eye position (EP_F), gain of final saccade (G_F), and gain of the primary saccade (G_P) were calculated along both the horizontal (x) and vertical (y) axes using the formulas provided by Heitger et al. (2002). A measure of amplitude error (AE) was also derived to represent the average deviation (%) in amplitude of the primary saccade from the target amplitude.

Memory-Guided Saccade Sequences. Adapting the paradigm initially used by Heitger et al. (2002), the MGS task involved the initial presentation of a yellow fixation cross centered on a dark gray screen. Once the participant has fixated on the central fixation cross for 500 ms, a peripheral target stimulus appeared at one of 24 possible target locations along 8 radial directions (0°, 45°, 90°, 135°, 180°, 225°, 270°, 315°) at eccentricities of 5°, 10°, or 15° from the central fixation cross (see Figure 3b). The target remained for 1000 ms before jumping successively to a different target location, where it also remained for 1000 ms. Upon the exit of the final target stimulus, a random delayed memory interval of 1650-2150 ms occurred prior to the disappearance of the fixation cross, at which time the examinee was instructed to mimic the stimuli's movements with their gaze upon a blank screen (see Figure 5). Two blocks of 24 trials each were presented. The first block consisted of 2-step trials, where the target jumped to two positions at random before exiting, and the second block consisted of 3-step trials, where the target jumped to three positions at random before exiting. Before beginning the first trial block, three 1-step and three 2-step practice trials were administered, and before beginning the second trial block, three 3-step practice trials were administered. If the participant looked away from the central fixation cross before it disappeared, they were prompted to keep their eyes on the central cross until it disappeared, and the trial was recycled to the end of the block. In addition to the 66 s required to complete the 9 practice trials, each 2-step trial required 7 s, each 3-step trial required 10 s, thus 474 s (7.9 mins) was required to complete the entire MGS task.

Following the removal of blink saccades, the following outcome measures were investigated as a function of step: primary saccade velocity (°/s), time to peak velocity (ms) of the primary saccade, duration (ms) of the primary saccade, and horizontal and vertical PE, G_F, and G_P. Additionally, AE was calculated for each step (AE_{step_k}) and mean AE was computed

across each sequence of steps (AE_{seq_j}), based on EP_f, using the formulas provided by Heitger et al. (2002). Finally, saccade frequency was calculated for each step, and the number of ordinal errors, the number of skipped steps, and an absolute time index (ATI = total response time divided by the total sequence duration) were calculated for the 2- and 3-step trials separately.

Predictive Smooth Pursuit Eye-Movement. Following an adaptation of the paradigms used by Maruta et al. (2014), Maruta, Suh, et al. (2010), and Diwakar et al. (2015), the predictive SPEM task involved the initial presentation of a blue fixation cross (28 × 28 pixels) on a dark gray screen, which indicated the start location of the target stimulus. The fixation cross remained until it was gazed upon for 200 ms, at which time it was replaced by the target stimulus, a blue disc with a diameter of 1° visual angle (28 pixels). The task consisted of two blocks of 30 revolutions, or cycles, in which the target stimulus moved at a fixed rate of 0.4 Hz in a clockwise or counter-clockwise, circular trajectory with a radius of 10° of visual angle (286 pixels), and thus at a speed of 25°/s. The start location of each target stimulus alternated randomly between the right (0°), top (90°), left (180°), or bottom (270°) quadrant axes of the unit circle. Each block included 15 continuous and 15 gap cycles, which were presented at random. In the continuous condition, the target was visible throughout the entire 2500 ms cycle. The gap conditions included a period of target blanking, where the target was visible for a random interval of 416–2083 ms (60°–300°) and then disappeared for 30° (208 ms), 45° (312 ms), or 60° (416 ms) before reappearing to complete the cycle. A blank screen appeared for 500 ms between each cycle. Refer to Figure 6 for an illustration of this paradigm. Participants were instructed to follow the target stimulus as it moved along a circular trajectory on the screen and to continue following its path by predicting the target's movement during gap periods. Each subject completed a single

practice block of 5 trials prior to beginning the test blocks. Each trial required 4 s; thus, a total of 260 s was required to complete the entire predictive SPEM task.

Outcome measures of spatial accuracy include the mean radius of gaze trajectory relative to target trajectory, which is expressed in units of degrees of visual angle, and measures of temporal accuracy include mean phase error, gaze stability, and smooth pursuit gain. Mean phase error was determined by the angle subtended by gaze versus the target position, averaged across all time points and expressed in units of degrees of phase angle. Gaze stability is characterized by the variability of gaze positional error in directions that are radial and tangential to the target trajectory. The variability of radial and tangential positional error is expressed in units of degree of visual angle and computed as the standard deviation of instantaneous gaze positional error in perpendicular (radial; SDRE) or orthogonal (tangential; SDTE) directions relative to the target's trajectory (Maruta et al., 2014; Maruta, Suh, et al., 2010); larger values for gaze stability measured indicate less stable tracking. Smooth pursuit gain was quantified as the ratio of eye velocity to target velocity after the first 100 ms, such that values below 1.0 indicate that the movement of the eye has fallen behind the target's movement and an increasing number of catch-up saccades are required to compensate for the slowness of the smooth pursuit system. Root mean-square error (RMSE) was also investigated as it provides an index of the extent to which the eye reproduces the movement of the target and quantifies gain as the cumulative distance between instantaneous gaze position and the target position during smooth pursuit. All measures were averaged across desaccaded trials and computed separately for the continuous cycles and for each of the three phases of the 30°, 45°, and 65° gap cycles (i.e., pre-gap, within-gap, post-gap). Saccade frequency (total saccade time ÷ trial duration) was also collected for each cycle

condition (Diwakar et al., 2015) prior to the isolation and removal of all blinks and saccades from the raw data samples.

Structural Neuroimaging

Acquisition

Neuroimaging data was acquired on a 3T Siemens TIM Trio whole-body scanner (Siemens, Erlangen, Germany) using a 32-channel head coil, and the total acquisition time was approximately 30 minutes. Each scan session began with a 10-second, three-plane localizer, and details regarding the acquisition parameters for each the following sequences can be found in Table 3. Structural data was collected using a T1-weighted magnetization-prepared rapid gradient echo (MP-RAGE) sequence, where 192 contiguous slices are acquired in the sagittal plane. To detect the presence of hemorrhage, edema, or microbleeds, which can affect the quality of HDFT (Geurts et al., 2012; Shin et al., 2014), susceptibility-weighted imaging (SWI) was used to acquire 72 axial slices via interleaved sampling. Multi-shell diffusion data was acquired in approximately 20 minutes using a free diffusion-encoding scheme with simultaneous multi-slice (SMS) optimization and multiband acceleration (factor of 3). A total of 300 volumes were acquired in interleaved slice order. Sampling in *q*-space included 256 non-colinear directions acquired across 3 shells of gradient-weighted data at b = 1000, 3000, and 5000 s/mm^2. For the b = 1000 and b = 3000 shells, 70 data points were acquired in the anterior-to-posterior phase encoding (PE) direction, corresponding to 64 diffusion directions and 6 non-gradient (b = 0 s/mm^2; b0) weighted images for each shell. For the b = 5000 shell, 138 data points were acquired in the anterior-to-posterior PE direction, corresponding to 128 diffusion directions and 10 b0 images. For each diffusion-weighted shell, a corresponding shell of six b0 images was acquired in the reversed PE direction (i.e., posterior-to-anterior) but with otherwise identical acquisition

parameters (Table 3); thus, a total of 6 shells of data were collected. The *b*0 shells were interleaved with their respective diffusion-weighted shell during acquisition so as to obtain better correspondence between the three PE-reversed shell pairs.

Preprocessing

The pipeline used for preprocessing of the multishell diffusion data was modeled after the Human Connectome Project diffusion preprocessing pipeline (Andersson & Sotiropoulos, 2016; Glasser et al., 2013; Sotiropoulos et al., 2013), and all bash scripts developed and used presently can be found in the OSF storage for this study at https://osf.io/89fpx/. Preprocessing included an initial intensity normalization of the mean *b*0 image across all six shells (three with positive phase encoding, three with negative phase encoding), where the mean *b*0 image from all series was extracted and rescaled to match the *b*0 image of the first series acquired. Finally, the *b*0 images from each series were merged with the *b*0 mean. The reversed phase encoding *b*0 pairs were then used to estimate the susceptibility-induced echo-planar imaging (EPI) distortion, which was accomplished using the topup tool from the FMRIB Software Library (FSL; Jenkinson et al., 2012). The resulting distortion field estimate was then fed into FSL's applytopup tool, which predicts the Gaussian Process in addition to estimating the eddy-current-induced inhomogeneities and extent of head motion for each volume. The resulting individual *b*0 volumes were then fed into FSL's BET brain extraction tool (Smith, 2002) to generate a skull-stripped brain mask for each subject. The estimates produced from topup and the brain mask generated after applytopup were finally fed into FSL's eddy tool, which corrects all of the distortions in a single resampling step. The skull-stripped brain mask was also used to constrain the area subjected to DSI data reconstruction using the GQI approach (Yeh et al., 2010), where

the ODFs were reconstructed to 362 discrete sampling directions with a diffusion sampling length ratio of 1.25.

Fiber Tractography

Fiber tractography was performed using DSI Studio (April 28 2020 build; https://dsi-studio.labsolver.org), which utilizes a generalized streamline fiber tracking method (Yeh et al., 2013) that has been recognized as producing the highest number of valid connections among other fiber tracking approaches (Maier-Hein et al., 2017). Atrophy, enlarged ventricles, and other structural abnormalities that often result from brain injury are known to complicate the automated registration of anatomical atlases to diffusion images (Irimia et al., 2011; Rijken et al., 2015); thus, human intervention in the registration process is necessary, and automated template registration is not recommended. A manual region-of-interest (ROI) approach has been suggested to increase the reproducibility of white matter tractography and to reduce the likelihood of false positive and false negative results, which may arise from noise, partial volume effects, and complex fiber architecture (Wakana et al., 2007). Multiple ROIs and/or regions of avoidance (ROAs) can be designated in order to anatomically constrain fibers bundles according to predefined trajectories, allowing for well-characterized, reproducible white matter tracts (Conturo et al., 1999; Huang et al., 2004; Wakana et al., 2007). The manual designation of ROIs on a subject-specific basis ensures that the extracted streamlines belong to the pathway of interest, and the necessity for registration and other normalization procedures that may introduce error are eliminated. Accordingly, the manual ROI approach is often regarded as the most anatomically accurate method for mapping white matter pathways in vivo (Sydnor et al., 2018).

For the previously described reasons, a multiple ROI approach was used, where the white matter directional vector field maps created by the diffusion *q*-space reconstruction process in

DSI Studio were used for the identification of obligatory tract trajectory landmarks for each pathway. Qualified researchers trained in tractography manually demarcated all ROIs and ROAs for each subject individually by selecting all voxels containing the appropriate fibers, which are determined by the color and direction of ODFs overlaid on the *b*0 image. A predefined ROI/ROA definition and fiber tracking protocol was followed by all tractographers, in which a total of 35 anatomical ROIs and/or ROAs were largely defined according to the procedures described by Wakana et al. (2007) for the FMa and SLF, by Catani and Thiebaut de Schotten (2008) for the IFO, and by Kalyvas et al. (2020), Makris et al. (2017), and (Wang et al., 2013) for the MdLF. Minor adaptations to these tractography protocols were made according to recent validation studies describing the trajectories of the SLF (Wang et al., 2016) and the IFO (Martino et al., 2010; Sarubbo et al., 2013) with greater precision through the use of advanced diffusion imaging methods and post-mortem fiber dissection techniques. The detailed manual used for all tractography-related procedures, including data reconstruction, region drawing, fiber tracking, tract editing, and data extraction, can be accessed in the OSF storage directory for the present study at https://osf.io/89fxp/.

The fiber trajectories of the FMa, IFO, MdLF, and SLF (Figure 8) were generated using an ODF-streamlined deterministic tractography algorithm (Basser et al., 2000; Yeh et al., 2010) with trilinear interpolation. Random-seeding was used to initiate fiber tracking in the direction of the most prominent fiber orientation. In the presence of multiple fiber orientations, tracking was initiated for each orientation individually, and fiber progression continued with a step size of 1.20 mm (half of the voxel size in one dimension; Yeh et al., 2013), a minimum/maximum fiber length threshold of 20/200 mm, a turning angle threshold of 60°, and a 20% smoothing weighting, which was determined using the protocol described in Wang et al. (2013). The

tracking progression ceased when the QA of the fiber orientation dropped below a subject-specific threshold, or until no fiber was selected within the 60° angular threshold. Rather than fixing the number of streamlines, 1,500,000 whole brain seeds (approximately 25 seeds per voxel) were fixed across all subjects to avoid artificial between-subject tract equalization and to allow for variation in the number of modeled streamlines according to an individual's anisotropy data (Presson, Krishnaswamy, et al., 2015). An optimal QA threshold between .03–.07 was chosen for each brain individually based on the visibility of ODF directions overlaid on an anisotropy map in an axial slice at the level of the internal and external capsules and was adjusted based on the relative signal-to-noise of each scan on a subject-specific basis. Subjective QA thresholds ranged from .038–.069 (M = .054, SD = .009), and there was no difference in QA thresholds used for the mTBI (M = .057, SD = .002) and healthy control groups (M = .050, SD = .003), $t(19) = 1.86$, $p = .078$.

Inter- and Intra-Rater Reliability. To ensure the reliability of the manual ROI protocol used for tractography, all data was independently analyzed by two of three adequately trained tractographers, and a random subset of the data was analyzed a twice by the same tractographer after a period of at least one month had passed since the initial analysis. Inter- and intra-rater reliability of the tractography protocol was established using Shrout-Fleiss intraclass correlation coefficients (ICCs; Shrout & Fleiss, 1979), which produced satisfactory reliability coefficients for inter-rater reliability (region ICCs ≥ 0.95, tract ICCs ≥ 0.93) as well as intra-rater reliability (region ICCs ≥ 0.96 and tract ICCs ≥ 0.95). All tractographers were blind to the injury status of the participants during data analysis.

Tract Editing. Fiber bundles were assessed for the presence of false tracts and excessive noise through comparison with anatomical and tractographic literature by two qualified

researchers with extensive training in neuroanatomy and specific knowledge of the anatomical structures of the FMa, IFO, MdLF, and SLF. Prior to manual editing, a maximum of two iterations of topology-informed pruning (TIP; Yeh et al., 2019) were performed to reduce the number of false fibers present in the rendered tracts, thus increasing their anatomical validity. Finally, a qualitative comparison of the fiber termination locations for each resulting fiber tract was conducted using the subject's anatomical data, which was skull-stripped using the Advanced Normalization Tools (Avants et al., 2011) brain extraction tool and aligned to the subject's diffusion map using a nonlinear registration algorithm implemented in DSI Studio. As a result, a 3D isosurface rendering of each subject's cortical surface was generated and used as a tract overlay, allowing for the examination of the agreement of fiber termination locations with gyral folding (Figure 9). Fibers that prematurely terminated in the white matter, belonged to a nearby tract, were determined to be false continuations (i.e., streamlines that originate in the desired tract but later merge with an adjacent tract), or followed anatomically impossible trajectories (i.e., looping fibers or fibers that "surf" across gyri) were identified and manually removed using the tract editing toolbox in DSI Studio.

Quantification. Several GQI-derived measures of diffusion density, diffusivity, and tract spread were used to quantify the structural integrity of white matter pathways reconstructed in DSI Studio using GQI. Due to Brownian motion, tensor-derived measures, such as FA and mean diffusivity (MD), quantify diffusivity from both restricted and non-restricted diffusion within a voxel; thus, FA and MD are unable to specify diffusion that is restricted by axonal myelination, which is a key contributor to the microstructural properties of biological tissue. As a result, changes in tensor-based measures of anisotropy and diffusivity reflect a complex assortment of biological changes that occur in the presence of edema, inflammation, crossing fibers, and other

factors (Yeh et al., 2013). Consequently, tensor-derived metrics are largely unreliable, particularly when derived from a small sample.

To correct for this, GQI-derived measures quantify how much water diffuses, or the *density* of restricted and less-restricted diffusion within a voxel and are robust against inflammation and edema. QA is calculated from the spin distribution function (SDF), which is estimated using GQI, and it is operationalized as the amount of anisotropic spins that diffuse along the fiber orientation (Yeh et al., 2013; Yeh et al., 2010). QA scales with spin density, and during its calculation, the isotropic background diffusion of the SDF is discarded and free water diffusion is scaled to 1; thus, QA is less susceptible to partial volume effects (Yeh et al., 2011), it is comparable across voxels and between subjects, and it is minimally impacted by the effects of free water diffusion. Additionally, QA outperforms tensor-derived FA when the signal-to-noise ratio is low, which is often the case when *b*-values exceed 1000 s/mm^2; therefore, QA-aided tractography is more reliable than that which is aided by FA (Zhang et al., 2013). Further, while tensor-based measures, such as FA, quantify the average anisotropy or diffusivity for all fiber populations within a voxel, QA is a fiber-specific measurement that is defined for each individual fiber orientation within a voxel. This allows the deterministic tractography algorithm to simultaneously eliminate noisy fibers selectively and define the accurate termination location of fibers. (Yeh et al., 2013). As a result, QA is robust in the presence of crossing fibers, allowing for more accurate and reliable estimations of complex white matter architecture.

To correct for free-water contamination within each voxel, a non-parametric GQI-derived tensor algorithm, called RDI, can be used to selectively quantify restricted diffusion that has been shown to strongly correlate ($r > .99$) with cell density (Yeh et al., 2017) and may be more sensitive to tissue reorganization after TBI than tensor-based measures, such as MD (Krishna et

al., 2019; Yeh et al., 2017). Changes in RDI reflect changes in cellularity, which is often a result of secondary brain injury pathologies, such as inflammation or edema. In conditions where restricted (e.g., caused by cytotoxic edema) and nonrestricted (e.g., caused by vasogenic edema) diffusion coexist, tensor-derived MD is unable to effectively describe areas of inflammation, because it is decreased by the former, increased by the latter, and unchanged when restricted and nonrestricted diffusion occur equally. RDI effectively separates restricted from nonrestricted and therefore has greater sensitivity and specificity for detecting changes in cellularity resulting from inflammation than tensor-derived MD.

When microstructural integrity is intact, GQI-derived measures of diffusion density will have greater variability between subjects than diffusivity-based measures, allowing for a better characterization of individuality across subjects; however, measures of diffusivity may be more sensitive to the integrity of microstructural architecture in the presence of pathology (Yeh et al., 2016). For this reason, gFA, which can also be quantified using GQI, is included as a measure of diffusivity in the present study. gFA is calculated from an ODF function (Yeh et al., 2013) and is highly correlated with DTI-derived FA (Fritzsche et al., 2010). Like FA, however, gFA is defined for all fiber populations within a voxel and decreases in the presence of crossing fibers, suffers from partial volume effects, and is influenced by biological changes in the tissue; therefore, caution must be taken when interpreting gFA, as results may be influenced by confounding factors.

Recent literature has suggested that HDFT-derived metrics of the spatial properties of white matter tracts, such as tract spread, may be better at indicating the presence of microstructural abnormalities in relation to cognitive deficits resulting from mTBI (Presson, Beers, et al., 2015; Presson, Krishnaswamy, et al., 2015). Tract spread is quantified as the

proportion of voxels encountered by a given tract, and it was calculated as the number of voxels contacted by at least one streamline of the tract divided by the total number of whole-brain voxels (Presson, Krishnaswamy, et al., 2015).

Experimental Design and Procedure

The present study adopted a cross-sectional, quasi-experimental design in which 11 participants with a history of mTBI and 10 healthy control participants were enrolled. Participants were recruited by the principal investigator and research assistants through local rehabilitation facilities, clinics, support groups, flyers, social networking, and word-of-mouth in the surrounding areas, and participants were identified as eligible upon completion of an online screening questionnaire and telephone interview. Recruitment and enrollment occurred between the Winter of 2019 and the Spring of 2020. All eligible participants attended one 3.5-hour session at Brigham Young University, where they were asked to provide informed consent before undergoing a visual acuity test, structural neuroimaging, an eye-tracking assessment, and neuropsychological testing.

A researcher properly trained and certified in the safety and use of MRI scanners conducted the structural imaging scan. The total time required for preparation and completion of each scan was approximately 45 minutes. Eye-tracking assessments were conducted by a researcher who was properly trained in the use of the eye-tracking apparatus and task administration procedures, and the eye-tracking typically occurred after the MRI but always prior to the neuropsychological testing. The total time required for the preparation and completion of the eye-tracking assessment was approximately 45 minutes. A qualified researcher or psychometrist trained in the appropriate standards and procedures of neuropsychological testing administered and scored all neuropsychological tests. The testing took place after the

completion of the neuroimaging scans and eye-tracking analysis, as some studies have suggested the poorer oculomotor function in TBI versus healthy controls may be due to greater vulnerability to fatigue following cognitive testing (Maruta, Palacios, et al., 2016; Maruta, Spielman, et al., 2016). The total time required for completion of the neuropsychological test battery was approximately 90 minutes.

Statistical Analysis

All statistical analyses were conducted using STATA 16.1 (2019; College Station, TX: StataCorp LP). The full dataset, a codebook for the data, and the script used to conduct all statistical analyses discussed below can be accessed from the OSF storage directory for the present study at https://osf.io/89fxp/. Neuropsychological tests were scored per their respective standards, and raw scores were converted into demographically-corrected, standardized *z*-scores according to the normative data provided in the testing manual unless otherwise specified above. Demographically-adjusted standardized scores were further converted into T-scores ($M = 50$, $SD = 10$), and three domain scores for measures of processing speed, attention, and working memory were generated by summing T-scores for all measures within each respective domain (see Table 2). A principal component analysis (PCA) was conducted on eye-tracking outcome measures that correlated with neuropsychological domain scores in order to reduce the number of comparisons to the number of components that individually explain a minimum of 5% of the total variance in the model. Prior to conducting the PCA, all eye-tracking outcome measures included in the model were converted to standardized scores.

All variables were initially screened for missing data, and those with greater than 5% of data missing were assessed for systematic patterns of missing data relating to the dependent variables. Any variables with values exceeding ± 3 IQR from the median value were considered

univariate outliers (Tukey, 1977) and fenced accordingly. The assumptions of homoscedasticity and normality were confirmed using Levene's and Shapiro-Wilks' tests, respectively, prior to all between-group comparisons of continuous variables. Assuming equal variance and normality, demographic characteristics were compared between groups using independent *t*-tests for continuous variables and Pearson's χ^2 or Fisher's exact test for categorical variables. Independent *t*-tests were also used to compare the extent of post-concussive symptoms between two groups. For continuous variables where the assumptions of homoscedasticity and/or normality were violated, a Wilcoxon Mann-Whitney U ranked-sums test was used to evaluate between group differences.

To compare performance between the healthy control and mTBI groups, one-way ANCOVAs were conducted for the three neuropsychological domains, after controlling for SEI, and one-way ANCOVAs, with age, sex, and SEI included as covariates, were conducted on each component extracted from the PCA performed on the eye-tracking outcome measures. One-way ANCOVAs were also used to evaluate between-group differences in QA, RDI, gFA, and tract spread of the FMa and right and left IFO, MdLF, and SLF, with age, sex, and SEI included as covariates. Covariates were selected based on the presence of high correlations with one or more of the outcome measures. Regression coefficients were post-estimated for each ANCOVA model and homoscedasticity was confirmed using Breusch-Pagan/Cook-Weisberg (Breusch & Pagan, 1979; Cook & Weisberg, 1983) tests with Holm's adjustment for multiple comparisons (Holm, 1979).

Discriminant function analysis was used to formulate three statistical models able to identify mTBI: the first model incorporated neuropsychological domain scores, the second model incorporated eye-tracking component scores, and the third model incorporated HDFT-derived

measures of tract integrity. For each model, the independent variables were selected according to the results of the previous ANCOVAs, where only variables demonstrating large effect sizes were included in each model. Discriminatory power of the models was quantified by the resultant overall classification accuracy, sensitivity, specificity, and positive and negative likelihood ratios (LR+, LR–), which are accompanied by resultant post-test probabilities computed using Baye's theorem.

To explore the relationships between cognitive functioning and the structural integrity of the underlying white matter within the mTBI group, partial correlations were conducted between QA, RDI, gFA, and tract spread of each white matter pathways and measures of attention, working memory, and processing speed obtained through neuropsychological testing and eye-tracking analysis, after removing the effects of age, sex, and SEI.

Multiple regression analysis was used to determine if attention, working memory, and processing speed abilities, measured through neuropsychological testing and eye-tracking, are able to predict the frequency and severity of persistent PCS in the mTBI group, after controlling for the effects of age, sex, and SEI. Finally, multiple regression analysis was also used to determine if measures of tract integrity extracted from the FMa and bilateral IFO, MdLF, and SLF are able to predict the frequency and severity of persistent PCS experienced by those with mTBI, after controlling for the effects of age, sex, and SEI. Due to non-normally distributed total and subscale scores on the NSI within the mTBI group, these variables were not suitable for linear regression analysis. Rather, a new variable was created to represent the frequency of PCS symptoms indicated on the NSI by dichotomizing item responses as 0 (no problem at all) and 1 (a mild, moderate, severe, or very severe problem), and these dichotomized items were summed to calculate the frequency of PCS symptoms experienced, which can range from 0 to 22. Due to

the extensive overlap in symptoms represented on the NSI and RPQ and the normally distributed total RPQ scores within the mTBI group, severity of PCS symptoms was measured as the total score on the RPQ.

To control for multiple comparisons, the Benjamini-Hochberg False Discovery Rate (FDR) procedure (Benjamini & Hochberg, 1995) was used for all null hypothesis tests, and statistical significance was thresholded at $\alpha = .05$. All *p*-values are reported with estimates of effect size and 99% confidence intervals (CIs). Null hypothesis significance testing was not used to evaluate the results of correlation and regression analyses; rather, the results were interpreted using measures of effect size. The following estimates of effect size are provided for each statistical analysis, and all are interpreted according to the conventions defined by Cohen (1988): Independent *t*-tests/Wilcoxon Mann-Whitney U ranked-sums tests are accompanied by Hedges's *g* (Hedges, 1981), one-way ANCOVAs are accompanied by Cohen's *f*, and partial correlations and standardized regression coefficients are accompanied by squared semipartial correlations.

Results

Participants

A total of 21 participants (11 mTBI, 10 healthy control) were recruited between November 2019 and March 2020, allowing for the detection of large effect sizes at an alpha of .05 with 41% power for between-group analyses with no covariates and 40% power for analyses with three covariates. Participants (43% female) were between 20–60 years of age ($M = 30.33$, $SD = 11.20$) with 12–20 years of education ($M = 15.43$, $SD = 2.04$). Group-level demographic and injury characteristics are reported in Table 4, and subject-specific injury characteristics for participants within the mTBI group are presented in Table 5.

Age, education, premorbid IQ, and SEI demonstrated homogeneity of variance, and education and premorbid IQ demonstrated normality between groups; however, Shapiro-Wilks test of normality demonstrated that age was not normally distributed in either group (z_{HC} = 2.61, p_{HC} = .005; z_{mTBI} = 2.51, p_{mTBI} = .006). A Wilcoxon Mann-Whitney U ranked-sums test was therefore used to demonstrate that the healthy control and mTBI groups did not differ in age, and independent *t*-tests demonstrated that the two groups did not differ in years of education, premorbid IQ, or SEI. Furthermore, Pearson's χ^2 and Fisher's exact tests demonstrated no significant differences in the distribution of sex, race, ethnicity, or handedness between the healthy control and mTBI groups (Table 4).

The measures of effort embedded within the WAIS-IV Digit Span and WMS-IV Symbol Span subtests indicated that adequate effort was put forth by all participants with mTBI; however, one healthy control participant scored within the suspect effort range on the Symbol Span (scaled score = 6). During testing, the participant was encouraged to put forth their best effort throughout all procedures. Given the lack of incentive for poor performance, a Digit Span RDS-R score within the adequate effort range, and no other indications of suspect effort, the participant's performance across neuropsychological testing procedures was determined to be valid, and the resultant data was not excluded from the present analysis.

Between-Group Comparisons

Post-Concussive Symptoms

While NSI total scores were normally distributed in the healthy control group, a non-normal distribution of total NSI scores was demonstrated in the mTBI group (z = 1.83, p = .034). Similarly, non-normal distributions were also present in the Vestibular, Somatosensory, and Cognitive subscale scores. Furthermore, the assumption of homogeneity of variance was violated

for NSI total scores and for the Somatosensory and Cognitive subscale scores. For these reasons, Wilcoxon Mann-Whitney U ranked-sums tests were used to evaluate the presence and extent of self-reported PCS between the two groups. As expected, total NSI scores were significantly higher in the mTBI group, as were the subscale scores for the Somatosensory, Cognitive, and Affective subscales of the NSI; large effect sizes were demonstrated for each of these differences. All descriptive and inferential statistics for NSI scores between the two groups are reported in Table 6.

Neuropsychological Domains

One-way ANCOVAs demonstrated no significant group differences in processing speed, attention, or working memory neuropsychological domain scores, after the effects of SEI were removed; however, a large effect size was found in favor of poorer working memory performance in the mTBI group relative to the healthy control group ($f = 0.48$). Summary statistics for neuropsychological domain scores between the two groups are found in Table 7.

Eye-Tracking Components

Due to technical difficulties, two subjects (1 mTBI, 1 HC) were unable to complete the eye-tracking procedures. Additionally, all eye-tracking data obtained from one healthy control subject was unusable for reasons related to eye color, and the MGS data from one mTBI subject was not included due to calibration failure. As a result, data was obtained from samples of the following sizes for each eye-tracking paradigm: VGS, $n = 18$ (10 mTBI, 8 HC); MGS, $n = 17$ (9 mTBI, 8 HC); SPEM, $n = 18$ (10 mTBI, 8 HC).

Pearson's correlation coefficients were used to investigate which of the various eye-tracking outcome measures were related to attention, working memory, and/or processing speed domain scores. Eye-tracking outcome measures with correlation coefficients $\geq |.30|$ were

included in the PCA, from which six components were retained that together explained 74% of the variance in the model (Table 8). Predicted scores from each component were transformed into T-scores, and the six scores were determined to broadly measure the following cognitive functions based on relationships with the individual neuropsychological test scores: psychomotor speed (component 1), cognitive flexibility (component 2), attention (component 3), working memory (component 4), general intelligence (component 5), and processing speed (component 6).

One-way ANCOVAs were conducted on each eye-tracking component score with age, sex, and SEI included as covariates. All results are reported along with group-wise descriptive statistics, standardized and unstandardized regression coefficients, 99% CIs, and Cohen's *f* as a measure of effect size in Table 9. A significant group difference and large effect size was found for the working memory component, $F(1, 12) = 5.20$, $p = .042$, $f = .66$, where scores were decreased by –23.79 ($SE = 10.43$, 99% CI [–55.66, 8.08]) in the mTBI group, relative to the healthy control group; however, this finding did not survive the multiple comparison correction. No other differences were found for the eye-tracking component scores; however, a small effect sizes were found for the attention, general intelligence, and processing speed three other components, where lower scores were observed in the mTBI group, relative to the healthy control group, on the attention and general intelligence components, and higher scores were observed in the mTBI group, relative to the healthy control group, for the processing speed component (Table 9).

High-Definition Fiber Tractography

One-way ANCOVAs were used to evaluate group differences in QA, gFA, RDI, and tract spread of the FMa and right and left IFO, MdLF, and SLF, with age, sex, and SEI included as

covariates. All results are reported along with group-wise descriptive statistics, standardized and unstandardized regression coefficients, 99% CIs, and Cohen's *f* as a measure of effect size in Table 10.

Forceps Major. After controlling for age, sex, and SEI, group differences were seen in QA of the FMa, $F(1, 16) = 5.09$, $p = .038$, $f = .56$, where QA was increased by .053 (*SE* = .024, 99% CI [–.016, .123]) in the mTBI group; however, this significant finding did not survive the multiple comparison correction. No group differences in gFA or RDI of the FMa were found; however, a large effect size was found for increased RDI in the mTBI group, and small effect sizes were found for increased gFA and reduced tract spread in the mTBI group.

Inferior Fronto-Occipital Fasciculus. After controlling for age, sex, and SEI, group differences were seen in QA of the right IFO, $F(1, 16) = 5.23$, $p = .036$, $f = .57$, where QA was increased by .030 (*SE* = .013, 99% CI [–.008, .068]) in the mTBI group. Group differences in RDI were also seen in the right IFO, $F(1, 16) = 5.61$, $p = .031$, $f = .59$, where RDI was increased by .040 (*SE* = .017, 99% CI [–.009, .089]) in the mTBI group; however, none of these significant findings survived the multiple comparison correction. No group differences in any measure of integrity of the left IFO; however, large effect sizes were seen for increased QA and RDI in the mTBI group, and a medium effect size was seen for decreased gFA in the left IFO of the mTBI group. No group differences in gFA or tract spread were seen for the right IFO; however, a small effect size was found for decreased gFA in the mTBI group.

Middle Longitudinal Fasciculus. After controlling for age, sex, and SEI, group differences were seen in RDI of the right MdLF, $F(1, 16) = 4.82$, $p = .043$, $f = .55$, where RDI was increased by .041 (*SE* = .019, 99% CI [–.013, .095]) in the mTBI group; however, this significant finding did not survive the multiple comparison correction. No group differences in

tract integrity were seen in the left MdLF; however, a large effect size was found for increased RDI in the mTBI group, and medium effect sizes were found for increased QA and decreased tract spread in the left MdLF of the mTBI group. No differences in QA, gFA, or tract spread were found for the right MdLF; however, a large effect size for increased QA and a medium effect size for reduced tract spread were seen in the mTBI group.

Superior Longitudinal Fasciculus. After controlling for age, sex, and SEI, group differences were seen in QA of the SLF in the left, $F(1, 16) = 5.69$, $p = .030$, $f = .60$, and right $F(1, 16) = 5.26$, $p = .036$, $f = .57$, hemispheres, where QA was increased by .033 ($SE = .014$, 99% CI [–.007, .074]) in the left SLF and by .032 ($SE = .014$, 99% CI [–.009, .074]) in the right SLF of the mTBI group. Differences were also seen in RDI of the left, $F(1, 16) = 4.57$, $p = .048$, $f = .53$, and right SLF, $F(1, 16) = 5.09$, $p = .038$, $f = .56$, where RDI was increased by .046 ($SE = .022$, 99% CI [–.017, .109]) in the left SLF and by .044 ($SE = .020$, 99% CI [–.013, .102]) in the right SLF of the mTBI group; however, none of these significant findings survived the multiple comparison correction. Additionally, small effect sizes were seen for reduced tract spread of the left SLF and reduced gFA and increased tract spread in the mTBI group.

Discriminant Function Analysis

Two linear discriminant analyses were conducted to identify patients with mTBI, each using one of the two measures of cognitive function that demonstrated large effect sizes in the results of the previous ANCOVA analyses. The first discriminant function comprised solely of the working memory neuropsychological domain score, correctly classified mTBI with an overall accuracy of 66.7% (sensitivity = 72.7%, specificity = 60%). Based on a pre-test probability of 52.4% in the present sample, the LR+ for this function is 1.82:1 (post-test probability = 66.7%), and the LR– is 0.45:1 (post-test probability = 33.1%). The discriminating

ability of this function is not significant (Wilks' λ = 0.814, F (1,19) = 4.36, *p* = .051). Likewise, the eigenvalue for these data (0.229) is low, with a canonical correlation of *r* = 0.43, thereby explaining only 19% of the variance in the dependent variable.

The second discriminant function, which was comprised solely of the eye-tracking component score associated with working memory, correctly classified mTBI with an overall accuracy of 64.7% (sensitivity = 55.6%, specificity = 75%). Based on a pre-test probability of 52.9% in the present sample, the LR+ for this function is 2.22:1 (post-test probability = 71.4%) and the LR– is 0.59:1 (post-test probability = 39.9%). Similar to the first function, the discriminating ability of the second function is not significant (Wilks' λ = 0.805, *F*(1, 15) = 3.63, *p* = .076). Likewise, the eigenvalue for these data (.242) is low, with a canonical correlation of *r* = .441, thereby explaining only 19% of the variance in the dependent variable.

A third linear discriminant analysis was conducted to identify patients with mTBI using the following 13 quantitative measures of tract integrity that demonstrated large effect sizes in the results of the previous ANCOVA analyses: QA and RDI of the FMa, left and right IFO, right MdLF, and left and right SLF, and RDI of the left MdLF. This function correctly classified mTBI with an overall accuracy of 85.7% (sensitivity = 81.8%, specificity = 90%). Based on a pre-test probability of 52.4% in the present sample, the LR+ for this function is 8.18:1 (post-test probability = 90%), and the LR– is 0.20:1 (post-test probability = 18.2%) The eigenvalue for these data (1.104) suggests that the discriminating ability of the function is high, with a canonical correlation of *r* = .724, thereby explaining 53% of the variance in the dependent variable; however, the function's discriminating ability did not reach the threshold for statistical significance (Wilks' λ = 0.475, *F*(13, 7) = 0.59, *p* = .802). The standardized canonical coefficient loadings for each of the 13 variables included in the structural function are reported in

Supplemental Table S1, which can be found in the study's OSF storage directory at https://osf.io/89fpx/.

Relationship Between Structure and Function

Partial correlations were conducted within the mTBI group to assess the relationship of HDFT metrics in each pathway and processing speed, attention, and working memory functions measured with neuropsychological testing and eye-tracking analysis, after controlling for the effects of age, sex, and SEI. The results of all correlational analyses are reported along with squared semipartial correlations in Table 11.

Tract Integrity and Neuropsychological Domain Scores

No relationships were observed between QA or RDI of any pathway and performance on neuropsychological domains of processing speed, attention, or working memory (Table 11). Interestingly, medium-to-large effect sizes indicated that increased gFA of various tracts was associated with lower scores across the neuropsychological domains. Specifically, poorer processing speed performance was associated with increased gFA of the left IFO, poorer performance on the attention domain was associated with increased gFA of the FMa, left IFO, and left SLF, and poorer working memory domain scores were associated with increased gFA of the FMa, left IFO, and right MdLF (Table 11). Fewer associations were observed between tract spread and neuropsychological domain scores, and the direction of these relationships were mixed. Specifically, medium-to-large effect sizes were observed for associations between increased tract spread of the right MdLF and poorer performance on all three neuropsychological domains, whereas large effect sizes were observed for associations between decreased tract spread of the left SLF and poorer performance on all three neuropsychological domains (Table 11).

Tract Integrity and Eye-Tracking Component Scores

In contrast to neuropsychological domain scores, strong relationships, with moderate-to-large effect sizes, were consistently seen between QA and RDI of all pathways and eye-tracking component scores of processing speed, attention, and working memory, after removing the effects of age, sex, and SEI. Specifically, medium effect sizes indicated that lower scores on the processing speed component were associated with increased QA of the FMa, left and right IFO, and left and right MdLF and increased RDI of the FMa, left IFO, left and right MdLF, and left SLF, and medium-to-large effect sizes indicated that lower scores on both the attention and working memory eye-tracking components were associated with increased QA and RDI of all white matter pathways assessed (Table 11). Similar to the associations observed with neuropsychological domain scores, medium-to-large effect sizes indicated that increased gFA was associated with poorer cognitive function when assessed using eye-tracking. Specifically, poorer processing speed was associated with increased gFA in the FMa, right IFO, and right MdLF, poorer attention was associated with increased gFA in the right IFO, left MdLF, and right and left SLF, and poorer working memory was associated with increased gFA of the FMa, left IFO, and right and left MdLF (Table 11). Finally, mixed results were also demonstrated for the relationship between tract spread and cognitive function when measure using eye-tracking. Medium-to-large effect sizes indicated that lower score on the processing speed component was associated with decreased tract spread of the right SLF but increased tract spread of the left MdLF, lower score on the attention component was associated with decreased tract spread of the FMa and right MdLF but increased tract spread of the left and right IFO and left and right SLF, and lower score on the working memory component was associated with decreased tract spread of the right IFO but increased tract spread of the left MdLF (Table 11).

Prediction of Post-Concussive Symptoms

Standardized regression coefficients and squared semipartial correlations were used to evaluate whether functional measures obtained through neuropsychological testing and eye-tracking analysis were able to predict the frequency and severity of PCS in the mTBI group, after controlling for the effects of age, sex, and SEI (Table 12). PCS frequency was operationalized by the number of self-reported symptoms indicated as at least a mild problem on the NSI (M = 12.55, SD = 3.11, range = 9–17), and PCS severity was operationalized as the total score on the RPQ (M = 15.46, SD = 14.58, range = 0–42).

Neither the processing speed nor working memory neuropsychological domain scores predicted PCS frequency or severity; however, improved performance on neuropsychological tests of attention predicted an increase in the frequency ($\beta = 0.42$) and severity ($\beta = 0.44$) of PCS with a medium effect size. Score on the attention component of the eye-tracking, however, did not predict level of self-reported PCS frequency or severity on either measure, but large and medium effect sizes were found for the prediction of increased PCS frequency ($\beta = 0.76$) and severity ($\beta = 0.45$), respectively, by higher score on the working memory component. As with neuropsychological measures of processing speed, there was no meaningful relationship between performance on the processing speed component of the eye-tracking and frequency or severity of PCS in the mTBI group.

Standardized regression coefficients and squared semipartial correlations were also used to evaluate whether HDFT-derived measures of tract integrity were able to predict the frequency and severity of PCS in the mTBI group, after removing the effects of age, sex, and SEI (Table 13).

Neither PCS frequency nor severity was predicted by changes QA of any pathway, and PCS severity was not predicted by changes in RDI of any pathway; however increased RDI of the right SLF predicted a decrease in PCS frequency ($\beta = –0.41$) with a medium effect size. Relative to QA and RDI, gFA and tract spread were better predictors of PCS, where medium-to-large effect sizes demonstrated that increased gFA in the FMa and left MdLF predicts a decrease in PCS frequency ($\beta_{FMa} = –0.63$, $\beta_{Left\ MdLF} = –0.45$), and increased gFA in the FMa and left SLF predicts a decrease in PCS severity ($\beta_{FMa} = –0.57$, $\beta_{Left\ SLF} = –0.52$). In contrast, increased gFA of the right IFO predicts an increase in PCS frequency ($\beta = 0.64$) with a large effect size. Medium-to-large effect sizes also demonstrated that increased tract spread of the right MdLF and right SLF predicts a decrease in PCS frequency ($\beta_{Right\ MdLF} = –0.43$, $\beta_{Right\ SLF} = –0.95$), and increased tract spread of the right SLF also predicts PCS severity ($\beta = –0.66$). In contrast, increased tract spread of the right IFO predicts an increase in both PCS frequency ($\beta = 0.66$) and severity (0.54) with large and medium effect sizes, respectively.

Discussion

Effective treatment and rehabilitation strategies are essential for improving the quality of life of individuals suffering from TBI-related disabilities, and a thorough understanding of the functional and structural impairments that persist chronically and contribute to the experience of persistent PCS is necessary to develop such strategies. While traditional outcome measures, such as neuropsychological testing and structural MRI, are sensitive to severe cognitive impairment and widespread tissue damage commonly seen in moderate-to-severe TBI, measures used in the assessment of recovery from mTBI must be sensitive to *subtle* changes in cognitive function and tissue microstructure that likely result in the persistent PCS experienced by approximately one-

third of this population. For this reason, valid biomarkers are necessary for effective treatment planning and rehabilitation in those with persistent PCS following mTBI.

The literature has begun to focus on alternative measures of functional outcome after mTBI, and studies using eye-tracking analysis have produced promising results (Heitger et al., 2008; Kraus et al., 2007; Kraus et al., 2010). Recent advances in diffusion imaging have paved the way for alternative measures of structural outcome after mTBI, particularly with the advent of HDFT, which has demonstrated a potential for substantial clinical utility in this population (Presson, Beers, et al., 2015; Presson, Krishnaswamy, et al., 2015; Shin, Okonkwo, et al., 2012; Shin et al., 2014; Ware et al., 2019). Despite these recent advances in the field, there are currently no published studies in the literature that have evaluated the sensitivity and specificity of HDFT as a biomarker for mTBI, and no studies have yet to evaluate the utility of eye-tracking analysis or HDFT for predicting persistent PCS after mTBI.

Sensitivity of Outcome Measures

Eye-Tracking Components Versus Neuropsychological Domains

The first aim of the present study was to examine the sensitivity of neuropsychological testing versus eye-tracking analysis for characterizing chronic impairments in attention, working memory, and processing speed in adults with mTBI, and it was hypothesized that eye-tracking analysis would be relatively more sensitive to such impairments and thus better able to classify individuals with mTBI when compared to healthy individuals. The results of between-group comparisons of neuropsychological function were largely as expected, where neuropsychological domain scores were similar between mTBI and healthy control groups; however, a large effect size was demonstrated for the working memory domain, where those with mTBI performed more poorly than the healthy controls. Similarly, mTBI and healthy control groups performed largely

the same across the cognitive components of the eye-tracking analysis, with the exception of the working memory component, where poorer performance was demonstrated by the mTBI group.

The consistent finding that working memory impairments are greatest in this sample are not entirely unexpected, as difficulties with memory are the most commonly reported cognitive symptoms associated with persistent PCS (Zeldovich et al., 2020). Working memory dysfunction often represents a downstream effect of deficits in attention and processing speed that impact the acquisition of information that is to be recalled (Prince & Bruhns, 2017). Some research has demonstrated that individuals with chronic mTBI may perform normally on simple tasks of attention and processing speed, however difficulties often arise on more complex measures of working memory that require the allocation of substantial attentional control (Ozen et al., 2013) and fast processing of incoming information (Ozen & Fernandes, 2012). This is also supported by functional MRI studies that have demonstrated that individuals with mTBI require an increased recruitment of cortical regions to perform the same task as a non-injured individual, suggesting an impairment to network efficiency in mTBI (Chen et al., 2012; McAllister et al., 1999; McAllister et al., 2001).

Overall, the discriminant function results for these functional measures do not support the hypothesis that eye-tracking analysis would be more sensitive to mTBI, relative to neuropsychological testing. While overall classification accuracy was similar between the two functions, neuropsychological domain scores for working memory were more sensitive than working memory component scores derived from eye-tracking analysis, suggesting that the former may have a greater utility in situations where ruling-out mTBI is the primary goal, as it results in fewer false positive results. On the other hand, for situations where ruling-in a history of mTBI is the primary goal, eye-tracking may be the better option, as the working memory

component scores derived from eye-tracking demonstrated relatively greater specificity, thus fewer false negative results. Receiver operating curves (ROC) are shown in Figure 10 for a further examination of the relative sensitivity and specificity of these two working memory measures. While the area under the ROC curve for each measure is quite similar and both demonstrate fair classification accuracy, the larger area under the curve for the eye-tracking working memory component score suggests that it may be a better classifier of mTBI than the neuropsychological domain score overall. Although the current results do not fully support those of Kraus et al. (2007), where eye-tracking was found to be more relatively more sensitive to mTBI than neuropsychological measures, they do support the idea that eye-tracking may be able to classify the subtle neurobehavioral deficits resulting from mTBI than neuropsychological testing, in general.

To determine whether or not the probabilities obtained from these discriminant functions are high or low enough for the measures to be considered clinically useful, several factors must be taken into consideration. Of particular importance is a consider the consequence of inaccurate classification (Kent & Hancock, 2016). It has been suggested that approximately 70% of individuals with co-occurring mental health disability and substance abuse (Corrigan & Deutschle, 2008) and 87% of persons within the county jail population (Slaughter, Fann, & Ehde, 2003) have a history of mTBI. Survivors of mTBI are at a higher risk of psychosocial and psychiatric difficulties that arise from the neurological and social aspects of head trauma. Mental health issues often occur following mTBI, with 15%–40% of survivors suffering from clinical depression (Teasdale & Engberg, 2001) and, compared to the 9% of soldiers returning from Iraq without mTBI, 44% of those with mTBI were also suffering from comorbid PTSD (Hoge et al., 2008). Further, there is evidence that suicide rates are four times as high among survivors of TBI

(Silver et al., 2001), and potentially the highest among survivors of mTBI (Teasdale & Engberg, 2001). These clear links between mTBI, mental illness, substance abuse, and criminal activity, demonstrate the major consequences of under- and misdiagnosis of mTBI. In light of this, the negative post-test probabilities of approximately 33% and 40% for the neuropsychological domain function and the eye-tracking component function, respectively, are much too high to be considered clinically useful *per se*, given the severe consequences associated with misdiagnosis mTBI; however, either of these classifiers may be useful enough to warrant the use of additional classification measures, such as those derived through neuroimaging.

High-Definition Fiber Tractography

The second aim of the present study was to examine the sensitivity of HDFT for characterizing changes to the microstructural integrity of major white matter pathways that underlie cognitive function in adults with chronic mTBI. It was hypothesized that quantitative metrics derived from HDFT would be sensitive to changes in microstructural integrity of the FMa, IFO, MdLF, and SLF and accurately discriminate individuals with mTBI from healthy controls. As expected, HDFT metrics demonstrated disruptions to white matter integrity in all of the examined pathways. The most consistent findings across tracts were moderate-to-large increases in QA and RDI in those with mTBI relative to the healthy controls (Figure 11), which indicates reduced microstructural integrity of the affected pathways. Additionally, decreased gFA was observed in the IFO and right SLF and decreased tract spread was observed in the FMa, MdLF, and left SLF in mTBI.

These results support those of previous studies, in which changes to the microstructural integrity of white matter have been shown to persist long after mTBI (for a review, see Lindsey et al., In press). Recent studies have demonstrated widespread increases in QA when compared

to healthy controls (Arulsamy et al., 2019; Ware et al., 2019), and QA has been shown to decrease in mTBI following 6-weeks of light therapy (Bajaj et al., 2017). Increased QA suggests an increase in the density or amount of diffusion, and such changes have been associated with the mechanical strain of TAI, as the stretching and deformation of axons leads to cytotoxic edema, thereby increasing the ratio of intra- to extra-cellular water concentration and increasing the diffusion density along the axons (Browne et al., 2011; Rosenblum, 2007). While these effects typically occur acutely post-injury, they have been shown to result in chronic neuroinflammatory responses (Simon et al., 2017). Alternatively, increased diffusion density may also indicate an increase in axonal diameter due to demyelination that is associated with axonal disruption, eventually leading to secondary axotomy (Maxwell, 2013).

While this is the first study within the TBI literature to use RDI as a measure of tract integrity, our finding that it is increased chronically in mTBI is in line with the limited research on its clinical utility, where it has been shown to be sensitive to changes in cellularity (Yeh et al., 2017) and the long-term effects of tissue reorganization (Sammartino et al., 2019) following tissue damage. Increased RDI in the chronic post-injury period indicates increased cellularity, which may be related to long-term consequences of TAI, such as glial scarring that results from reactive astrogliosis or changes to cell morphology, including axonal varicosities and neurite beading, which restrict diffusion along the axon (Mac Donald et al., 2007; Sofroniew, 2005; Tu et al., 2016).

Some level of lateralization was present in these results related to QA and RDI, as the largest effect sizes for these measures were almost exclusively seen in the right hemisphere when compared to the homologous tract in the left hemisphere. More extensive damage to the right hemisphere in mTBI is consistently seen in the literature (Munivenkatappa et al., 2017; Narayana

et al., 2015; Presson, Krishnaswamy, et al., 2015; Taber et al., 2015), and this may be due to less densely packed axon branching in the right hemisphere rendering it more vulnerable to the biomechanical forces associated with a head trauma (Klingberg et al., 1999).

Differences in gFA are less prevalent in the current data, and the direction of change is particularly more variable than that which is demonstrated by the other metrics. In general, longitudinal DTI studies suggest that partial normalization of FA and other measures of diffusivity can occur in chronic mTBI (Mayer et al., 2010; Munivenkatappa et al., 2017; Yin et al., 2019), but relatively decreased FA is nonetheless commonly demonstrated in chronic mTBI, particularly within the association tracts (Alhilali et al., 2015; Metting et al., 2013; Veeramuthu et al., 2015; Wada et al., 2012). Furthermore, variations in MD, AD, and RD are often reported in the FMa, IFO, and SLF in the chronic mTBI literature (Cubon et al., 2011; Messe et al., 2012; Munivenkatappa et al., 2017; Wilde et al., 2016), and these changes can drive increases in FA (Alexander et al., 2007; Beaulieu, 2002; Jones et al., 2013; Shenton et al., 2012). The only meaningful difference in gFA presently demonstrated is a moderate decrease in gFA of the left IFO; however, the lack of differences in gFA of other tracts may more likely be a result of low statistical power due to the limited sample size and what is expected to be a relatively small effect size for gFA.

Nonetheless, the overall findings are line with previous research using HDFT, where gFA was not able to capture the subtle changes to microstructural integrity that occur following mTBI as robustly as GQI-derived measures (Presson, Beers, et al., 2015; Presson, Krishnaswamy, et al., 2015; Ware et al., 2019). It has been suggested that diffusivity metrics, such as gFA, are more suitable measures of changes in tract integrity in the presence of pathology, whereas density metrics, such as QA and RDI, are more suitable measures of inter-individuality in

physiological heterogeneity when microstructural integrity is largely intact (Yeh et al., 2016). In chronic mTBI, the extent of neuropathology may be diminished to a point where diffusivity metrics are no longer suitable measures of tract integrity; instead, density-based measures, which are well-equipped to detect to physiological differences in the absence of acute pathology, appear to have greater utility for detecting the subtle microstructural changes that persist chronically in mTBI.

Similarly, tract spread was less robust to chronic changes in tract integrity following mTBI than the measures of diffusion density; however, the pattern demonstrated in differences in tract spread between the two groups is somewhat more in line with expectations than those of gFA. In support of previous research using tract spread (Presson, Beers, et al., 2015; Presson, Krishnaswamy, et al., 2015), consistently lower spread was seen in mTBI when compared to the healthy controls, particularly in the MdLF. Critics of traditional diffusion-weighted imaging methodology have argued that new methods must be developed to account for changes in the morphology of white matter tracts for diffusion-based measures to be more biologically relevant (Jones et al., 2013). Tract spread is largely dependent on the volume, diameter, length, and surface area of the tract and should be used along with diffusion-based metrics as an indicator of tract quality. Atrophy of the gray and white matter and dilation of the ventricles are consistently demonstrated years after mTBI (Maxwell et al., 2010; Mohammed Sulaiman et al., 2011; Zhou et al., 2013), and diffusion-based metrics only utilize a small amount of information about the effects this has on the morphological features of the tract. Furthermore, the size of a white matter tract is relevant to its function (Bigler, 2015), and changes to the size of a tract only occur in the presence of atrophy or plasticity. The pattern of decreased tract spread in the present data

suggests that the quality of the white matter is reduced long after mTBI, likely as a result of atrophy.

The results of the discriminant function analysis support the present hypothesis that HDFT-derived measures of white matter integrity would accurately discriminate between mTBI and healthy controls, as these measures were highly sensitive and specific to mTBI when used together. Furthermore, the negative post-test probability of approximately 18% suggests that HDFT has moderate clinical utility for mTBI classification when used alone (Jaeschke et al., 1994). Given the risks associated with misdiagnosis described above, the use of multiple classifiers may be necessary to move the negative post-test probability across a more acceptable diagnostic threshold, such as a post-test probability of 10% (Straus et al., 2019). If HDFT is used as a follow-up to classification based on either neuropsychological testing or eye-tracking, the post-test probability is shifted to approximately 7%. It is of note, however, that the generalizability of the HDFT function is weak, given the ratio of sample size to the number of variables included (Rencher & Christensen, 2012). For this reason, these results should be interpreted with caution until they are replicated in a larger sample.

Structure-Function Relationship

The third aim of the present study was to evaluate the relationship between measures of processing speed, attention, and working memory obtained from traditional neuropsychological tests versus more recently developed eye-tracking techniques, and the structural integrity of the underlying white matter measured through the use of HDFT. The current findings are in line those of other studies linking the FMa, IFO, MdLF, and SLF to attention (Cabeza et al., 2008; Chechlacz et al., 2015; Makris, Preti, Wassermann, et al., 2013; Sarubbo et al., 2013), working memory (Cabeza et al., 2008; Chung et al., 2019; Golestani et al., 2014), and processing speed

(Menegaux et al., 2017; Niogi et al., 2008; Presson, Beers, et al., 2015; Turken et al., 2008), and support our hypothesis that reduced structural integrity of these tracts would be associated with impairments in attention, working memory, and processing speed, particularly when these functions are measured using eye-tracking analysis. Specifically, we demonstrated that widespread increases in QA and RDI, indicating reduced axonal integrity, are associated with impairments in processing speed, and to a greater extent, with impairments in attention and working memory abilities in chronic mTBI; however, this association is only present when attention, processing speed, and working memory are measured through eye-tracking analysis. While this is the first study to evaluate RDI in relation to cognition, it has been suggested that cellularity is the putative feature linking white matter to working memory capacity, as larger cell densities allow for a larger capacity for working memory (Golestani et al., 2014). Additionally, impairments to aspects of cognitive control, including inattention, have been shown to be related to alterations in gray and white matter density in the parietal and occipital lobes in chronic mTBI (Little et al., 2014) and other neurological populations (Galaburda et al., 2002), as well as atrophy of the fronto-parietal network (Cerami et al., 2015). Such findings may help to explain the relatively stronger associations between increased RDI of the FMa, IFO, and MdLF and increased QA of the SLF, respectively, with attention abilities seen in the present sample of mTBI.

Interestingly, gFA was related to cognitive performance measured using neuropsychological testing and, to a greater extent, eye-tracking analysis, as expected; however, the direction of these associations is opposite to that which was hypothesized. Although gFA is nonspecifically affected by a myriad of pathophysiological changes, including demyelination, axonal loss, edema, and disorganized microstructure, a reduction in anisotropy almost

exclusively indicates some extent of disruption has occurred to the axonal microstructure (Hutchinson et al., 2018). An exception has been shown to occur during glial scar formation, however, which involves the formation of a very dense region of highly oriented astrocytes with elongated morphology, which lack any neuronal projections or vasculature. The glial scar environment restricts the diffusion of water and has been shown to increase anisotropic diffusion in rodent models of TBI (Budde et al., 2011). While its purpose is to protect viable tissue from damaged or toxic tissue, the glial scar tissue ultimately prevents the regeneration of axons and hinders the recovery of neuronal connectivity following injury due to the formation of physical and chemical barriers to axon elongation and the production of growth-inhibitory components (Cregg et al., 2014; Silver & Miller, 2004; Wanner et al., 2008; Zhou et al., 2020). Furthermore, this explanation for increased gFA in relation to poorer cognitive function supports the suggestion that the observed increases in RDI may be due to increased cell-packing density from glial scarring that occurs chronically as a result of reactive astrogliosis (Mac Donald et al., 2007; Sofroniew, 2005). It is important to note that, like DTI-derived FA, HDFT-derived gFA is also impacted by several other factors, including thermal and physiologic noise, motion and eddy-current artifacts, partial volume effects, and crossing fiber orientations; thus, it is recommended that caution is taken when interpreting results related to changes in anisotropy, particularly without additional information from measures of diffusivity (Alexander et al., 2007; Assaf & Pasternak, 2008; Yeh et al., 2013).

Associations were also present between tract spread and performance on neuropsychological and eye-tracking measures of processing speed, attention, and working memory, and a greater number of associations were demonstrated with the eye-tracking component scores; however, the directions of the associations present with tract spread were

largely inconsistent across tracts and between neuropsychological domain versus eye-tracking component scores (Figure 12). Previous research relating tract spread to cognitive function in mTBI found it to be a better indicator of neuropsychological impairment than gFA (Presson, Beers, et al., 2015); however, this is not supported by the present results. It is possible that the more consistent relationship demonstrated between cognitive function and measures of microstructural integrity relative to that with tract spread indicates that, while axons may appear to be intact, they have disrupted microstructural physiology, which is a greater contributor to cognitive dysfunction. It is important to note that the current understanding of the directionality of HDFT-derived measures and their associations with cognitive function are limited, given the novelty of HDFT as a diffusion-weighted imaging technique, particularly within the mTBI literature. Furthermore, it has been said that "with a structure as complex as the human brain, it should come as no surprise that for most brain areas there is not a linear relationship between the size and location of a particular 'lesion' and neuropsychological deficit" (Bigler, 2001, p. 120).

Prediction of Post-Concussive Symptoms

The final two aims of the present study were to determine the utility of (1) eye-tracking analysis versus neuropsychological testing and (2) HDFT for predicting the frequency and severity of persistent PCS experienced by individuals with chronic mTBI. It was hypothesized that both measures of cognitive function would have similar predictive value and that increases in QA and RDI and decreases in gFA and tract spread of each pathway would predict greater frequency and severity of PCS experienced in chronic mTBI.

While our results support the hypothesis that both neuropsychological domain and eye-tracking component scores would have similar predictive value, neither were particularly strong predictors of PCS, and the direction of the relationship was opposite to that which was expected.

Higher scores on the neuropsychological domain of attention predicted a moderate increase in both the frequency and severity of PCS. Similarly, higher scores on the eye-tracking component of working memory predicted a large increase in PCS frequency and a moderate increase in PCS severity. Interestingly, problems with attention and memory were among the most commonly reported in the current mTBI sample (Figure 13). Given the strong associations between demographic factors and the development of PCS (Ryan & Warden, 2003; Zeldovich et al., 2020), it is important to note that these relationships were seen after removing the effects of age, sex, and SEI, the latter of which accounts for educational attainment, occupational status, and socioeconomic status.

We also found that, with the exception of a moderate relationship between RDI of the right SLF and frequency of PCS, no other meaningful relationships were present between QA and RDI and self-reported PCS; however, a distinct pattern of negative associations is seen (Table 13), where increased QA and RDI of all pathways are consistently shown to predict a decrease in the frequency and severity of PCS. This finding neither supports the hypothesis nor is it consistent with findings reported in the literature, where reduced tract integrity is either related to increased symptom reporting after TBI or there is no relationship found between the microstructural integrity of white matter and PCS (for a review, see Khong et al., 2016). Mixed results are demonstrated when gFA and tract spread are used to predict PCS, however. Specifically, our hypothesis was supported by the finding that more extensive PCS is predicted by reduced gFA of the MdLF and reduced tract spread of the MdLF and right SLF; however, similar to the results pertaining to QA and RDI, unexpected relationships are also demonstrated between reduced gFA and tract spread of the IFO and reduced frequency and severity of PCS. Given the inconsistency of these results, along with the unexpected relationships between

cognitive performance and the frequency and severity of PCS in the present mTBI sample, it is likely that some level of symptom exaggeration may have occurred.

There are a number of reasons why symptom exaggeration occurs after mTBI (Iverson, 2006b), including psychological comorbidities, differential interpretation of instructions, lack of attention during assessment, sociocultural differences, lack of insight, and primary and secondary gain. Symptom exaggeration results in inflated scores on measures of PCS and attempts have been made to develop measures of symptom validity. One such measure, the Validity-10 (Vanderploeg et al., 2014), is embedded within the NSI, involves the summing of responses across 10 items (vision problems, hearing problems, noise sensitivity, change in taste or smell, difficulty making decisions, slowed thinking, dizziness, balance problems, coordination difficulties/clumsiness, and nausea), and has been shown to be a useful screening tool for symptom exaggeration (Dretsch et al., 2017; Lange, Brickell, & French, 2015; Lange, Brickell, Lippa, et al., 2015; Sullivan et al., 2016). Based on the results of an analogue simulation study designed to examine the classification accuracy of the Val-10 in subjects who are feigning PCS (Sullivan et al., 2016), a cut-off score of ≥ 10 was suggested to classify probable symptom exaggeration (sensitivity = 75%, specificity = 100%). Based on this cut-off score, 3 of the 11 participants in the present mTBI sample meet the criteria for probable symptom exaggeration.

Upon reviewing the present results, a secondary analysis of the utility of neuropsychological domain scores, eye-tracking component scores, and HDFT as predictors of PCS in chronic mTBI was conducted for exploratory purposes with the effects of probable symptom exaggeration controlled for. The results of this secondary analysis are no longer largely inconsistent with the literature (see Supplemental Tables S2 and S3 at https://osf.io/89fpx/); rather, after controlling for the effects of symptom exaggeration, PCS frequency and severity

was not predicted by neuropsychological domain scores or eye-tracking component scores, with the exception of a moderate relationship present between increased working memory component scores and increased frequency of PCS, which remains to be in opposition to expectations. As for the prediction of PCS by HDFT, after controlling for the effects of symptom exaggeration, the pattern of negative associations between decreased QA and RDI with increased symptom reporting remains; however, these associations have been substantially reduced, with less than 10% of the variance in PCS explained by QA or RDI of a given tract. Similar results are present with gFA and tract spread, with the exception of one moderate association between increased PCS frequency predicted by a decreased in gFA of the right MdLF, which is in line with expectations.

There are various factors related to expectation, awareness, and other psychological conditions that impact the subjective experience of persistent PCS and can lead to symptom exaggeration and overreporting. It is suggested that some individuals who report a high number of symptoms may be more likely to underestimate past problems, akin to the "good-old-days" bias on symptom reporting (Iverson et al., 2010; Lange et al., 2010). Alternatively, longitudinal studies have found that patients who initially viewed their mTBI as being serious, experienced heightened levels of emotional distress, and expected persistent, negative consequences report experiencing a greater number of symptoms in the chronic post-injury period (Whittaker et al., 2007). Persistent PCS has also been shown to occur more commonly in the presence of depression and anxiety than in mTBI alone (Lange et al., 2011), and it has been suggested that PCS severity is related more to a patient's premorbid psychiatric condition than to neuropsychological factors (Meares et al., 2008). Furthermore, mental health has been shown to be a better predictor of cognitive dysfunction than self-reported PCS (Schiehser et al., 2011). The

coexistence of a myriad of other mental health disorders and psychological states with PCS complicates the processes by which PCS can truly be assessed in mTBI. In fact, studies of PCS in healthy adults have demonstrated similar patterns of symptom reporting to those seen in the present and other mTBI samples (Ettenhofer & Barry, 2012; Wang et al., 2006). In particular, healthy individuals with have been shown to report similarly high rates of fatigue, slowed processing speed, difficulties with concentration, and forgetfulness despite having no history of brain trauma. Such findings underscore the complexity of evaluating relationships between objective measures of cognitive function and subjective reports of PCS in mTBI and warrant careful consideration when interpreting related results.

An alternative explanation for the small, yet persistent relationships found been reduced QA and RDI—the measures hitherto shown to be the most sensitive to abnormal microstructure and cognitive dysfunction—and increased PCS symptom frequency and severity in chronic mTBI is a lack of awareness for or denial of functional impairment. Although anosognosia is most commonly reported following severe TBI (Prigatano & Altman, 1990; Robertson & Schmitter-Edgecombe, 2015), it can occur to some extent after mTBI (Bach & David, 2006; Gasquoine, 1992; Hart et al., 2003; Richardson et al., 2015; Sherer et al., 2003). Patients who acknowledge the presence of symptoms are more likely to follow through with restorative therapy and other rehabilitative efforts post-injury (Fleming & Ownsworth, 2006; Halligan, 2006), and self-awareness has been shown to be a critical determinant of vocational and general functional outcome (Ezrachi et al., 1991; Griffen et al., 2011; Vossel et al., 2013; Wise et al., 2005). Anosognosia has historically been conceptualized as a disconnection syndrome, where connections with the frontal and temporal lobe regions responsible for self-awareness are damaged, restricting information flow (Geschwind, 1965), and it is generally reported that no

associations exist between a lack of self-awareness for impairment and performance on neuropsychological tests (Allen & Ruff, 1990; Morton & Barker, 2010; Vuilleumier, 2004). A lack of self-awareness for injury-related impairments may have some role in the present results that suggest that reduced microstructural integrity is related to impairments in cognition yet predictive of fewer and less severe PCS; however, given the relatively uncommon occurrence in mTBI, it is unlikely that this is the only factor at play.

Limitations

There are important limitations that must be considered with interpreting the results of the current study. The greatest limitation is the small sample size, which negatively impacts the statistical power to detect effects and restricts the generalizability of the results. The PCA on eye-tracking measures was particularly affected by the small sample size, and this likely reduced the internal validity of the eye-tracking component scores used in the analysis. Furthermore, the inclusion of three covariates in the majority of analyses further reduced their statistical power. Due to the influence of age, sex, and socioeconomic status on eye-tracking performance, white matter integrity, and persistent PCS seen in the present data and demonstrated in the literature, however, control over the effects of these variables was determined to be necessary. The small sample size also exacerbates the heterogeneity in our participants with mTBI and prevented us from considering the impact that age at injury, TSI, duration of PTA, or other injury-related factors have on the results. Although no injury-related factors demonstrated meaningful associations with the outcome measures, these variables should be controlled for in future studies. An important limitation to the interpretation of the results lies in the lack of data regarding a history of pre- or post-injury neuropsychiatric disturbances. Given the impact of conditions, such as anxiety and depression, on the frequency and severity of PCS and cognitive

functioning, any confounding influence these factors may have on the results related the prediction of PCS by structure or function cannot be ruled out. Finally, the assessments used presently were exclusively cross-sectional, and do not shed light on the functional or structural changes that occur overtime following mTBI. A more complete understanding of the relationship between structure, function, and outcome will require larger mTBI cohorts followed longitudinally. Despite these limitations, the results of this study should be considered as a first step toward understanding the utility of HDFT and eye-tracking for predicting outcome in chronic mTBI.

Conclusions and Future Directions

Mild TBI is not a transient event but a chronic progressive disease that results in long-term physical, cognitive, behavioral, emotional and neurological consequences. It is often suggested in the literature that individuals with mTBI fully recover after the first year post-injury based on normal performance on traditional neuropsychological measures of cognitive function (Dikmen et al., 2017) and a lack of positive neuroimaging findings using conventional measures, despite the high occurrence of self-reported PCS long after mTBI. Considering the high proportion of those with mTBI who complain of long-term symptoms related to poor cognitive function, it is essential that more sensitive measures are used to assess outcome. The present findings suggest that eye-tracking analysis and HDFT may be better suited for assessing outcome in chronic mTBI, particularly when used together; however, additional studies with larger, more homogenous samples are necessary to establish their utility in this domain. Additionally, future research should examine the role white matter integrity may have as a mediator of the relationship between cognitive function and the experience of persistent PCS in chronic mTBI. This is particularly important given the potential utility of HDFT to identify biomarkers

indicative of outcome long after mTBI. It is also important to consider the complex interplay of biopsychosocial factors that influence recovery from mTBI, and more research is needed in this area. While the results of the present study are promising for the utility of advanced measures of functional and structural outcome, the findings should be replicated and further validation of these findings from prospective, large-scale studies is necessary to increase our understanding of the changes in structural and functional connectivity that occur in the brain in chronic mTBI.

References

Abhinav, K., Yeh, F. C., Mansouri, A., Zadeh, G., & Fernandez-Miranda, J. C. (2015). High-definition fiber tractography for the evaluation of perilesional white matter tracts in high-grade glioma surgery. *Neuro Oncology, 17*(9), 1199-1209. https://doi.org/10.1093/neuonc/nov113

Abhinav, K., Yeh, F. C., Pathak, S., Suski, V., Lacomis, D., Friedlander, R. M., & Fernandez-Miranda, J. C. (2014). Advanced diffusion MRI fiber tracking in neurosurgical and neurodegenerative disorders and neuroanatomical studies: A review. *Biochimica et Biophysica Acta, 1842*(11), 2286-2297. https://doi.org/10.1016/j.bbadis.2014.08.002

Alexander, A. L., Hasan, K. M., Lazar, M., Tsuruda, J. S., & Parker, D. L. (2001). Analysis of partial volume effects in diffusion-tensor MRI. *Magnetic Resonance in Medicine, 45*, 770-780.

Alexander, A. L., Lee, J. E., Lazar, M., & Field, A. S. (2007). Diffusion tensor imaging of the brain. *The Journal of the American Society for Experimental NeuroTherapeutics, 4*, 316-329.

Alhilali, L. M., Delic, J. A., Gumus, S., & Fakhran, S. (2015). Evaluation of white matter injury patterns underlying neuropsychiatric symptoms after mild traumatic brain injury. *Radiology, 277*(3), 793-800. https://doi.org/10.1148/radiol.2015142974

Allen, C. C., & Ruff, R. M. (1990). Self-rating versus neuropsychological performance of moderate versus severe head-injured patients. *Brain Injury, 4*(1), 7-17. https://doi.org/10.3109/02699059009026143

Andersson, J. L. R., & Sotiropoulos, S. N. (2016). An integrated approach to correction for off-resonance effects and subject movement in diffusion MR imaging. *Neuroimage, 125*, 1063-1078. https://doi.org/10.1016/j.neuroimage.2015.10.019

Arulsamy, A., Corrigan, F., & Collins-Praino, L. E. (2019). Cognitive and neuropsychiatric impairments vary as a function of injury severity at 12 months post-experimental diffuse traumatic brain injury: Implications for dementia development. *Behavioral Brain Research, 365*, 66-76. https://doi.org/10.1016/j.bbr.2019.02.045

Asikainen, I., Nybo, T., Muller, K., Sarna, S., & Kaste, M. (1999). Speed performance and long-term functional and vocational outcome in a group of young patients with moderate or severe traumatic brain injury. *European Journal of Neurology, 6*(2), 179-185.

Assaf, Y., & Pasternak, O. (2008). Diffusion tensor imaging (DTI)-based white matter mapping in brain research: A review. *Journal of Molecular Neuroscience, 34*(1), 51-61. https://doi.org/10.1007/s12031-007-0029-0

Avants, B. B., Tustison, N. J., Song, G., Cook, P. A., Klein, A., & Gee, J. C. (2011). A reproducible evaluation of ANTs similarity metric performance in brain image registration. *Neuroimage, 54*(3), 2033-2044. https://doi.org/10.1016/j.neuroimage.2010.09.025

Bach, L. J., & David, A. S. (2006). Self-awareness after acquired and traumatic brain injury. *Neuropsychological Rehabilitation, 16*(4), 397-414. https://doi.org/10.1080/09602010500412830

Bajaj, S., Vanuk, J. R., Smith, R., Dailey, N. S., & Killgore, W. D. S. (2017). Blue-light therapy following mild traumatic brain injury: Effects on white matter water diffusion in the brain. *Frontiers in Neurology, 8*, Article 616. https://doi.org/10.3389/fneur.2017.00616

Basser, P. J., Mattiello, J., & LeBihan, D. (1994). Estimation of the effective self-diffusion tensor from the NMR spin echo. *Journal of Magnetic Resononance, Series B, 103*(3), 247-254.

Basser, P. J., Pajevic, S., Pierpaoli, C., Duda, J., & Aldroubi, A. (2000). In vivo fiber tractography using DT-MRI data. *Magnetic Resonance in Medicine, 44*(4), 625-632. https://doi.org/10.1002/1522-2594

Bate, A. J., Mathias, J. L., & Crawford, J. R. (2001). Performance on the Test of Everday Attention and standard tests of attention following severe traumatic brain injury. *The Clinical Neuropsychologist, 15*(3), 405-422.

Beaulieu, C. (2002). The basis of anisotropic water diffusion in the nervous system - A technical review. *NMR Biomedicine, 15*(7-8), 435-455. https://doi.org/10.1002/nbm.782

Beaulieu, C., Does, M. D., Snyder, R. E., & Allen, P. S. (1996). Changes in water diffusion due to Wallerian degeneration in peripheral nerve. *Magnetic Resonance in Medicine, 36*(4), 627-631.

Benjamini, Y., & Hochberg, Y. (1995). Controlling the False Discovery Rate: A practical and powerful approach to multiple testing. *Journal of the Royal Statistical Society. Series B (Methodological), 57*(1), 289-300.

Bigler, E. D. (2001). Distinguished Neuropsychologist Award Lecture 1999. The lesion(s) in traumatic brain injury: Implications for clinical neuropsychology. *Applied Neuropsychology: Adult, 16*(2), 95-131.

Bigler, E. D. (2008). Neuropsychology and clinical neuroscience of persistent post-concussive syndrome. *Journal of the International Neuropsychological Society, 14*(1), 1-22. https://doi.org/10.1017/S135561770808017X

Bigler, E. D. (2013). Neuroimaging biomarkers in mild traumatic brain injury (mTBI). *Neuropsychology Review, 23*(3), 169-209. https://doi.org/10.1007/s11065-013-9237-2

Bigler, E. D. (2015). Structural Image analysis of the brain in neuropsychology using magnetic resonance imaging (MRI) techniques. *Neuropsychology Review, 25*(3), 224-249. https://doi.org/10.1007/s11065-015-9290-0

Bigler, E. D., & Maxwell, W. L. (2011). Neuroimaging and neuropathology of TBI. *NeuroRehabilitation, 28*(2), 63-74. https://doi.org/10.3233/NRE-2011-0633

Bigler, E. D., & Maxwell, W. L. (2012). Neuropathology of mild traumatic brain injury: Relationship to neuroimaging findings. *Brain Imaging and Behavior, 6*(2), 108-136. https://doi.org/10.1007/s11682-011-9145-0

Bigler, E. D., & Stern, Y. (2015). Traumatic brain injury and reserve. *Handbook of Clinical Neurology, 128*, 691-710. https://doi.org/10.1016/B978-0-444-63521-1.00043-1

Bigler, E. D., & Wilde, E. A. (2010). Quantitative neuroimaging and the prediction of rehabilitation outcome following traumatic brain injury. *Frontiers in Human Neuroscience, 4*, Article 228. https://doi.org/10.3389/fnhum.2010.00228

Borgaro, S. R., Prigatano, G. P., Kwasnica, C., & Rexer, J. L. (2003). Cognitive and affective sequelae in complicated and uncomplicated mild traumatic brain injury. *Brain Injury, 17*(3), 189-198. https://doi.org/10.1080/0269905021000013183

Bouix, S., Pasternak, O., Rathi, Y., Pelavin, P. E., Zafonte, R., & Shenton, M. E. (2013). Increased gray matter diffusion anisotropy in patients with persistent post-concussive symptoms following mild traumatic brain injury. *PLoS One, 8*(6), Article e66205. https://doi.org/10.1371/journal.pone.0066205

Breusch, T. S., & Pagan, A. R. (1979). A simple test for heteroscedasticity and random cefficient variation. *Econometrica, 47*(5), 1287-1294.

Brown, A. W., Malec, J. F., McClelland, R. L., Diehl, N. N., Englander, J., & Cifu, D. X. (2005). Clinical elements that predict outcome after traumatic brain injury: A prospective multicenter recursive partitioning (decision-tree) analysis. *Journal of Neurotrauma, 22*(10), 1040-1051. https://doi.org/10.1089/neu.2005.22.1040

Brown, J. (1958). Some tests of the decay theory of immediate memory. *Quarterly Journal of Experimental Psychology, 10*, 12-21.

Browne, K. D., Chen, X. H., Meaney, D. F., & Smith, D. H. (2011). Mild traumatic brain injury and diffuse axonal injury in swine. *Journal of Neurotrauma, 28*(9), 1747-1755. https://doi.org/10.1089/neu.2011.1913

Budde, M. D., Janes, L., Gold, E., Turtzo, L. C., & Frank, J. A. (2011). The contribution of gliosis to diffusion tensor anisotropy and tractography following traumatic brain injury: Validation in the rat using Fourier analysis of stained tissue sections. *Brain, 134*(Pt 8), 2248-2260. https://doi.org/10.1093/brain/awr161

Cabeza, R., Ciaramelli, E., Olson, I. R., & Moscovitch, M. (2008). The parietal cortex and episodic memory: An attentional account. *Nature Reviews Neuroscience, 9*(8), 613-625. https://doi.org/10.1038/nrn2459

Carlozzi, N. E., Grech, J., & Tulsky, D. S. (2013). Memory functioning in individuals with traumatic brain injury: An examination of the Wechsler Memory Scale-Fourth Edition (WMS-IV). *Journal of Clinical and Experimental Neuropsychology, 35*(9), 906-914. https://doi.org/10.1080/13803395.2013.833178

Carlozzi, N. E., Kirsch, N. L., Kisala, P. A., & Tulsky, D. S. (2015). An examination of the Wechsler Adult Intelligence Scales (WAIS-IV) in individuals with complicated mild, moderate and severe traumatic brain injury (TBI). *The Clinical Neuropsychologist, 29*(1), 21-37.

Carroll, L. J., Cassidy, J. D., Holm, L., Kraus, J., Coronado, V. G., & members of the WHO Collaborating Centre Task Force on Mild Traumatic Brain Injury. (2004). Methodological issues and research recommendations for mild traumatic brain injury: The WHO Collaborating Centre Task Force on Mild Traumatic Brain Injury. *Journal of Rehabilitation Medicine* (Suppl 43), 113-125. https://doi.org/10.1080/16501960410023877

Catani, M., & de Schotten, M. T. (2012). *Atlas of human brain connections.* Oxford University Press.

Catani, M., & Thiebaut de Schotten, M. (2008). A diffusion tensor imaging tractography atlas for virtual in vivo dissections. *Cortex, 44*(8), 1105-1132. https://doi.org/10.1016/j.cortex.2008.05.004

CDC National Center for Injury Prevention and Control (2017). *Rates of TBI-related emergency department visits, hospitalizations, and deaths - United States, 2001 – 2010*. https://data.cdc.gov/Traumatic-Brain-Injury-/Rates-of-TBI-related-Emergency-Department-Visits-H/45um-c62r

Cerami, C., Crespi, C., Della Rosa, P. A., Dodich, A., Marcone, A., Magnani, G., Coppi, E., Falini, A., Cappa, S. F., & Perani, D. (2015). Brain changes within the visuo-spatial attentional network in posterior cortical atrophy. *Journal of Alzheimers Disease, 43*(2), 385-395. https://doi.org/10.3233/JAD-141275

Chan, R. C. (2000). Attentional deficits in patients with closed head injury: A further study to the discriminative validity of the test of everyday attention. *Brain Injury, 14*(3), 227-236.

Chan, R. C., Hoosain, R., Lee, T. M., Fan, Y. W., & Fong, D. (2003). Are there sub-types of attentional deficits in patients with persisting post-concussive symptoms? A cluster analytical study. *Brain Injury, 17*(2), 131-148.

Chechlacz, M., Gillebert, C. R., Vangkilde, S. A., Petersen, A., & Humphreys, G. W. (2015). Structural variability within frontoparietal networks and individual differences in attentional functions: An approach using the theory of visual attention. *Journal of Neuroscience, 35*(30), 10647-10658. https://doi.org/10.1523/JNEUROSCI.0210-15.2015

Chen, C. J., Wu, C. H., Liao, Y. P., Hsu, H. L., Tseng, Y. C., Liu, H. L., & Chiu, W. T. (2012). Working memory in patients with mild traumatic brain injury: Functional MR imaging analysis. *Radiology, 264*(3), 844-851. https://doi.org/10.1148/radiol.12112154

Chmura, J., Presson, N., Benso, S., Puccio, A. M., Fissel, K., Hachey, R., Braun, E., Okonkwo, D. O., & Schneider, W. (2015). A high-definition fiber tracking report for patients with traumatic brain injury and their doctors. *Military Medicine, 180*(Suppl 3), 122-134. https://doi.org/10.7205/MILMED-D-14-00441

Chung, S., Wang, X., Fieremans, E., Rath, J. F., Amorapanth, P., Foo, F. A., Morton, C. J., Novikov, D. S., Flanagan, S. R., & Lui, Y. W. (2019). Altered relationship between working memory and brain microstructure after mild traumatic brain injury. *American Journal of Neuroradiology, 40*(9), 1438-1444. https://doi.org/10.3174/ajnr.A6146

Cicerone, K. D., & Azulay, J. (2002). Diagnostic utility of attention measures in postconcussion syndrome. *Clinical Neuropsychology, 16*(3), 280-289. https://doi.org/10.1076/clin.16.3.280.13849

Cicerone, K. D., & Kalmar, K. (1995). Persistent postconcussion syndrome: The structure of subjective complaints after mild traumatic brain injury. *Journal of Head Trauma Rehabilitation, 10*, 1-17. https://doi.org/10.1097/00001199-199510030-00002

Cifu, D. X., Wares, J. R., Hoke, K. W., Wetzel, P. A., Gitchel, G., & Carne, W. (2015). Differential eye movements in mild traumatic brain injury versus normal controls. *Journal of Head Trauma Rehabilitation, 30*(1), 21-28. https://doi.org/10.1097/HTR.0000000000000036

Ciuffreda, K. J., Ludlam, D. P., Thiagarajan, P., Yadav, N. K., & Capo-Aponte, J. (2014). Proposed objective visual system biomarkers for mild traumatic brain injury. *Military Medicine, 179*(11), 1212-1217. https://doi.org/10.7205/MILMED-D-14-00059

Cohen, J. (1988). *Statistical power analysis for the behavioral sciences* (2nd ed.). Lawrence Erlbaum.

Cohen, J. (1992). A power primer. *Psychological Bulliten, 112*(1), 155-159.

Conner, A. K., Briggs, R. G., Rahimi, M., Sali, G., Baker, C. M., Burks, J. D., Glenn, C. A., Battiste, J. D., & Sughrue, M. E. (2018). A connectomic atlas of the human cerebrum–Chapter 12: Tractographic description of the middle longitudinal fasciculus. *Operational Neurosurgery (Hagerstown), 15* (Suppl 1), S429-S435. https://doi.org/10.1093/ons/opy266

Conturo, T. E., Lori, N. F., Cull, T. S., Akbudak, E., Snyder, A. Z., Shimony, J. S., McKinstry, R. C., Burton, H., & Raichle, M. E. (1999). Tracking neuronal fiber pathways in the living human brain. *Proceedings of the National Academy of Sciences USA, 96*(18), 10422-10427. https://doi.org/10.1073/pnas.96.18.10422

Cook, R. D., & Weisberg, S. (1983). Diagnostics for heteroscedasticity in regression. *Biometrika, 70*(1), 1-10.

Corrigan, J. D., & Deutschle Jr, J. J. (2008). The presence and impact of traumatic brain injury among clients in treatment for co-occurring mental illness and substance abuse. *Brain Injury, 22*(3), 223-231. https://doi.org/10.1080/02699050801938967

Crawford, J. R., Obonsawin, M. C., & Allan, K. M. (1998). PASAT and components of WAIS-R performance: Convergent and divergent validity. *Neuropsychological Rehabilitation, 8*(3), 255-272.

Cregg, J. M., DePaul, M. A., Filous, A. R., Lang, B. T., Tran, A., & Silver, J. (2014). Functional regeneration beyond the glial scar. *Exp Neurol, 253*, 197-207. https://doi.org/10.1016/j.expneurol.2013.12.024

Cristofori, I., & Levin, H. S. (2015). Traumatic brain injury and cognition. In J. Grafman & A. M. Salazar (Eds.), *Handbook of clinical neurology* (Vol. 128, pp. 579-611). Elsevier.

Cubon, V. A., Putukian, M., Boyer, C., & Dettwiler, A. (2011). A diffusion tensor imaging study on the white matter skeleton in individuals with sports-related concussion. *Journal of Neurotrauma, 28*(2), 189-201. https://doi.org/10.1089/neu.2010.1430

de Schotten, M. T., Dell'Acqua, F., Forkel, S. J., Simmons, A., Vergani, F., Murphy, D. G. M., & Catani, M. (2012). A lateralized brain network for visuospatial attention. *Nature Proceedings*. https://doi.org/10.1038/npre.2011.5549.1

Dean, P. J., Sato, J. R., Vieira, G., McNamara, A., & Sterr, A. (2015). Multimodal imaging of mild traumatic brain injury and persistent postconcussion syndrome. *Brain and Behavior, 5*(1), 45-61. https://doi.org/10.1002/brb3.292

Dick, A. S., & Tremblay, P. (2012). Beyond the arcuate fasciculus: consensus and controversy in the connectional anatomy of language. *Brain, 135*(12), 3529-3550. https://doi.org/10.1093/brain/aws222

Dikmen, S., Machamer, J., & Temkin, N. (2017). Mild traumatic brain injury: Longitudinal study of cognition, functional status, and post-traumatic symptoms. *Journal of Neurotrauma, 34*(8), 1524-1530. https://doi.org/10.1089/neu.2016.4618

Dikmen, S. S., Corrigan, J. D., Levin, H. S., Machamer, J., Stiers, W., & Weisskopf, M. G. (2009). Cognitive outcome following traumatic brain injury. *Journal of Head Trauma Rehabilitation, 24*(6), 430-438.

Dikmen, S. S., Machamer, J. E., Powell, J. M., & Temkin, N. R. (2003). Outcome 3 to 5 years after moderate to severe traumatic brain injury. *Archives of Physical Medicine & Rehabilitation, 84*(10), 1449-1457.

Diwakar, M., Harrington, D. L., Maruta, J., Ghajar, J., El-Gabalawy, F., Muzzatti, L., Corbetta, M., Huang, M. X., & Lee, R. R. (2015). Filling in the gaps: Anticipatory control of eye movements in chronic mild traumatic brain injury. *Neuroimage: Clinical, 8*, 210-223. https://doi.org/10.1016/j.nicl.2015.04.011

Dretsch, M. N., Williams, K., Staver, T., Grammer, G., Bleiberg, J., DeGraba, T., & Lange, R. T. (2017). Evaluating the clinical utility of the Validity-10 for detecting amplified symptom reporting for patients with mild traumatic brain injury and comorbid psychological health conditions. *Applied Neuropsychology: Adult, 24*(4), 376-380. https://doi.org/10.1080/23279095.2016.1220947

Emanuelson, I., Andersson Holmkvist, E., Björklund, R., & Stålhammar, D. (2003). Quality of life and post-concussion symptoms in adults after mild traumatic brain injury: A

population-based study in Western Sweden. *Acta Neurologica Scandinavica, 108*(5), 332-338. https://doi.org/10.1046/j.1600-0404.2003.00155.x

Englander, J., Hall, K., Stimpson, T., & Chaffin, S. (1992). Mild traumatic brain injury in an insured population: Subjective complaints and return to employment. *Brain Injury, 6*(2), 161-166. https://doi.org/10.3109/02699059209029654

Ettenhofer, M. L., & Barry, D. M. (2012). A comparison of long-term postconcussive symptoms between university students with and without a history of mild traumatic brain injury or orthopedic injury. *Journal of the International Neuropsychological Society, 18*(3), 451-460. https://doi.org/10.1017/S1355617711001895

Eyres, S., Carey, A., Gilworth, G., Neumann, V., & Tennant, A. (2005). Construct validity and reliability of the Rivermead Post-Concussion Symptoms Questionnaire. *Clinical Rehabilitation, 19*(8), 878-887. https://doi.org/10.1191/0269215505cr905oa

Ezrachi, O., Ben-Yishay, Y., Kay, T., Diller, L., & Rattok, J. (1991). Predicting employment in traumatic brain injury following neuropsychological rehabilitation. *Journal of Head Trauma Rehabilitation, 6*, 71-84.

Faul, F., Erdfelder, E., Buchner, A., & Lang, A. G. (2009). Statistical power analyses using G*Power 3.1: Tests for correlation and regression analyses. *Behavior Research Methods, 41*(4), 1149-1160. https://doi.org/10.3758/BRM.41.4.1149

Faul, F., Erdfelder, E., Lang, A. G., & Buchner, A. (2007). G*Power 3: A flexible statistical power analysis program for the social, behavioral, and biomedical sciences. *Behavior Research Methods, 39*(2), 175-191.

Faul, M., & Coronado, V. (2015). Epidemiology of traumatic brain injury. *Handbook of Clinical Neurology, 127*, 3-13. https://doi.org/10.1016/B978-0-444-52892-6.00001-5

Felmingham, K. L., Baguley, I. J., & Green, A. M. (2004). Effects of diffuse axonal injury on speed of information processing following severe traumatic brain injury. *Neuropsychology, 18*(3), 564-571. https://doi.org/10.1037/0894-4105.18.3.564

Fernandez-Miranda, J. C., Pathak, S., Engh, J., Jarbo, K., Verstynen, T., Yeh, F. C., Wang, Y., Mintz, A., Boada, F., Schneider, W., & Friedlander, R. (2012). High-definition fiber tractography of the human brain: Neuroanatomical validation and neurosurgical applications. *Neurosurgery, 71*(2), 430-453. https://doi.org/10.1227/NEU.0b013e3182592faa

Fijalkowski, R. J., Ellingson, B. M., Stemper, B. D., Yoganandan, N., Gennarelli, T. A., & Pintar, F. A. (2006). Interface parameters of impact-induced mild traumatic brain injury. *Biomedical Scientific Instruments, 42*, 108-113.

Finnanger, T. G., Skandsen, T., Andersson, S., Lydersen, S., Vik, A., & Indredavik, M. (2013). Differentiated patterns of cognitive impairment 12 months after severe and moderate traumatic brain injury. *Brain Injury, 27*(13-14), 1606-1616. https://doi.org/10.3109/02699052.2013.831127

Fleming, J. M., & Ownsworth, T. (2006). A review of awareness interventions in brain injury rehabilitation. *Neuropsychological Rehabilitation, 16*(4), 474-500. https://doi.org/10.1080/09602010500505518

Frieden, T. R., Houry, D., & Baldwin, G. (2015). *Report to Congress on traumatic brain injury in the United States: Epidemiology and rehabilitation*. https://www.cdc.gov/traumaticbraininjury/pdf/tbi_report_to_congress_epi_and_rehab-a.pdf

Fritzsche, K. H., Laun, F. B., Meinzer, H. P., & Stieltjes, B. (2010). Opportunities and pitfalls in the quantification of fiber integrity: What can we gain from Q-ball imaging? *Neuroimage, 51*(1), 242-251. https://doi.org/10.1016/j.neuroimage.2010.02.007

Fukushima, K., Fukushima, J., Warabi, T., & Barnes, G. R. (2013). Cognitive processes involved in smooth pursuit eye movements: behavioral evidence, neural substrate and clinical correlation. *Frontiers in Systems Neuroscience, 7*(4), 1-28. https://doi.org/doi.org/10.3389/fnsys.2013.00004

Funahashi, S. (2014). Saccade-related activity in the prefrontal cortex: Its role in eye movement control and cognitive functions. *Frontiers in Integrational Neuroscience, 8*, Article 54. https://doi.org/10.3389/fnint.2014.00054

Galaburda, A. M., Holinger, D. P., Bellugi, U., & Sherman, G. F. (2002). Williams syndrome: neuronal size and neuronal-packing density in primary visual cortex. *Archives of Neurology, 59*(9), 1461-1467. https://doi.org/10.1001/archneur.59.9.1461

Gasquoine, P. G. (1992). Affective state and awareness of sensory and cognitive effects after closed head injury. *Neuropsychology, 6*, 187-196.

Geschwind, N. (1965). Disconnection syndromes in animals and man. *Brain, 88*, 237-294.

Geurts, B. H., Andriessen, T. M., Goraj, B. M., & Vos, P. E. (2012). The reliability of magnetic resonance imaging in traumatic brain injury lesion detection. *Brain Injury, 26*(12), 1439-1450. https://doi.org/10.3109/02699052.2012.694563

Glasser, M. F., Sotiropoulos, S. N., Wilson, J. A., Coalson, T. S., Fischl, B., Andersson, J. L., Xu, J., Jbabdi, S., Webster, M., Polimeni, J. R., Van Essen, D. C., Jenkinson, M., & Consortium, W. U.-M. H. (2013). The minimal preprocessing pipelines for the Human

Connectome Project. *Neuroimage, 80*, 105-124. https://doi.org/10.1016/j.neuroimage.2013.04.127

Golestani, A. M., Miles, L., Babb, J., Castellanos, F. X., Malaspina, D., & Lazar, M. (2014). Constrained by our connections: White matter's key role in interindividual variability in visual working memory capacity. *Journal of Neuroscience, 34*(45), 14913-14918. https://doi.org/10.1523/JNEUROSCI.2317-14.2014

Green, R. E., Melo, B., Christensen, B., Ngo, L. A., Monette, G., & Bradbury, C. (2008). Measuring premorbid IQ in traumatic brain injury: An examination of the validity of the Wechsler Test of Adult Reading (WTAR). *Journal of Clinical and Experimental Neuropsychology, 30*(2), 163-172. https://doi.org/10.1080/13803390701300524

Griffen, J. A., Rapport, L. J., Bryer, R. C., Bieliauskas, L. A., & Burt, C. (2011). Awareness of deficits and on-road driving performance. *Clinical Neuropsychology, 25*(7), 1158-1178. https://doi.org/10.1080/13854046.2011.609841

Gronwall, D., & Wrightson, P. (1974). Recovery after minor head injury (Letter). *Lancet, 2*(7894), 1452.

Gronwall, D., & Wrightson, P. (1981). Memory and information processing capacity after closed head injury. *Journal of Neurology, Neurosurgery, and Psychiatry, 44*(10), 889-895.

Gronwall, D. M. (1977). Paced Auditory Serial-Addition Task: A measure of recovery from concussion. *Perceptual Motor Skills, 44*(2), 367-373. https://doi.org/10.2466/pms.1977.44.2.367

Guise, C., Fernandes, M. M., Nobrega, J. M., Pathak, S., Schneider, W., & Fangueiro, R. (2016). Hollow polypropylene yarns as a biomimetic brain phantom for the validation of high-

definition fiber tractography imaging. *ACS Applied Material Interfaces, 8*(44), 29960-29967. https://doi.org/10.1021/acsami.6b09809

Halligan, P. W. (2006). Awareness and knowing: implications for rehabilitation. *Neuropsychological Rehabilitation, 16*(4), 456-473. https://doi.org/10.1080/09602010500309762

Hart, T., Novack, T. A., Temkin, N., Barber, J., Dikmen, S. S., Diaz-Arrastia, R., Ricker, J., Hesdorffer, D. C., Jallo, J., Hsu, N. H., & Zafonte, R. (2016). Duration of posttraumatic amnesia predicts neuropsychological and global outcome in complicated mild traumatic brain injury. *Journal of Head Trauma Rehabilitation, 31*(6), E1-E9. https://doi.org/10.1097/HTR.0000000000000210

Hart, T., Whyte, J., Polansky, M., Millis, S., Hammond, F. M., Sherer, M., Bushnik, T., Hanks, R., & Kreutzer, J. (2003). Concordance of patient and family report of neurobehavioral symptoms at 1 year after traumatic brain injury. *Archives of Physical Medicine & Rehabilitation, 84*(2), 204-213. https://doi.org/10.1053/apmr.2003.50019

Hawryluk, G. W., & Manley, G. T. (2015). Classification of traumatic brain injury: Past, present, and future. *Handbook of Clinical Neurology, 127*, 15-21. https://doi.org/10.1016/B978-0-444-52892-6.00002-7

Heaton, R. K., Miller, S. W., Taylor, M. J., & Grant, I. (2004). *Revised comprehensive norms for an expanded Halstead-Reitan battery: Demographically adjusted neuropsychological norms for African American and Caucasian adults.* PAR Inc.

Hedges, L. V. (1981). Distribution theory for Glass's estimator of effect size and related estimators. *Journal of Educational Statistics, 6*(2), 107-128.

Heitger, M. H., Anderson, T. J., & Jones, R. D. (2002). Saccade sequences as markers for cerebral dysfunction following mild closed head injury. In J. Hyönä, D. P. Munoz, W. Heide, & R. Radach (Eds.), *Progress in brain research* (Vol. 140, pp. 433-448). Elsevier.

Heitger, M. H., Jones, R. D., & Anderson, T. J. (2008, August 20-24). *A new approach to predicting postconcussion syndrome after mild traumatic brain injury based upon eye movement function.* Paper presented at the 30th Annual International IEEE EMBS Conference, Vancouver, British Columbia, Canada.

Hessen, E., & Nestvold, K. (2009). Indicators of complicated mild TBI predict MMPI-2 scores after 23 years. *Brain Injury, 23*(3), 234-242. https://doi.org/10.1080/02699050902748349

Hessen, E., Nestvold, K., & Sundet, K. (2006). Neuropsychological function in a group of patients 25 years after sustaining minor head injuries as children and adolescents. *Scandinavian Journal of Psychology, 47*(4), 245-251. https://doi.org/10.1111/j.1467-9450.2006.00514.x

Hilgetag, C. C., Burns, G. A., O'Neill, M. A., Scannell, J. W., & Young, M. P. (2000). Anatomical connectivity defines the organization of clusters of cortical areas in the macaque monkey and the cat. *Philosophical Transactions of the Royal Society B: Biological Sciences, 355*(1393), 91-110. https://doi.org/10.1098/rstb.2000.0551

Hoge, C. W., McGurk, D., Thomas, J. L., Cox, A. L., Engel, C. C., & Castro, C. A. (2008). Mild traumatic brain injury in US soldiers returning from Iraq. *New England Journal of Medicine*, *358*(5), 453-463. https://doi.org/10.1056/NEJMoa072972

Holdnack, J. A., Schoenberg, M. R., Lange, R. T., & Iverson, G. L. (2013). Predicting premorbid ability for WAIS-IV, WMS-IV, and WASI-II. In J. A. Holdnack, L. Drozdick, L. G.

Weiss, & G. L. Iverson (Eds.), *WAIS-IV, WMS-IV, and ACS: Advanced Clinical Interpretation* (pp. 217-278). Academic Press.

Holm, S. (1979). A simple sequentially rejective multiple test procedure. *Scandinavian Journal of Statistics, 6*, 65-70.

Huang, H., Zhang, J., van Zijl, P. C., & Mori, S. (2004). Analysis of noise effects on DTI-based tractography using the brute-force and multi-ROI approach. *Magnetic Resonance in Medicine, 52*(3), 559-565. https://doi.org/10.1002/mrm.20147

Hui, E. S., Cheung, M. M., Chan, K. C., & Wu, E. X. (2010). B-value dependence of DTI quantitation and sensitivity in detecting neural tissue changes. *Neuroimage, 49*(3), 2366-2374. https://doi.org/10.1016/j.neuroimage.2009.10.022

Huisman, T. A., Loenneker, T., Barta, G., Bellemann, M. E., Hennig, J., Fischer, J. E., & Il'yasov, K. A. (2006). Quantitative diffusion tensor MR imaging of the brain: field strength related variance of apparent diffusion coefficient (ADC) and fractional anisotropy (FA) scalars. *Europeanj Radiology, 16*(8), 1651-1658. https://doi.org/10.1007/s00330-006-0175-8

Hulkower, M. B., Poliak, D. B., Rosenbaum, S. B., Zimmerman, M. E., & Lipton, M. L. (2013). A decade of DTI in traumatic brain injury: 10 years and 100 articles later. *American Journal of Neuroradiology, 34*(11), 2064-2074. https://doi.org/10.3174/ajnr.A3395

Hunt, A. W., Mah, K., Reed, N., Engel, L., & Keightley, M. (2015). Oculomotor-based vision assessment in mild traumatic brain injury: A systematic review. *Journal of Head Trauma Rehabilitation, 31*(4), 252-261. https://doi.org/0.1097/HTR.0000000000000174

Hutchinson, E. B., Schwerin, S. C., Avram, A. V., Juliano, S. L., & Pierpaoli, C. (2018). Diffusion MRI and the detection of alterations following traumatic brain injury. *Journal of Neuroscience Research, 96*(4), 612-625. https://doi.org/10.1002/jnr.24065

Hutton, S. B. (2008). Cognitive control of saccadic eye movements. *Brain and Cognition, 68*(3), 327-340. https://doi.org/10.1016/j.bandc.2008.08.021

Irimia, A., Chambers, M. C., Alger, J. R., Filippou, M., Prastawa, M. W., Wang, B., Hovda, D. A., Gerig, G., Toga, A. W., Kikinis, R., Vespa, P. M., & Van Horn, J. D. (2011). Comparison of acute and chronic traumatic brain injury using semi-automatic multimodal segmentation of MR volumes. *Journal of Neurotrauma, 28*(11), 2287-2306. https://doi.org/10.1089/neu.2011.1920

Iverson, G. L. (2006a). Complicated vs uncomplicated mild traumatic brain injury: Acute neuropsychological outcome. *Brain Injury, 20*(13-14), 1335-1344. https://doi.org/10.1080/02699050601082156

Iverson, G. L. (2006b). Misdiagnosis of the persistent postconcussion syndrome in patients with depression. *Archives of Clinical Neuropsychology, 21*(4), 303-310. https://doi.org/10.1016/j.acn.2005.12.008

Iverson, G. L., & Lange, R. T. (2003). Examination of "postconcussion-like" symptoms in a healthy sample. *Applied Neuropsychology, 10*(3), 137-144. https://doi.org/10.1207/S15324826AN1003_02

Iverson, G. L., Lange, R. T., Brooks, B. L., & Rennison, V. L. (2010). "Good old days" bias following mild traumatic brain injury. *Clinical Neuropsychology, 24*(1), 17-37. https://doi.org/10.1080/13854040903190797

Iverson, G. L., Zasler, N. D., & Lange, R. T. (Eds.). (2007). *Post-concussion disorder*. Demos.

Jaeschke, R., Guyatt, G. H., & Sackett, D. L. (1994). Users' guides to the medical literature. III. How to use an article about a diagnostic test. What are the results and will they help me in caring for my patients? The Evidence-Based Medicine Working Group. *JAMA, 271*(9), 703-707. https://doi.org/10.1001/jama.271.9.703

Jansons, K. M., & Alexander, D. C. (2003). Persistent angular structure: New insights from diffusion MRI data. Dummy version. *Information Processing in Medical Imaging, 18*, 672-683.

Jarbo, K., Verstynen, T., & Schneider, W. (2012). In vivo quantification of global connectivity in the human corpus callosum. *Neuroimage, 59*(3), 1988-1996. https://doi.org/10.1016/j.neuroimage.2011.09.056

Jenkinson, M., Beckmann, C. F., Behrens, T. E., Woolrich, M. W., & Smith, S. M. (2012). FSL. *Neuroimage, 62*(2), 782-790. https://doi.org/10.1016/j.neuroimage.2011.09.015

Johansen-Berg, H., & Rushworth, M. F. (2009). Using diffusion imaging to study human connectional anatomy. *Annual Review of Neuroscience, 32*(3), 75-94.

Jones, D. K., Knosche, T. R., & Turner, R. (2013). White matter integrity, fiber count, and other fallacies: The do's and don'ts of diffusion MRI. *Neuroimage, 73*, 239-254. https://doi.org/10.1016/j.neuroimage.2012.06.081

Jung, J., Cloutman, L. L., Binney, R. J., & Lambon Ralph, M. A. (2016). The structural connectivity of higher order association cortices reflects human functional brain networks. *Cortex*. https://doi.org/10.1016/j.cortex.2016.08.011

Kalyvas, A., Koutsarnakis, C., Komaitis, S., Karavasilis, E., Christidi, F., Skandalakis, G. P., Liouta, E., Papakonstantinou, O., Kelekis, N., Duffau, H., & Stranjalis, G. (2020). Mapping the human middle longitudinal fasciculus through a focused anatomo-imaging

study: Shifting the paradigm of its segmentation and connectivity pattern. *Brain Structure and Function, 225*(1), 85-119. https://doi.org/10.1007/s00429-019-01987-6

Kashluba, S., Hanks, R. A., Casey, J. E., & Millis, S. R. (2008). Neuropsychologic and functional outcome after complicated mild traumatic brain injury. *Archives of Physical Medicine & Rehabilitation, 89*(5), 904-911. https://doi.org/10.1016/j.apmr.2007.12.029

Katz, D. I., & Alexander, M. P. (1994). Traumatic brain injury. Predicting course of recovery and outcome for patients admitted to rehabilitation. *Archives of Neurology, 51*(7), 661-670. https://doi.org/10.1001/archneur.1994.00540190041013

Kent, P., & Hancock, M. J. (2016). Interpretation of dichotomous outcomes: Sensitivity, specificity, likelihood ratios, and pre-test and post-test probability. *Journal of Physiotherapy, 62*(4), 231-233. https://doi.org/10.1016/j.jphys.2016.08.008

Kersel, D. A., Marsh, N. V., Havill, J. H., & Sleigh, J. W. (2001). Neuropsychological functioning during the year following severe traumatic brain injury. *Brain Injury, 15*(4), 283-296.

Khong, E., Odenwald, N., Hashim, E., & Cusimano, M. D. (2016). Diffusion tensor imaging findings in post-concussion syndrome patients after mild traumatic brain injury: A systematic review. *Frontiers in Neurology, 7*, Article 156. https://doi.org/10.3389/fneur.2016.00156

King, N. S., Crawford, S., Wenden, F. J., Moss, N. E., & Wade, D. T. (1995). The Rivermead Post Concussion Symptoms Questionnaire: A measure of symptoms commonly experienced after head injury and its reliability. *Journal of Neurology, 242*(9), 587-592. https://doi.org/10.1007/bf00868811

King, P. R., Donnelly, K. T., Donnelly, J. P., Dunnam, M., Warner, G., Kittleson, C. J., Bradshaw, C. B., Alt, M., & Meier, S. T. (2012). Psychometric study of the Neurobehavioral Symptom Inventory. *Journal of Rehabilitation Research and Development, 49*(6), 879-888. https://doi.org/10.1682/jrrd.2011.03.0051

Klingberg, T., Vaidya, C. J., Gabrieli, J. D., Moseley, M. E., & Hedehus, M. (1999). Myelination and organization of the frontal white matter in children: A diffusion tensor MRI study. *Neuroreport, 10*(13), 2817-2821. https://doi.org/10.1097/00001756-199909090-00022

Kotter, R., & Sommer, F. T. (2000). Global relationship between anatomical connectivity and activity propagation in the cerebral cortex. *Philosophical Transactions of the Royal Society B: Biological Sciences, 355*(1393), 127-134. https://doi.org/10.1098/rstb.2000.0553

Kraus, M. F., Little, D. M., Donnel, A. J., Reilly, J. L., Simonian, N., & Sweeney, J. A. (2007). Oculomotor function in chronic traumatic brain injury. *Cognitive Behavioral Neurology, 20*(3), 170-178.

Kraus, M. F., Little, D. M., Wojtowicz, S. M., & Sweeney, J. A. (2010). Procedural learning impairments identified via predictive saccades in chronic traumatic brain injury. *Cognitive Behavioral Neurology, 23*(4), 210-217.

Krishna, V., Yeh, F. C., & Sammartino, F. (2019). Restricted diffusion imaging: A novel algorithm to study micro-structural changes after brain injury [Abstract]. *Journal of Neurotrauma*, A-64. https://doi.org/10.1089/neu.2019.29100.abstracts

Kuo, L. W., Chen, J. H., Wedeen, V. J., & Tseng, W. Y. (2008). Optimization of diffusion spectrum imaging and Q-ball imaging on clinical MRI system. *Neuroimage, 41*(1), 7-18. https://doi.org/10.1016/j.neuroimage.2008.02.016

Lange, R. T., Brickell, T. A., & French, L. M. (2015). Examination of the Mild Brain Injury Atypical Symptom Scale and the Validity-10 Scale to detect symptom exaggeration in US military service members. *Journal of Clinical and Experimental Neuropsychology, 37*(3), 325-337. https://doi.org/10.1080/13803395.2015.1013021

Lange, R. T., Brickell, T. A., Lippa, S. M., & French, L. M. (2015). Clinical utility of the Neurobehavioral Symptom Inventory validity scales to screen for symptom exaggeration following traumatic brain injury. *Journal of Clinical and Experimental Neuropsychology, 37*(8), 853-862. https://doi.org/10.1080/13803395.2015.1064864

Lange, R. T., Iverson, G. L., & Franzen, M. D. (2009). Neuropsychological functioning following complicated vs. uncomplicated mild traumatic brain injury. *Brain Injury, 23*(2), 83-91. https://doi.org/10.1080/02699050802635281

Lange, R. T., Iverson, G. L., & Rose, A. (2010). Post-concussion symptom reporting and the "good-old-days" bias following mild traumatic brain injury. *Archives of Clinical Neuropsychology, 25*(5), 442-450. https://doi.org/10.1093/arclin/acq031

Lange, R. T., Iverson, G. L., & Rose, A. (2011). Depression strongly influences postconcussion symptom reporting following mild traumatic brain injury. *Journal of Head Trauma Rehabilitation, 26*(2), 127-137. https://doi.org/10.1097/HTR.0b013e3181e4622a

Lannsjo, M., Borg, J., Bjorklund, G., Af Geijerstam, J. L., & Lundgren-Nilsson, A. (2011). Internal construct validity of the Rivermead Post-Concussion Symptoms Questionnaire. *Journal of Rehabilitation Medicine, 43*(11), 997-1002. https://doi.org/10.2340/16501977-0875

Lazar, M. (2017). Working memory: How important is white matter? *The Neuroscientist, 23*(2), 197-210. https://doi.org/10.1177/1073858416634298

Lencer, R., & Trillenberg, P. (2008). Neurophysiology and neuroanatomy of smooth pursuit in humans. *Brain and Cognition, 68*(3), 219-228. https://doi.org/10.1016/j.bandc.2008.08.013

Levin, H. S., Hanten, G., Roberson, G., Li, X., Ewing-Cobbs, L., Dennis, M., Chapman, S., Max, J. E., Hunter, J., Schachar, R., Luerssen, T. G., & Swank, P. (2008). Prediction of cognitive sequelae based on abnormal computed tomography findings in children following mild traumatic brain injury. *Journal of Neurosurgery: Pediatrics, 1*(6), 461-470. https://doi.org/10.3171/PED/2008/1/6/461

Levine, B., Fujiwara, E., O'Connor, C., Richard, N., Kovacevic, N., Mandic, M., Restagno, A., Easdon, C., Robertson, I. H., Graham, S. J., Cheung, G., Gao, F., Schwartz, M. L., & Black, S. E. (2006). In vivo characterization of traumatic brain injury neuropathology with structural and functional neuroimaging. *Journal of Neurotrauma, 23*(10), 1396-1411. https://doi.org/10.1089/neu.2006.23.1396

Lindsey, H. M., Hodges, C. B., Greer, K. M., Wilde, E. A., & Merkley, T. (In press). Diffusion-weighted imaging in mild traumatic brain injury: A systematic review of the literature. *Neuropsychology Review*.

Little, D. M., Geary, E. K., Moynihan, M., Alexander, A., Pennington, M., Glang, P., Schulze, E. T., Dretsch, M., Pacifico, A., Davis, M. L., Stevens, A. B., & Huang, J. H. (2014). Imaging chronic traumatic brain injury as a risk factor for neurodegeneration. *Alzheimers Dementia, 10*(Suppl 3), S188-195. https://doi.org/10.1016/j.jalz.2014.04.002

Liversedge, S. P., & Findlay, J. M. (2000). Saccadic eye movements and cognition. *Trends in Cognitive Sciences, 4*(1), 6-14.

Mac Donald, C. L., Dikranian, K., Song, S. K., Bayly, P. V., Holtzman, D. M., & Brody, D. L. (2007). Detection of traumatic axonal injury with diffusion tensor imaging in a mouse model of traumatic brain injury. *Experimental Neurology, 205*(1), 116-131. https://doi.org/10.1016/j.expneurol.2007.01.035

Maier-Hein, K. H., Neher, P. F., Houde, J. C., Cote, M. A., Garyfallidis, E., Zhong, J., Chamberland, M., Yeh, F. C., Lin, Y. C., Ji, Q., Reddick, W. E., Glass, J. O., Chen, D. Q., Feng, Y., Gao, C., Wu, Y., Ma, J., He, R., Li, Q., . . . (2017). The challenge of mapping the human connectome based on diffusion tractography. *Nature Communications, 8*(1), 1349. https://doi.org/10.1038/s41467-017-01285-x

Makris, N., Kennedy, D. N., McInerney, S., Sorensen, A. G., Wang, R., Caviness, V. S., Jr., & Pandya, D. N. (2005). Segmentation of subcomponents within the superior longitudinal fascicle in humans: A quantitative, in vivo, DT-MRI study. *Cerebral Cortex, 15*(6), 854-869. https://doi.org/10.1093/cercor/bhh186

Makris, N., Papadimitriou, G. M., Kaiser, J. R., Sorg, S., Kennedy, D. N., & Pandya, D. N. (2009). Delineation of the middle longitudinal fascicle in humans: A quantitative, in vivo, DT-MRI study. *Cerebral Cortex, 19*(4), 777-785. https://doi.org/10.1093/cercor/bhn124

Makris, N., Preti, M. G., Asami, T., Pelavin, P., Campbell, B., Papadimitriou, G. M., Kaiser, J., Baselli, G., Westin, C. F., Shenton, M. E., & Kubicki, M. (2013). Human middle longitudinal fascicle: Variations in patterns of anatomical connections. *Brain Struct Funct, 218*(4), 951-968. https://doi.org/10.1007/s00429-012-0441-2

Makris, N., Preti, M. G., Wassermann, D., Rathi, Y., Papadimitriou, G. M., Yergatian, C., Dickerson, B. C., Shenton, M. E., & Kubicki, M. (2013). Human middle longitudinal fascicle: Segregation and behavioral-clinical implications of two distinct fiber

connections linking temporal pole and superior temporal gyrus with the angular gyrus or superior parietal lobule using multi-tensor tractography. *Brain Imaging and Behavior, 7*(3), 335-352. https://doi.org/10.1007/s11682-013-9235-2

Makris, N., Zhu, A., Papadimitriou, G. M., Mouradian, P., Ng, I., Scaccianoce, E., Baselli, G., Baglio, F., Shenton, M. E., Rathi, Y., Dickerson, B., Yeterian, E., & Kubicki, M. (2017). Mapping temporo-parietal and temporo-occipital cortico-cortical connections of the human middle longitudinal fascicle in subject-specific, probabilistic, and stereotaxic Talairach spaces. *Brain Imaging and Behavior, 11*(5), 1258-1277. https://doi.org/10.1007/s11682-016-9589-3

Maldonado, I. L., de Champfleur, N. M., Velut, S., Destrieux, C., Zemmoura, I., & Duffau, H. (2013). Evidence of a middle longitudinal fasciculus in the human brain from fiber dissection. *Journal of Anatomy, 223*(1), 38-45. https://doi.org/10.1111/joa.12055

Martino, J., Brogna, C., Robles, S. G., Vergani, F., & Duffau, H. (2010). Anatomic dissection of the inferior fronto-occipital fasciculus revisited in the lights of brain stimulation data. *Cortex, 46*(5), 691-699. https://doi.org/10.1016/j.cortex.2009.07.015

Maruta, J., Heaton, K. J., Maule, A. L., & Ghajar, J. (2014). Predictive visual tracking: Specificity in mild traumatic brain injury and sleep deprivation. *Military Medicine, 179*(6), 619-625. https://doi.org/10.7205/MILMED-D-13-00420

Maruta, J., Lee, S. W., Jacobs, E. F., & Ghajar, J. (2010). A unified science of concussion. *Annals of the New York Academy of Sciences, 1208*, 58-66. https://doi.org/10.1111/j.1749-6632.2010.05695.x

Maruta, J., Palacios, E. M., Zimmerman, R. D., Ghajar, J., & Mukherjee, P. (2016). Chronic post-concussion neurocognitive deficits I. Relationship with white matter integrity.

Frontiers in Human Neuroscience, 10, Article 35. https://doi.org/10.3389/fnhum.2016.00035

Maruta, J., Spielman, L. A., Yarusi, B. B., Wang, Y., Silver, J. M., & Ghajar, J. (2016). Chronic post-concussion neurocognitive deficits II. Relationship with persistent symptoms. *Frontiers in Human Neuroscience, 10*, Article 45. https://doi.org/10.3389/fnhum.2016.00045

Maruta, J., Suh, M., Niogi, S. N., Mukherjee, P., & Ghajar, J. (2010). Visual tracking synchronization as a metric for concussion screening. *Journal of Head Trauma Rehabilitation, 25*(4), 293-305.

Maruta, J., Tong, J., Lee, S. W., Iqbal, Z., Schonberger, A., & Ghajar, J. (2012, May 4). *EYE-TRAC: Monitoring attention and utility for mTBI.* Proceedings of The International Society for Optics and Photonics (volume 8371), Sensing Technologies for Global Health, Military Medicine, Disaster Response, and Environmental Monitoring II; and Biometric Technology for Human Identification IX, 83710L. https://doi.org/10.1117/12.927790

Mathias, J. L., Bowden, S. C., Bigler, E. D., & Rosenfeld, J. V. (2007). Is performance on the Wechsler test of adult reading affected by traumatic brain injury? *British Journal of Clinical Psychology, 46*(4), 457-466. https://doi.org/10.1348/014466507X190197

Maxwell, W. L. (2013). Damage to myelin and oligodendrocytes: A role in chronic outcomes following traumatic brain injury? *Brain Science, 3*(3), 1374-1394. https://doi.org/10.3390/brainsci3031374

Maxwell, W. L., MacKinnon, M. A., Stewart, J. E., & Graham, D. I. (2010). Stereology of cerebral cortex after traumatic brain injury matched to the Glasgow outcome score. *Brain, 133*(1), 139-160. https://doi.org/10.1093/brain/awp264

Mayer, A. R., Ling, J., Mannell, M. V., Gasparovic, C., Phillips, J. P., Doezema, D., Reichard, R., & Yeo, R. A. (2010). A prospective diffusion tensor imaging study in mild traumatic brain injury. *Neurology, 74*(8), 643-650. https://doi.org/10.1212/WNL.0b013e3181d0ccdd

McAllister, T. W., Saykin, A. J., Flashman, L. A., Sparling, M. B., Johnson, S. C., Guerin, S. J., Mamourian, A. C., Weaver, J. B., & Yanofsky, N. (1999). Brain activation during working memory 1 month after mild traumatic brain injury: A functional MRI study. *Neurology, 53*(6), 1300-1308. https://doi.org/10.1212/wnl.53.6.1300

McAllister, T. W., Sparling, M. B., Flashman, L. A., Guerin, S. J., Mamourian, A. C., & Saykin, A. J. (2001). Differential working memory load effects after mild traumatic brain injury. *Neuroimage, 14*(5), 1004-1012. https://doi.org/10.1006/nimg.2001.0899

McCaffrey, R. J., Krahula, M. M., Heimberg, R. G., Keller, K. E., & Purcell, M. J. (1988). A comparison of the Trail Making Test, Symbol Digit Modalities Test, and the Hooper Visual Organization Test in an inpatient substance abuse population. *Archives of Clinical Neuropsychology, 3*(2), 181-187.

McDonald, C. M., Jaffe, K. M., Fay, G. C., Polissar, N. L., Martin, K. M., Liao, S., & Rivara, J. B. (1994). Comparison of indices of traumatic brain injury severity as predictors of neurobehavioral outcome in children. *Archives of Physical Medicine & Rehabilitation, 75*(3), 328-337. https://doi.org/10.1016/0003-9993(94)90038-8

McDowell, J. E., Dyckman, K. A., Austin, B. P., & Clementz, B. A. (2008). Neurophysiology and neuroanatomy of reflexive and volitional saccades: Evidence from studies of humans. *Brain and Cognition, 68*(3), 255-270. https://doi.org/10.1016/j.bandc.2008.08.016

McInerney, R. J. (2004). *The Victoria Computerized Adaptation of the Paced Auditory Serial Addition Task (PASAT)* [Computer software]. University of Victoria. http://www.mcinerney.ca/pasat.html

McKee, A. C., & Daneshvar, D. H. (2015). The neuropathology of traumatic brain injury. In J. Grafman & A. M. Salazar (Eds.), *Handbook of Clinical Neurology* (Vol. 127, pp. 45-66). Elsevier.

Meares, S., Shores, E. A., Taylor, A. J., Batchelor, J., Bryant, R. A., Baguley, I. J., Chapman, J., Gurka, J., Dawson, K., Capon, L., & Marosszeky, J. E. (2008). Mild traumatic brain injury does not predict acute postconcussion syndrome. *Journal of Neurology, Neurosurgery, and Psychiatry, 79*(3), 300-306. https://doi.org/10.1136/jnnp.2007.126565

Menegaux, A., Meng, C., Neitzel, J., Bauml, J. G., Muller, H. J., Bartmann, P., Wolke, D., Wohlschlager, A. M., Finke, K., & Sorg, C. (2017). Impaired visual short-term memory capacity is distinctively associated with structural connectivity of the posterior thalamic radiation and the splenium of the corpus callosum in preterm-born adults. *Neuroimage, 150*, 68-76. https://doi.org/10.1016/j.neuroimage.2017.02.017

Messe, A., Caplain, S., Pelegrini-Issac, M., Blancho, S., Montreuil, M., Levy, R., Lehericy, S., & Benali, H. (2012). Structural integrity and postconcussion syndrome in mild traumatic brain injury patients. *Brain Imaging and Behavior, 6*(2), 283-292. https://doi.org/10.1007/s11682-012-9159-2

Mesulam, M. M. (1998). From sensation to cognition. *Brain, 121*(6), 1013-1052.

Mesulam, M. M. (2000). Brain, mind, and the evolution of connectivity. *Brain and Cognition, 42*(1), 4-6. https://doi.org/10.1006/brcg.1999.1145

Meterko, M., Baker, E., Stolzmann, K. L., Hendricks, A. M., Cicerone, K. D., & Lew, H. L. (2012). Psychometric assessment of the Neurobehavioral Symptom Inventory-22: The structure of persistent postconcussive symptoms following deployment-related mild traumatic brain injury among veterans. *Journal of Head Trauma Rehabilitation, 27*(1), 55-62. https://doi.org/10.1097/HTR.0b013e318230fb17

Metting, Z., Cerliani, L., Rodiger, L. A., & van der Naalt, J. (2013). Pathophysiological concepts in mild traumatic brain injury: Diffusion tensor imaging related to acute perfusion CT imaging. *PLoS One, 8*(5), Article e64461. https://doi.org/10.1371/journal.pone.0064461

Mild Traumatic Brain Injury Committee of the Head Injury Interdisciplinary Special Interest Group of the American Congress of Rehabilitation Medicine. (1993). Definition of mild traumatic brain injury. *Journal of Head Trauma Rehabilitation, 8*(3), 86-87.

Miles, W. R. (1929). Ocular dominance demonstrated by unconscious sighting. *Journal of Experimental Psychology, 12*(2), 113-126.

Millis, S. R., Rosenthal, M., Novack, T. A., Sherer, M., Nick, T. G., Kreutzer, J. S., High, W. M., & Ricker, J. H. (2001). Long-term neuropsychological outcome after traumatic brain injury. *Journal of Head Trauma Rehabilitation, 16*(4), 343-355.

Mohammed Sulaiman, A., Denman, N., Buchanan, S., Porter, N., Vijay, S., Sharpe, R., Graham, D. I., & Maxwell, W. L. (2011). Stereology and ultrastructure of chronic phase axonal and cell soma pathology in stretch-injured central nerve fibers. *Journal of Neurotrauma, 28*(3), 383-400. https://doi.org/10.1089/neu.2010.1707

Morgan, S. F., & Wheelock, G. D. (1992). Digit Symbol and Symbol Digit Modalities Test: Are they directly interchangeable? *Neuropsychology, 4*(6), 327-330.

Mori, S., Crain, B. J., Chacko, V. P., & van Zijl, P. C. (1999). Three-dimensional tracking of axonal projections in the brain by magnetic resonance imaging. *Annals of Neurology, 45*(2), 265-269.

Mori, S., & Zhang, J. (2006). Principles of diffusion tensor imaging and its applications to basic neuroscience research. *Neuron, 51*(5), 527-539. https://doi.org/10.1016/j.neuron.2006.08.012

Morton, N., & Barker, L. (2010). The contribution of injury severity, executive and implicit functions to awareness of deficits after traumatic brain injury (TBI). *Journal of the International Neuropsychological Society, 16*(6), 1089-1098. https://doi.org/10.1017/S1355617710000925

Munivenkatappa, A., Bhagavatula, I. D., Shukla, D. P., & Rajeswaran, J. (2017). A longitudinal study of changes in diffusion tensor value and their association with cognitive sequelae among patients with mild head injury. *Journal of Neurosurgical Science, 61*(3), 283-290. https://doi.org/10.23736/S0390-5616.16.03112-X

Nakase-Thompson, R., Sherer, M., Yablon, S. A., Nick, T. G., & Trzepacz, P. T. (2004). Acute confusion following traumatic brain injury. *Brain Injury, 18*(2), 131-142. https://doi.org/10.1080/0269905031000149542

Narayana, P. A., Yu, X., Hasan, K. M., Wilde, E. A., Levin, H. S., Hunter, J. V., Miller, E. R., Patel, V. K., Robertson, C. S., & McCarthy, J. J. (2015). Multi-modal MRI of mild traumatic brain injury. *Neuroimage: Clinical, 7*, 87-97. https://doi.org/10.1016/j.nicl.2014.07.010

Ni, H., Kavcic, V., Zhu, T., Ekholm, S., & Zhong, J. (2006). Effects of number of diffusion gradient directions on derived diffusion tensor imaging indices in human brain. *American Journal of Neuroradiology, 27*(8), 1776-1781.

Niogi, S. N., Mukherjee, P., Ghajar, J., Johnson, C. E., Kolster, R., Lee, H., Suh, M., Zimmerman, R. D., Manley, G. T., & McCandliss, B. D. (2008). Structural dissociation of attentional control and memory in adults with and without mild traumatic brain injury. *Brain, 131*(12), 3209-3221. https://doi.org/10.1093/brain/awn247

Oishi, K., Faria, A., van Zijl, P. C. M., & Mori, S. (2011). *MRI Atlas of Human White Matter* (2nd ed.). Elsevier.

Oouchi, H., Yamada, K., Sakai, K., Kizu, O., Kubota, T., Ito, H., & Nishimura, T. (2007). Diffusion anisotropy measurement of brain white matter is affected by voxel size: Underestimation occurs in areas with crossing fibers. *American Journal of Neuroradiology, 28*(6), 1102-1106. https://doi.org/10.3174/ajnr.A0488

Ozen, L. J., & Fernandes, M. A. (2012). Slowing down after a mild traumatic brain injury: A strategy to improve cognitive task performance? *Archives of Clinical Neuropsychology, 27*(1), 85-100. https://doi.org/10.1093/arclin/acr087

Ozen, L. J., Itier, R. J., Preston, F. F., & Fernandes, M. A. (2013). Long-term working memory deficits after concussion: Electrophysiological evidence. *Brain Injury, 27*(11), 1244-1255. https://doi.org/10.3109/02699052.2013.804207

Palacios, E. M., Fernandez-Espejo, D., Junque, C., Sanchez-Carrion, R., Roig, T., Tormos, J. M., Bargallo, N., & Vendrell, P. (2011). Diffusion tensor imaging differences relate to memory deficits in diffuse traumatic brain injury. *BMC Neurology, 11*, 24. https://doi.org/10.1186/1471-2377-11-24

Pathak, S. K. (2015). *Improved quantification of connectivity in human brain mapping* [Dissertation, University of Pittsburgh]. Pittsburgh, PA.

Pearson. (2009a). *Advanced Clinical Solutions for WAIS-IV and WMS-IV: Administration and Scoring Manual*. Author.

Pearson. (2009b). *Advanced Clinical Solutions for WAIS-IV and WMS-IV: Clinical and Interpretive Manual*. Author.

Peterson, L. R., & Peterson, M. J. (1959). Short-term retention of individual verbal items. *Journal of Experimental Psychology, 58*(3), 193-198.

Petrides, M., & Pandya, D. N. (1984). Projections to the frontal cortex from the posterior parietal region in the rhesus monkey. *Journal of Comparative Neurology, 228*(1), 105-116. https://doi.org/10.1002/cne.902280110

Pierpaoli, C., & Basser, P. J. (1996). Toward a quantitative assessment of diffusion anisotropy. *Magnetic Resonance in Medicine, 36*, 893-906.

Pierpaoli, C., Jezzard, P., Basser, P. J., Barnett, A., & Di Chiro, G. (1996). Diffusion tensor MR imaging of the human brain. *Radiology, 201*, 637-648.

Ponsford, J., & Kinsella, G. (1992). Attentional deficits following closed-head injury. *Journal of Clinical and Experimental Neuropsychology, 14*(5), 822-838. https://doi.org/10.1080/01688639208402865

Potter, S., Leigh, E., Wade, D., & Fleminger, S. (2006). The Rivermead Post Concussion Symptoms Questionnaire: A confirmatory factor analysis. *Journal of Neurology, 253*(12), 1603-1614. https://doi.org/10.1007/s00415-006-0275-z

Povlishock, J. T., & Katz, D. I. (2005). Update of neuropathology and neurological recovery after traumatic brain injury. *Journal of Head Trauma Rehabilitation, 20*(1), 76-94.

Presson, N., Beers, S. R., Morrow, L., Wagener, L. M., Bird, W. A., Van Eman, G., Krishnaswamy, D., Penderville, J., Borrasso, A. J., Benso, S., Puccio, A., Fissell, C., Okonkwo, D. O., & Schneider, W. (2015). An exploratory analysis linking neuropsychological testing to quantification of tractography using high definition fiber tracking (HDFT) in military TBI. *Brain Imaging and Behavior, 9*(3), 484-499. https://doi.org/10.1007/s11682-015-9386-4

Presson, N., Krishnaswamy, D., Wagener, L., Bird, W., Jarbo, K., Pathak, S., Puccio, A. M., Borasso, A., Benso, S., Okonkwo, D. O., & Schneider, W. (2015). Quantifying white matter structural integrity with high-definition fiber tracking in traumatic brain injury. *Military Medicine, 180*(Suppl 3), 109-121. https://doi.org/10.7205/MILMED-D-14-00413

Prigatano, G. P., & Altman, I. M. (1990). Impaired awareness of behavioral limitations after traumatic brain injury. *Archives of Physical Medicine & Rehabilitation, 71*(13), 1058-1064.

Prigatano, G. P., & Fordyce, D. J. (1986). The neuropsychological rehabilitation program at Presbyterian hospital, Oklahoma City. In B. P. Uzzell & Y. Gross (Eds.), *Neuropsychological rehabilitation after brain injury* (pp. 96-118). Johns Hopkins University Press.

Prigatano, G. P., Pepping, M., & Klonoff, P. (1986). Cognitive, personality, and psychosocial factors in the neuropsychological assessment of brain-injured patients. In B. P. Uzzell & Y. Gross (Eds.), *Clinical Neuropsychology of Intervention* (pp. 135-166). Springer.

Prince, C., & Bruhns, M. E. (2017). Evaluation and treatment of mild traumatic brain injury: the role of neuropsychology. *Brain Science, 7*(8). https://doi.org/10.3390/brainsci7080105

Rabinowitz, A. R., & Levin, H. S. (2014). Cognitive sequelae of traumatic brain injury. *Psychiatric Clinics of North America, 37*(1), 1-11. https://doi.org/10.1016/j.psc.2013.11.004

Ramnani, N. (2012). Frontal lobe and posterior parietal contributions to the cortico-cerebellar system. *Cerebellum, 11*(2), 366-383. https://doi.org/10.1007/s12311-011-0272-3

Rassovsky, Y., Levi, Y., Agranov, E., Sela-Kaufman, M., Sverdlik, A., & Vakil, E. (2015). Predicting long-term outcome following traumatic brain injury (TBI). *Journal of Clinical and Experimental Neuropsychology, 37*(4), 354-366. https://doi.org/10.1080/13803395.2015.1015498

Rassovsky, Y., Satz, P., Alfano, M. S., Light, R. K., Zaucha, K., McArthur, D. L., & Hovda, D. (2006). Functional outcome in TBI II: Verbal memory and information processing speed mediators. *Journal of Clinical and Experimental Neuropsychology, 28*(4), 581-591. https://doi.org/10.1080/13803390500434474

Rees, P. M. (2003). Contemporary issues in mild traumatic brain injury. *Archives of Physical Medicine & Rehabilitation, 84*(12), 1885-1894. https://doi.org/10.1016/j.apmr.2003.03.001

Reese, C. S., Suhr, J. A., & Riddle, T. L. (2012). Exploration of malingering indices in the Wechsler Adult Intelligence Scale – Digit Span subtest. *Archives of Clinical Neuropsychology, 27*(2), 176-181.

Reilly, J. L., Lencer, R., Bishop, J. R., Keedy, S., & Sweeney, J. A. (2008). Pharmacological treatment effects on eye movement control. *Brain and Cognition, 68*(3), 415-435. https://doi.org/10.1016/j.bandc.2008.08.026

Reitan, R. M., & Wolfson, D. (1985). *The Halstead-Reitan Neuropsychological Test Battery*. Neuropsychology Press.

Reitan, R. M., & Wolfson, D. (1993). *The Halstead-Reitan Neuropsychological Battery: Theory and Clinical Implications*. Neuropsychology Press.

Rencher, A. C., & Christensen, W. F. (2012). *Methods of multivariate analysis* (3rd ed.). John Wiley & Sons.

Richardson, C., McKay, A., & Ponsford, J. L. (2015). Factors influencing self-awareness following traumatic brain injury. *Journal of Head Trauma Rehabilitation, 30*(2), E43-54. https://doi.org/10.1097/HTR.0000000000000048

Rijken, B. F., Leemans, A., Lucas, Y., van Montfort, K., Mathijssen, I. M., & Lequin, M. H. (2015). Diffusion tensor imaging and fiber tractography in children with craniosynostosis syndromes. *American Journal of Neuroradiology, 36*(8), 1558-1564. https://doi.org/10.3174/ajnr.A4301

Robertson, K., & Schmitter-Edgecombe, M. (2015). Self-awareness and traumatic brain injury outcome. *Brain Injury, 29*(7-8), 848-858. https://doi.org/10.3109/02699052.2015.1005135

Rohling, M. L., Binder, L. M., Demakis, G. J., Larrabee, G. J., Ploetz, D. M., & Langhinrichsen-Rohling, J. (2011). A meta-analysis of neuropsychological outcome after mild traumatic brain injury: Re-analyses and reconsiderations of Binder et al. (1997), Frencham et al. (2005), and Pertab et al. (2009). *Clinical Neuropsychology, 25*(4), 608-623. https://doi.org/10.1080/13854046.2011.565076

Rosenblum, W. I. (2007). Cytotoxic edema: Monitoring its magnitude and contribution to brain swelling. *J Neuropathol Exp Neurol, 66*(9), 771-778. https://doi.org/10.1097/nen.0b013e3181461965

Ruff, R. M., & Allen, C. C. (1996). *Ruff 2 & 7 Selective Attention Test professional manual.* PAR.

Ryan, L. M., & Warden, D. L. (2003). Post concussion syndrome. *International Review of Psychiatry, 15*(4), 310-316. https://doi.org/10.1080/09540260310001606692

Sammartino, F., Yeh, F. C., & Krishna, V. (2019). Longitudinal analysis of structural changes following unilateral focused ultrasound thalamotomy. *Neuroimage: Clinical, 22*, 101754. https://doi.org/10.1016/j.nicl.2019.101754 \

Sarubbo, S., De Benedictis, A., Maldonado, I. L., Basso, G., & Duffau, H. (2013). Frontal terminations for the inferior fronto-occipital fascicle: Anatomical dissection, DTI study and functional considerations on a multi-component bundle. *Brain Structure and Function, 218*(1), 21-37. https://doi.org/10.1007/s00429-011-0372-3

Satz, P. S., Alfano, M. S., Light, R. F., Morgenstern, H. F., Zaucha, K. F., Asarnow, R. F., & Newton, S. (1999). Persistent post-concussive syndrome: A proposed methodology and literature review to determine the effects, if any, of mild head and other bodily injury. *Journal of Clinical and Experimental Neuropsychology, 21*(5), 620-628. https://doi.org/10.1076/jcen.21.5.620.870

Schiehser, D. M., Delis, D. C., Filoteo, J. V., Delano-Wood, L., Han, S. D., Jak, A. J., Drake, A. I., & Bondi, M. W. (2011). Are self-reported symptoms of executive dysfunction associated with objective executive function performance following mild to moderate

traumatic brain injury? *Journal of Clinical and Experimental Neuropsychology, 33*(6), 704-714. https://doi.org/10.1080/13803395.2011.553587

Schmahmann, J. D., Pandya, D. N., Wang, R., Dai, G., D'Arceuil, H. E., de Crespigny, A. J., & Wedeen, V. J. (2007). Association fibre pathways of the brain: Parallel observations from diffusion spectrum imaging and autoradiography. *Brain, 130*(3), 630-653. https://doi.org/10.1093/brain/awl359

Schulz, D., Kopp, B., Kunkel, A., & Faiss, J. H. (2006). Cognition in the early stage of multiple sclerosis. *Journal of Neurology, 253*(8), 1002-1010. https://doi.org/10.1007/s00415-006-0145-8

Sharp, D. J., Beckmann, C. F., Greenwood, R., Kinnunen, K. M., Bonnelle, V., De Boissezon, X., Powell, J. H., Counsell, S. J., Patel, M. C., & Leech, R. (2011). Default mode network functional and structural connectivity after traumatic brain injury. *Brain, 134*(Pt 8), 2233-2247. https://doi.org/10.1093/brain/awr175

Sharpe, J. A. (2008). Neurophysiology and neuroanatomy of smooth pursuit: Lesion studies. *Brain and Cognition, 68*(3), 241-254. https://doi.org/10.1016/j.bandc.2008.08.015

Shenton, M. E., Hamoda, H. M., Schneiderman, J. S., Bouix, S., Pasternak, O., Rathi, Y., Vu, M. A., Purohit, M. P., Helmer, K., Koerte, I., Lin, A. P., Westin, C. F., Kikinis, R., Kubicki, M., Stern, R. A., & Zafonte, R. (2012). A review of magnetic resonance imaging and diffusion tensor imaging findings in mild traumatic brain injury. *Brain Imaging and Behavior, 6*(2), 137-192. https://doi.org/10.1007/s11682-012-9156-5

Sherer, M., Hart, T., Nick, T. G., Whyte, J., Thompson, R. N., & Yablon, S. A. (2003). Early impaired self-awareness after traumatic brain injury. *Archives of Physical Medicine & Rehabilitation, 84*(2), 168-176. https://doi.org/10.1053/apmr.2003.50045

Sherer, M., Struchen, M. A., Yablon, S. A., Wang, Y., & Nick, T. G. (2008). Comparison of indices of traumatic brain injury severity: Glasgow Coma Scale, length of coma and post-traumatic amnesia. *Journal of Neurology, Neurosurgery, and Psychiatry, 79*(6), 678-685. https://doi.org/10.1136/jnnp.2006.111187

Shin, S. S., Okonkwo, D. O., Schneider, B., & Verstynen, T. (2012). Using high resolution white matter mapping to detect traumatic brain injury. *University of Pittsburgh Neurosurgery News, 13*(1). http://www.neurosurgery.pitt.edu/news/neuronews/pdf/2012winter.pdf

Shin, S. S., Pathak, S., Presson, N., Bird, W., Wagener, L., Schneider, W., Okonkwo, D. O., & Fernandez-Miranda, J. C. (2014). Detection of white matter injury in concussion using high-definition fiber tractography. *Progress in Neurological Surgery, 28*, 86-93. https://doi.org/10.1159/000358767

Shin, S. S., Verstynen, T., Pathak, S., Jarbo, K., Hricik, A. J., Maserati, M., Beers, S. R., Puccio, A. M., Boada, F. E., Okonkwo, D. O., & Schneider, W. (2012). High-definition fiber tracking for assessment of neurological deficit in a case of traumatic brain injury: Finding, visualizing, and interpreting small sites of damage. *Journal of Neurosurgery, 116*, 1062-1069. https://doi.org/10.3171/2012.1.JNS111282)

Shrout, P. E., & Fleiss, J. L. (1979). Intraclass correlations: Uses in assessing rater reliability. *Psychological Bulletin, 86*(2), 420-428.

Shum, D. H. K., McFarland, K. A., & Bain, J. D. (1990). Construct validity of eight tests of attention: Comparison of normal and closed head injured samples. *The Clinical Neuropsychologist, 4*, 151-162.

Shura, R. D., Rowland, J. A., & Miskey, H. M. (2016). Auditory Consonant Trigrams: A psychometric update. *Archives of Clinical Neuropsychology, 31*(1), 47-57. https://doi.org/10.1093/arclin/acv083

Sigurdardottir, S., Andelic, N., Roe, C., Jerstad, T., & Schanke, A. K. (2009). Post-concussion symptoms after traumatic brain injury at 3 and 12 months post-injury: A prospective study. *Brain Injury, 23*(6), 489-497. https://doi.org/10.1080/02699050902926309

Silver, J., & Miller, J. H. (2004). Regeneration beyond the glial scar. *Nature Reviews Neuroscience, 5*(2), 146-156. https://doi.org/10.1038/nrn1326

Silver, J. M., Kramer, R., Greenwald, S., & Weissman, M. (2001). The association between head injuries and psychiatric disorders: Findings from the New Haven NIMH Epidemiologic Catchment Area Study. *Brain Injury*, *15*(11), 935-945. https://doi.org/10.1080/02699050110065295

Simon, D. W., McGeachy, M. J., Bayir, H., Clark, R. S., Loane, D. J., & Kochanek, P. M. (2017). The far-reaching scope of neuroinflammation after traumatic brain injury. *Nature Reviews Neurolology, 13*(3), 171-191. https://doi.org/10.1038/nrneurol.2017.13

Slaughter, B., Fann, J. R., & Ehde, D. (2003). Traumatic brain injury in a county jail population: Prevalence, neuropsychological functioning and psychiatric disorders. *Brain Injury*, *17*(9), 731-741. https://doi.org/10.1080/0269905031000088649

Smith, A. (2000). *Symbol Digit Modalities Test: SDMT*. Testzentrale.

Smith, S. M. (2002). Fast robust automated brain extraction. *Human Brain Mapping, 17*(3), 143-155. https://doi.org/10.1002/hbm.10062

Sofroniew, M. V. (2005). Reactive astrocytes in neural repair and protection. *Neuroscientist, 11*(5), 400-407. https://doi.org/10.1177/1073858405278321

Sotiropoulos, S. N., Jbabdi, S., Xu, J., Andersson, J. L., Moeller, S., Auerbach, E. J., Glasser, M. F., Hernandez, M., Sapiro, G., Jenkinson, M., Feinberg, D. A., Yacoub, E., Lenglet, C., Van Essen, D. C., Ugurbil, K., Behrens, T. E., & members of the WU-Minn HCP Consortium. (2013). Advances in diffusion MRI acquisition and processing in the Human Connectome Project. *Neuroimage, 80*, 125-143. https://doi.org/10.1016/j.neuroimage.2013.05.057

SR Research. *Data Viewer* (Version 2.6.1) [Computer software]. https://www.sr-research.com/data-viewer/

SR Research. *Experiment Builder* (Version 1.10.1630) [Computer software]. https://www.sr-research.com/experiment-builder/

SR Research. (2017). *EyeLink 1000 Plus* (Version 1.0.12) [Apparatus and software]. https://www.sr-research.com/eyelink1000plus.html

Stocchetti, N., & Zanier, E. R. (2016). Chronic impact of traumatic brain injury on outcome and quality of life: A narrative review. *Critical Care, 20*(1), Article 148. https://doi.org/10.1186/s13054-016-1318-1

Straus, S. E., Glasziou, P., Richardson, W. S., & Haynes, R. B. (2019). *Evidence-based medicine: How to practice and teach EBM* (5 ed.). Elsevier.

Strauss, E., Sherman, E. M. S., & Spreen, O. (2006). *A compendium of neuropsychological tests: Administration, norms, and commentary* (3rd ed.). Oxford University Press.

Stuss, D. T., Stethem, L. L., & Pelchat, G. (1988). Three tests of attention and rapid information processing: An extension. *Clinical Neuropsychologist, 2*(3), 246-250. https://doi.org/10.1080/13854048808520107

Suh, M., Basu, S., Kolster, R., Sarkar, R., McCandliss, B., Ghajar, J., Cognitive, & the members of the Cognitive and Neurobiological Research Consortium (2006). Increased oculomotor deficits during target blanking as an indicator of mild traumatic brain injury. *Neuroscience Letters, 410*(3), 203-207. https://doi.org/10.1016/j.neulet.2006.10.001

Suh, M., Kolster, R., Sarkar, R., McCandliss, B., Ghajar, J., & the members of the Cognitive and Neurobiological Research Consortium (2006). Deficits in predictive smooth pursuit after mild traumatic brain injury. *Neuroscience Letters, 401*(1-2), 108-113. https://doi.org/10.1016/j.neulet.2006.02.074

Sullivan, K. A., Lange, R. T., & Edmed, S. L. (2016). Utility of the Neurobehavioral Symptom Inventory Validity-10 index to detect symptom exaggeration: An analogue simulation study. *Applied Neuropsychology: Adult, 23*(5), 353-362. https://doi.org/10.1080/23279095.2015.1079714

Sydnor, V. J., Rivas-Grajales, A. M., Lyall, A. E., Zhang, F., Bouix, S., Karmacharya, S., Shenton, M. E., Westin, C. F., Makris, N., Wassermann, D., O'Donnell, L. J., & Kubicki, M. (2018). A comparison of three fiber tract delineation methods and their impact on white matter analysis. *Neuroimage, 178*, 318-331. https://doi.org/10.1016/j.neuroimage.2018.05.044

Taber, K. H., Hurley, R. A., Haswell, C. C., Rowland, J. A., Hurt, S. D., Lamar, C. D., & Morey, R. A. (2015). White matter compromise in veterans exposed to primary blast forces. *Journal of Head Trauma Rehabilitation, 30*(1), E15-25. https://doi.org/10.1097/HTR.0000000000000030

Taoka, T., Iwasaki, S., Sakamoto, M., Nakagawa, H., Fukusumi, A., Myochin, K., Hirohashi, S., Hoshida, T., & Kichikawa, K. (2006). Diffusion anisotropy and diffusivity of white

matter tracts within the temporal stem in Alzheimer disease: Evaluation of the "tract of interest" by diffusion tensor tractography. *American Journal of Neuroradiology, 27*(5), 1040-1045.

Taylor, C. A., Bell, J. M., Breiding, M. J., & Xu, L. (2017). Traumatic Brain Injury-Related Emergency Department Visits, Hospitalizations, and Deaths — United States, 2007 and 2013. *MMWR Surveillance Summaries, 66*(SS-9), 116.

Taylor, H. G., Dietrich, A., Nuss, K., Wright, M., Rusin, J., Bangert, B., Minich, N., & Yeates, K. O. (2010). Post-concussive symptoms in children with mild traumatic brain injury. *Neuropsychology, 24*(2), 148-159. https://doi.org/10.1037/a0018112

Teasdale, G., & Jennett, B. (1974). Assessment of coma and impaired consciousness. A practical scale. *Lancet, 2*(7872), 81-84.

Teasdale, T. W., & Engberg, A. W. (2001). Suicide after traumatic brain injury: A population study. *Journal of Neurology, Neurosurgery & Psychiatry*, *71*(4), 436-440.

The Management of Concussion/mTBI Working Group (2009). VA/DoD clinical practice guideline for management of concussion/mild traumatic brain injury. *Journal of Rehabilitation and Research Development, 46*(6), CP1-68. https://doi.org/10.1682/JRRD.2009/06.0076

Thiebaut de Schotten, M., Dell'Acqua, F., Forkel, S. J., Simmons, A., Vergani, F., Murphy, D. G., & Catani, M. (2011). A lateralized brain network for visuospatial attention. *Nature Neuroscience, 14*(10), 1245-1246. https://doi.org/10.1038/nn.2905

Thiebaut de Schotten, M., Dell'Acqua, F., Valabregue, R., & Catani, M. (2012). Monkey to human comparative anatomy of the frontal lobe association tracts. *Cortex, 48*(1), 82-96. https://doi.org/10.1016/j.cortex.2011.10.001

Thiebaut de Schotten, M., Ffytche, D. H., Bizzi, A., Dell'Acqua, F., Allin, M., Walshe, M., Murray, R., Williams, S. C., Murphy, D. G., & Catani, M. (2011). Atlasing location, asymmetry and inter-subject variability of white matter tracts in the human brain with MR diffusion tractography. *Neuroimage, 54*(1), 49-59. https://doi.org/10.1016/j.neuroimage.2010.07.055

Thier, P., & Ilg, U. J. (2005). The neural basis of smooth-pursuit eye movements. *Current Opinions in Neurobiology, 15*(6), 645-652. https://doi.org/10.1016/j.conb.2005.10.013

Tomaiuolo, F., Carlesimo, G. A., Di Paola, M., Petrides, M., Fera, F., Bonanni, R., Formisano, R., Pasqualetti, P., & Caltagirone, C. (2004). Gross morphology and morphometric sequelae in the hippocampus, fornix, and corpus callosum of patients with severe non-missile traumatic brain injury without macroscopically detectable lesions: a T1 weighted MRI study. *Journal of Neurology, Neurosurgery, and Psychiatry, 75*(9), 1314-1322. https://doi.org/10.1136/jnnp.2003.017046

Tu, T. W., Williams, R. A., Lescher, J. D., Jikaria, N., Turtzo, L. C., & Frank, J. A. (2016). Radiological-pathological correlation of diffusion tensor and magnetization transfer imaging in a closed head traumatic brain injury model. *Annals of Neurology, 79*(6), 907-920. https://doi.org/10.1002/ana.24641

Tuch, D. S. (2004). Q-ball imaging. *Magnetic Resonance in Medicine, 52*(6), 1358-1372. https://doi.org/10.1002/mrm.20279

Tuch, D. S., Reese, T. G., Wiegell, M. R., Makris, N., Belliveau, J. W., & Wedeen, V. J. (2002). High angular resolution diffusion imaging reveals intravoxel white matter fiber heterogeneity. *Magnetic Resonance in Medicine, 48*(4), 577-582. https://doi.org/10.1002/mrm.10268

Tuch, D. S., Reese, T. G., Wiegell, M. R., & Wedeen, V. J. (2003). Diffusion MRI of complex neural architecture. *Neuron, 40*(5), 885-895.

Tukey, J. W. (1977). *Exploratory data analysis* (Vol. 2). Addison-Wesley.

Ture, U., Yasargil, M. G., Friedman, A. H., & Al-Mefty, O. (2000). Fiber dissection technique: Lateral aspect of the brain. *Neurosurgery, 47*(2), 417-426.

Turken, A., Whitfield-Gabrieli, S., Bammer, R., Baldo, J. V., Dronkers, N. F., & Gabrieli, J. D. (2008). Cognitive processing speed and the structure of white matter pathways: convergent evidence from normal variation and lesion studies. *Neuroimage, 42*(2), 1032-1044. https://doi.org/10.1016/j.neuroimage.2008.03.057

Tusa, R. J., & Ungerleider, L. G. (1988). Fiber pathways of cortical areas mediating smooth pursuit eye movements in monkeys. *Annals of Neurology, 23*(2), 174-183. https://doi.org/10.1002/ana.410230211

Vander Vorst, M., Ono, K., Chan, P., & Stuhmiller, J. (2007). Correlates to traumatic brain injury in nonhuman primates. *Journal of Trauma, 62*(1), 199-206. https://doi.org/10.1097/01.ta.0000238665.09611.4b

Vanderploeg, R. D., Cooper, D. B., Belanger, H. G., Donnell, A. J., Kennedy, J. E., Hopewell, C. A., & Scott, S. G. (2014). Screening for postdeployment conditions: Development and cross-validation of an embedded validity scale in the Neurobehavioral Symptom Inventory. *Journal of Head Trauma Rehabilitation, 29*(1), 1-10. https://doi.org/10.1097/HTR.0b013e318281966e

Vanderploeg, R. D., Silva, M. A., Soble, J. R., Curtiss, G., Belanger, H. G., Donnell, A. J., & Scott, S. G. (2015). The structure of postconcussion symptoms on the Neurobehavioral

Symptom Inventory: A comparison of alternative models. *Journal of Head Trauma Rehabilitation, 30*(1), 1-11. https://doi.org/10.1097/HTR.0000000000000009

Veeramuthu, V., Narayanan, V., Kuo, T. L., Delano-Wood, L., Chinna, K., Bondi, M. W., Waran, V., Ganesan, D., & Ramli, N. (2015). Diffusion tensor imaging parameters in mild traumatic brain injury and its correlation with early neuropsychological impairment: A longitudinal study. *Journal of Neurotrauma, 32*(19), 1497-1509. https://doi.org/10.1089/neu.2014.3750

Ventura, R. E., Balcer, L. J., & Galetta, S. L. (2014). The neuro-ophthalmology of head trauma. *The Lancet Neurology, 13*(10), 1006-1016. https://doi.org/10.1016/s1474-4422(14)70111-5

Verstynen, T., Jarbo, K., Pathak, S., & Schneider, W. (2011). In vivo mapping of microstructural somatotopies in the human corticospinal pathways. *Journal of Neurophysiology, 105*(1), 336-346. https://doi.org/10.1152/jn.00698.2010

Viano, D. C., Casson, I. R., Pellman, E. J., Bir, C. A., Zhang, L., Sherman, D. C., & Boitano, M. A. (2005). Concussion in professional football: Comparison with boxing head impacts — Part 10. *Neurosurgery, 57*(6), 1154-1172. https://doi.org/10.1227/01.neu.0000187541.87937.d9

Vossel, S., Weiss, P. H., Eschenbeck, P., & Fink, G. R. (2013). Anosognosia, neglect, extinction and lesion site predict impairment of daily living after right-hemispheric stroke. *Cortex, 49*(7), 1782-1789. https://doi.org/10.1016/j.cortex.2012.12.011

Vuilleumier, P. (2004). Anosognosia: The neurology of beliefs and uncertainties. *Cortex, 40*(1), 9-17. https://doi.org/10.1016/s0010-9452(08)70918-3

Wada, T., Asano, Y., & Shinoda, J. (2012). Decreased fractional anisotropy evaluated using tract-based spatial statistics and correlated with cognitive dysfunction in patients with mild traumatic brain injury in the chronic stage. *American Journal of Neuroradiology, 33*(11), 2117-2122. https://doi.org/10.3174/ajnr.A3141

Wakana, S., Caprihan, A., Panzenboeck, M. M., Fallon, J. H., Perry, M., Gollub, R. L., Hua, K., Zhang, J., Jiang, H., Dubey, P., Blitz, A., van Zijl, P., & Mori, S. (2007). Reproducibility of quantitative tractography methods applied to cerebral white matter. *Neuroimage, 36*(3), 630-644. https://doi.org/10.1016/j.neuroimage.2007.02.049

Wang, X., Pathak, S., Stefaneanu, L., Yeh, F. C., Li, S., & Fernandez-Miranda, J. C. (2016). Subcomponents and connectivity of the superior longitudinal fasciculus in the human brain. *Brain Structure and Function, 221*(4), 2075-2092. https://doi.org/10.1007/s00429-015-1028-5

Wang, Y., Chan, R. C., & Deng, Y. (2006). Examination of postconcussion-like symptoms in healthy university students: Relationships to subjective and objective neuropsychological function performance. *Archives of Clinical Neuropsychology, 21*(4), 339-347. https://doi.org/10.1016/j.acn.2006.03.006

Wang, Y., Fernandez-Miranda, J. C., Verstynen, T., Pathak, S., Schneider, W., & Yeh, F. C. (2013). Rethinking the role of the middle longitudinal fascicle in language and auditory pathways. *Cerebral Cortex, 23*(10), 2347-2356. https://doi.org/10.1093/cercor/bhs225

Wanner, I. B., Deik, A., Torres, M., Rosendahl, A., Neary, J. T., Lemmon, V. P., & Bixby, J. L. (2008). A new in vitro model of the glial scar inhibits axon growth. *Glia, 56*(15), 1691-1709. https://doi.org/10.1002/glia.20721

Ware, A. L., Biekman, B., Hachey, R., MacLeod, M., Bird, W., Pathak, S., Clarke, E., Borrasso, A., Puccio, A. M., Glavin, K., Pomiecko, K., Moretti, P., Beers, S. R., Levin, H. S., Schneider, W., Okonkwo, D. O., & Wilde, E. A. (2019). A preliminary high-definition fiber tracking study of the executive control network in blast-induced traumatic brain injury. *Journal of Neurotrauma, 36*(5), 686-701. https://doi.org/10.1089/neu.2018.5725

Wechsler, D. (2008a). *Wechsler Adult Intelligence Scale – Fourth edition: Administration and Scoring Manual*. Pearson.

Wechsler, D. (2008b). *Wechsler Adult Intelligence Scale – Fourth edition: Technical and Interpretive Manual*. Pearson.

Wechsler, D. (2009a). *Wechsler Memory Scale – Fourth edition: Administrative and scoring manual*. Pearson.

Wechsler, D. (2009b). *Wechsler Memory Scale – Fourth edition: Technical and interpretive manual*. Pearson.

Wechsler, D. (2011). *Wechsler Abbreviated Scale of Intelligence – Second edition*. Pearson.

Wedeen, V. J., Hagmann, P., Tseng, W. Y., Reese, T. G., & Weisskoff, R. M. (2005). Mapping complex tissue architecture with diffusion spectrum magnetic resonance imaging. *Magnetic Resonance in Medicine, 54*(6), 1377-1386. https://doi.org/10.1002/mrm.20642

Whiteneck, G. G., Cuthbert, J. P., Corrigan, J. D., & Bogner, J. A. (2016). Risk of negative outcomes after traumatic brain injury: A statewide population-based survey. *Journal of Head Trauma Rehabilitation, 31*(1), E43-E54. https://doi.org/10.1097/HTR.0000000000000141

Whittaker, R., Kemp, S., & House, A. (2007). Illness perceptions and outcome in mild head injury: A longitudinal study. *Journal of Neurology, Neurosurgery, and Psychiatry, 78*(6), 644-646. https://doi.org/10.1136/jnnp.2006.101105

Wilde, E. A., Bigler, E. D., Pedroza, C., & Ryser, D. K. (2006). Post-traumatic amnesia predicts long-term cerebral atrophy in traumatic brain injury. *Brain Injury, 20*(7), 695-699. https://doi.org/10.1080/02699050600744079

Wilde, E. A., Li, X., Hunter, J. V., Narayana, P. A., Hasan, K., Biekman, B., Swank, P., Robertson, C., Miller, E., McCauley, S. R., Chu, Z. D., Faber, J., McCarthy, J., & Levin, H. S. (2016). Loss of consciousness is related to white matter injury in mild traumatic brain injury. *Journal of Neurotrauma, 33*(22), 2000-2010. https://doi.org/10.1089/neu.2015.4212

Wilde, E. A., Whiteneck, G. G., Bogner, J., Bushnik, T., Cifu, D. X., Dikmen, S., French, L., Giacino, J. T., Hart, T., Malec, J. F., Millis, S. R., Novack, T. A., Sherer, M., Tulsky, D. S., Vanderploeg, R. D., & von Steinbuechel, N. (2010). Recommendations for the use of common outcome measures in traumatic brain injury research. *Archives of Physical Medicine & Rehabilitation, 91*(11), 1650-1660 e1617. https://doi.org/10.1016/j.apmr.2010.06.033

Willer, B., & Leddy, J. J. (2006). Management of concussion and post-concussion syndrome. *Current Treatment Options in Neurology, 8*, 415-426.

Williams, D. H., Levin, H. S., & Eisenberg, H. M. (1990). Mild head injury classification. *Neurosurgery, 27*(3), 422-428.

Wise, K., Ownsworth, T., & Fleming, J. (2005). Convergent validity of self-awareness measures and their association with employment outcome in adults following acquired brain injury. *Brain Injury, 19*(10), 765-775. https://doi.org/10.1080/0269905050019977

Yeh, F. C., Liu, L., Hitchens, T. K., & Wu, Y. L. (2017). Mapping immune cell infiltration using restricted diffusion MRI. *Magnetic Resonance in Medicine, 77*(2), 603-612. https://doi.org/10.1002/mrm.26143

Yeh, F. C., Panesar, S., Barrios, J., Fernandes, D., Abhinav, K., Meola, A., & Fernandez-Miranda, J. C. (2019). Automatic removal of false connections in diffusion MRI tractography using topology-informed pruning (TIP). *Neurotherapeutics, 16*(1), 52-58. https://doi.org/10.1007/s13311-018-0663-y

Yeh, F. C., Verstynen, T. D., Wang, Y., Fernandez-Miranda, J. C., & Tseng, W. Y. (2013). Deterministic diffusion fiber tracking improved by quantitative anisotropy. *PLoS One, 8*(11), Article e80713. https://doi.org/10.1371/journal.pone.0080713

Yeh, F. C., Vettel, J. M., Singh, A., Poczos, B., Grafton, S. T., Erickson, K. I., Tseng, W. I., & Verstynen, T. D. (2016). Quantifying differences and similarities in whole-brain white matter architecture using local connectome fingerprints. *PLoS Computational Biology, 12*(11), Article e1005203. https://doi.org/10.1371/journal.pcbi.1005203

Yeh, F. C., Wedeen, V. J., & Tseng, W. Y. (2010). Generalized Q-sampling imaging. *IEEE Translational Medical Imaging, 29*(9), 1626-1635. https://doi.org/10.1109/TMI.2010.2045126

Yeh, F. C., Wedeen, V. J., & Tseng, W. Y. (2011). Estimation of fiber orientation and spin density distribution by diffusion deconvolution. *Neuroimage, 55*(3), 1054-1062. https://doi.org/10.1016/j.neuroimage.2010.11.087

Yendiki, A., Koldewyn, K., Kakunoori, S., Kanwisher, N., & Fischl, B. (2014). Spurious group differences due to head motion in a diffusion MRI study. *Neuroimage, 88*, 79-90. https://doi.org/10.1016/j.neuroimage.2013.11.027

Yin, B., Li, D. D., Huang, H., Gu, C. H., Bai, G. H., Hu, L. X., Zhuang, J. F., & Zhang, M. (2019). Longitudinal changes in diffusion tensor imaging following mild traumatic brain injury and correlation with outcome. *Frontal Neural Circuits, 13*, Article 28. https://doi.org/10.3389/fncir.2019.00028

Young, J. C., Sawyer, R. J., Roper, B. L., & Baughman, B. C. (2012). Expansion and re-examination of Digit Span effort indices on the WAIS-IV. *The Clinical Neuropsychologist, 26*(1), 147-159.

Zeldovich, M., Wu, Y. J., Gorbunova, A., Mikolic, A., Polinder, S., Plass, A. M., Covic, A., Asendorf, T., Andelic, N., Voormolen, D. C., von Steinbuchel, N., & on the behalf of the Center-TBI Participants & Investigators. (2020). Influence of sociodemographic, premorbid, and injury-related factors on post-concussion symptoms after traumatic brain injury. *Journal of Clinical Medicine, 9*(6), Article 1931. https://doi.org/10.3390/jcm9061931

Zhang, H., Wang, Y., Lu, T., Qiu, B., Tang, Y., Ou, S., Tie, X., Sun, C., Xu, K., & Wang, Y. (2013). Differences between generalized Q-sampling imaging and diffusion tensor imaging in the preoperative visualization of the nerve fiber tracts within peritumoral edema in brain. *Neurosurgery, 73*(6), 1044-1053; discussion 1053. https://doi.org/10.1227/NEU.0000000000000146

Zhou, Y., Kierans, A., Kenul, D., Ge, Y., Rath, J., Reaume, J., Grossman, R. I., & Lui, Y. W. (2013). Mild traumatic brain injury: Longitudinal regional brain volume changes. *Radiology, 267*(3), 880-890. https://doi.org/10.1148/radiol.13122542

Zhou, Y., Shao, A., Yao, Y., Tu, S., Deng, Y., & Zhang, J. (2020). Dual roles of astrocytes in plasticity and reconstruction after traumatic brain injury. *Cell Communication and Signaling, 18*(1), Article 62. https://doi.org/10.1186/s12964-020-00549-2

Table 1

Eye-Tracking Paradigms and Associated Cognitive Domains

Task	Domains	Protocol
Visually-guided saccades	Attention Processing Speed	The subject fixates on a central fixation cross until a target stimulus appears, at which time the subject is instructed to generate a saccade to the target.
Memory-guided saccade sequences	Working Memory	The subject fixates on a central fixation cross while target stimuli are presented in a sequence elsewhere on the screen. When cued, the subject is instructed to look away from the fixation cross and make saccades to the same locations and in the same order as the target stimuli appeared on the screen.
Predictive smooth pursuit eye movement	Attention Processing Speed Working Memory	The subject tracks a moving stimulus around a known, circular trajectory. The object will be transiently extinguished on its course for some periods of time, and the subject is instructed to continue tracking the known trajectory of the target during this time.

Table 2

Neuropsychological Test Protocols and Primary Cognitive Domain Assessed

Task	Modality	Protocol
Processing Speed		
PASAT	Auditory	Over four trials with decreasing inter-stimulus intervals, the subject is required to add 60 pairs of randomly presented digits by summing each with the digit immediately preceding it.
SDMT	Visual	The subject is given a paired symbol-digit key and is instructed to fill the appropriate number into several rows of blank squares paired with the symbols as quickly and accurately as possible within 90 seconds.
TMTA	Visual	The subject is instructed to draw lines connecting circles that are consecutively numbered from 1 to 25 and presented randomly across a worksheet as quickly as possible.
Attention		
DSF	Auditory	The subject is required to repeat strings of random numbers of increasing sequence length exact order as they were presented.
SSP	Visual	The subject is presented with series of nonsense designs of increasing length, and then asked to choose the correct designs from foils in the same sequence as they were presented.
2 & 7	Visual	The subject is instructed to mark all of the 2s and 7s they find embedded within several rows of random letters or numbers as quickly and accurately as possible.
Working Memory		
ACT	Auditory	The subject is required to hold consonant trigrams in mind while counting backwards by 3s until instructed to stop and to recall the trigram after a 3-, 9-, or 18- second delay.
DSB	Auditory	The subject is required to repeat strings of random numbers of increasing sequence length in the exact reversed order as they were presented.
DSS	Auditory	The subject is required to recall strings of random numbers of increasing sequence length in numerical order, starting with the smallest number.
TMTB	Visual	The subject is instructed to draw lines, alternating alphanumerically, to connect 25 circles that are consecutively numbered and lettered and presented randomly across a worksheet as quickly as possible.

Note. PASAT = Paced Auditory Serial Addition Task; SDMT = Symbol Digit Modalities Test; TMTA = Trail Making Test part A; DSF = Wechsler Adult Intelligence Scale – Fourth edition (WAIS-IV) Digit Span Forward; SSP = Wechsler Memory Scale – Fourth edition (WMS-IV) Symbol Span; 2 & 7 = Ruff 2 & 7 Test of Selective Attention; ACT = Auditory Consonant Trigrams; DSB = WAIS-IV Digit Span Backward; DSS = WAIS-IV Digit Span Sequencing; TMTB = Trail Making Test part B.

Table 3

Acquisition Parameters of Structural Neuroimaging Sequences

	MP-RAGE	SWI	dMRI	dMRI	dMRI	dMRI	dMRI	dMRI
TA (m:s)	4:26	3:44	4:37	0:50	9:58	0:57	3:38	0:41
Voxel size (mm)	0.9×0.9×0.9	0.9×0.9×1.5	2.4×2.4×2.4	2.4×2.4×2.4	2.4×2.4×2.4	2.4×2.4×2.4	2.4×2.4×2.4	2.4×2.4×2.4
Slices	192	72	63	63	63	63	63	63
Orientation	Sagittal	Transversal	Transversal	Transversal	Transversal	Transversal	Transversal	Transversal
PE Direction	A >> P	R >> L	A >> P	P >> A	A >> P	P >> A	A >> P	P >> A
FOV read (mm)	230	230	230	230	230	230	230	230
FOV phase (%)	100	75	100	100	100	100	100	100
Slice thickness (mm)	0.9	1.5	2.4	2.4	2.4	2.4	2.4	2.4
Matrix size	256×256	256×173	96×96	96×96	96×96	96×96	96×96	96×96
TR (ms)	1900	27	3600	3600	4100	4100	3100	3100
TE (ms)	2.32	20	127	127	149	149	94	94
TI (ms)	900							
Flip angle (°)	9	15						
GRAPPA acceleration	2	2						
Multiband acceleration			3	3	3	3	3	3
Multi-slice mode	Single shot	Interleaved	Interleaved	Interleaved	Interleaved	Interleaved	Interleaved	Interleaved
Bandwidth (Hz/Px)	200	120	2264	2264	2264	2264	2264	2264
Echo spacing (ms)	7.1		0.55	0.55	0.55	0.55	0.55	0.55
Diffusion mode			Free	Free	Free	Free	Free	Free
Low b-value (s/mm^2)			0	0	0	0	0	0
Max b-value (s/mm^2)			3000	3000	5000	5000	1000	1000
Diffusion directions			69	6	138	6	69	6
EPI Factor			96	96	96	96	96	96

Note. MP-RAGE = ; SWI = susceptibility-weighted imaging; dMRI = diffusion-weighted magnetic resonance imaging; TA = acquisition time; PE = phase encoding; A = anterior; P = posterior; R = right; L = left; FOV = field-of-view; TR = repetition time; TE = echo time; TI = inversion time; GRAPPA = generalized autocalibrating partially parallel acquisition; EPI = echo-planar imaging.

Table 4

Demographic and Injury Characteristics of the Present Sample

Sample characteristic	Mild TBI (*n* = 11)			Healthy Control (*n* = 10)			Statistics		
	n	%		*n*	%		χ^2	*df*	*p*
Sex							0.40	1	.670
Male	7	63.6		5	50.0				
Female	4	36.4		5	50.0				
Ethnicity							2.01	2	.366
Caucasian	10	90.9		9	90.0				
Hispanic	1	9.1		0	0.0				
Asian	0	0.0		1	10.0				
Dominant Hand							0.40	1	.635
Right	9	81.8		7	70.0				
Left	2	18.2		3	30.0				
Mechanism									
MVA	4	36.4							
Fall	1	9.1							
SRC	3	27.3							
BFT	2	18.2							
Blast	1	9.1							
	M	*SD*	Range	*M*	*SD*	Range	*z*		*p*
Age	32.00	12.14	21–60	28.50	10.38	20-54	–0.99		.399
							t (19)		*p*
Education	15.18	2.23	12–20	15.70	1.89	13-20	0.57		.574
FSIQ	109.73	3.35	102–114	112.8	3.88	107-120	1.95		.066
SEI	-0.03	0.93	–1.14–1.72	0.03	1.12	–2.44–1.72	0.13		.896
TSI (mo)	114.45	80.89	29–289						
Age at Injury	22.27	12.09	13–56						
PTA (min)	94.09	214.46	0–720						
LOC (min)	3.91	8.28	0–25						
LOS (hr)	3.00	7.07	0–24						
Previous TBIs	0.73	1.10	0–3						

Note. TBI = traumatic brain injury; MVA = motorized vehicle accident; BFT = blunt force trauma; FSIQ = estimated premorbid full scale IQ (standard score); SEI = socioeconomic index (*z*-score); TSI = time-since-injury; PTA = duration of posttraumatic amnesia; LOC = duration of loss of consciousness; LOS = length of hospital stay.

Table 5

Patient-Specific Injury Characteristics

Sex (Age, Education)	Age at Injury	TSI (mo)	Injury Mechanism	PTA (min)	LOC (min)	LOS (hr)	Previous TBIs	NSI Total	NSI Frequency	RPQ Total
Male (29, 16)	25	54	30-foot Fall	0	1	0	0	16	10	9
Male (28, 16)	20	90	MVA	0	0	1	0	24	14	10
Female (50, 16)	25	289	MVA	720	25	24	0	15	13	17
Male (33, 16)	16	213	BMX crash	180	0	2	2	12	9	0
Male (30, 14)	16	165	Assault	60	15	4	3	19	14	12
Male (29, 16)	26	29	Blast	30	1	0	0	12	9	0
Female (26, 15)	18	90	BFT	0	0	0	0	16	9	6
Female (60, 20)	56	44	MVA	0	0	0	0	42	15	42
Female (21, 14)	14	74	Sledding	0	0	1	0	14	11	8
Male (21, 12)	16	62	Football	45	0	1	2	36	17	26
Male (25, 12)	13	149	Rugby	0	1	0	1	32	17	40

Note. TSI = time since injury; PTA = duration of posttraumatic amnesia; LOC = duration of loss of consciousness; LOS = length of hospital stay; TBIs = traumatic brain injuries; NSI = Neurobehavioral Symptom Inventory; RPQ = Rivermead Postconcussion Symptom Questionnaire; MVA = motorized vehicle accident (passenger); BFT = blunt force trauma.

Table 6

Neurobehavioral Symptom Inventory Scores Between Groups

Scale	HC (n = 10)			mTBI (n = 11)			z	p[a]	g	99% CI for g	
	M	*SD*	Σ*R*	*M*	*SD*	Σ*R*				*LL*	*UL*
Vestibular	0.40	0.97	95.5	1.00	1.26	135.5	1.22	.290	0.51	–0.60	1.60
Somatosensory	**1.10**	**0.57**	**77.0**	**3.73**	**2.72**	**154.0**	**2.52**	**.010**	**1.25**	**0.04**	**2.44**
Cognitive	**1.90**	**1.85**	**71.0**	**6.64**	**4.30**	**160.0**	**2.77**	**.004**	**1.35**	**0.12**	**2.56**
Affective	**2.50**	**2.01**	**62.0**	**8.36**	**3.93**	**169.0**	**3.42**	**.000**	**1.78**	**0.46**	**3.07**
Total	**6.10**	**4.15**	**57.5**	**21.64**	**10.45**	**173.5**	**3.70**	**.000**	**1.84**	**0.51**	**3.15**

Note. Bold text indicates large effect sizes. Hedges's g is interpreted as small, medium, and large when $g \geq 0.30$, 0.50, and 0.80, respectively (Hedges, 1981). HC = healthy control; mTBI = mild traumatic brain injury; ΣR = rank sum.

[a] exact statistics.

Table 7

Neuropsychological Domain Scores Between Groups

Domain	HC (n = 10)		mTBI (n = 11)		F(1,18)	p	$FDR_{.05}$	f	β	b	SE	99% CI for b	
	M	SD	M	SD								LL	IL
PS	154.80	23.83	149.55	29.72	0.22	.647	.033	.110	–0.11	–5.56	11.93	–39.91	28.79
AT	211.10	26.74	207.09	19.37	0.13	.720	.050	.086	–0.08	–3.66	10.04	–32.57	25.25
WM	**228.10**	**27.38**	**205.18**	**22.91**	**4.12**	**.058**	**.017**	**.478**	**–0.43**	**–22.75**	**11.21**	**–55.01**	**9.52**

Note. Bold text indicates large effect sizes. Effect sizes are interpreted as small, medium, and large when Cohen's $f \geq .10$, .25, and .40, respectively (Cohen, 1988). HC = healthy control. mTBI = mild traumatic brain injury. PS = processing speed; AT = attention; WM = working memory.

Table 8

Principal Components Retained from Eye-Tracking Outcome Measures

Principal Components	Component Loading					
	1	2	3	4	5	6
Component 1: Psychomotor Speed (PM)						
VGS 5° velocity	**.185**	–.083	–.005	–.012	.036	.143
VGS 25° vertical PE	**.106**	.056	.049	.015	.065	–.011
MGS Step 1 duration	**.207**	.078	.077	.112	.028	–.146
MGS Step 2 duration	**.194**	–.001	.139	–.044	–.076	–.044
MGS Step 2 horizontal PE	**.189**	.057	.147	.086	.160	–.077
MGS Step 2 time to peak velocity	**.206**	–.068	.158	.015	–.006	–.062
MGS Step 2 velocity	**.210**	–.077	.107	.042	–.025	.164
MGS Step 3 duration	**.184**	.102	.123	.045	–.033	–.102
MGS Step 3 velocity	**.210**	–.144	.050	.062	–.022	.141
MGS 3-step sequence horizontal mean PE	**.186**	.016	.169	.118	.149	–.082
SPEM within-30°-gap phase error	**.171**	.170	–.048	–.005	–.100	–.024
SPEM within-45°-gap phase error	**.169**	.099	–.130	–.021	–.004	–.037
SPEM within-60°-gap phase error	**.187**	.143	.063	.119	.018	–.067
SPEM within-60°-gap RMSE	**.166**	.157	–.053	.096	–.145	.015
SPEM post-45°-gap SDTE	**.195**	.083	–.051	–.087	–.055	.170
SPEM post-60°-gap SDTE	**.217**	.165	–.056	–.068	–.027	–.023
SPEM post-60°-gap RMSE	**.168**	.150	–.057	.031	–.113	.048
Component 2: Cognitive Flexibility (CF)						
VGS 5° horizontal G_F	–.115	**.209**	.089	.031	.140	.100
VGS 5° horizontal G_P	–.069	**.209**	.172	.075	.051	–.035
VGS 10° horizontal G_F	–.121	**.188**	.144	.092	.095	.126
VGS 10° horizontal G_P	–.109	**.180**	.134	.148	.034	.058
VGS 15° horizontal G_P	–.161	**.147**	.109	.132	.061	.125
VGS 20° horizontal G_F	–.159	**.168**	.116	.073	.030	.132
VGS 20° velocity	.125	**–.194**	.065	.117	.073	.131
VGS 25° duration	–.010	**.269**	–.028	–.032	.082	–.136
VGS 25° velocity	.131	**–.210**	.085	.066	.057	.117
VGS 30° velocity	.112	**–.239**	.079	–.029	–.045	.099
MGS Step 2 saccade frequency	–.076	**–.156**	.139	.138	.088	.019
MGS Step 3 saccade frequency	.011	**–.223**	.070	.145	.078	–.019
MGS Step 3 horizontal G_P	–.105	**.169**	–.080	.045	–.137	–.159
MGS 2-step sequence ATI	–.139	**–.149**	.125	–.056	–.031	–.003
SPEM pre-60°-gap phase error	.090	**.126**	.077	–.105	.051	.016
SPEM post-30°-gap phase error	.106	**.148**	.064	.106	–.056	.130
SPEM post-45°-gap gain	.066	**–.198**	.001	.159	.042	–.157
Component 3: Attention (AT)						
VGS 25° vertical G_P	–.081	–.034	**–.209**	.194	–.058	–.049
VGS 25° horizontal PE	.048	.013	**–.235**	–.102	.025	–.134
VGS 30° horizontal PE	.088	–.080	**–.187**	.054	.167	.002
MGS Step 1 saccade frequency	–.143	–.120	**.159**	.133	.005	–.090
MGS Step 1 amplitude error	–.027	.112	**.184**	.040	.179	.000
MGS Step 1 horizontal G_F	–.142	.077	**–.223**	.055	.062	–.096
MGS 2-step sequence vertical mean PE	–.037	.018	**–.214**	–.027	.143	.147
Component 4: Working Memory (WM)						
VGS 5° vertical G_F	–.043	–.119	–.064	**.274**	.093	–.021
VGS 5° vertical G_P	–.070	–.130	–.123	**.248**	.081	–.049
VGS 5° vertical PE	.033	–.010	–.141	**.245**	–.189	.017
VGS 15° vertical PE	–.059	.000	–.042	**.218**	–.191	.151

Principal Components	Component Loading					
	1	2	3	4	5	6
VGS 20° latency	–.069	–.076	.077	**–.225**	.088	.008
VGS 30° vertical G_P	–.032	–.003	–.065	**.299**	–.067	.033
Component 5: General Intelligence (GI)						
VGS 10° latency	–.057	–.029	.061	–.185	**.186**	.120
VGS 10° vertical PE	.028	–.023	–.092	.223	**–.253**	.121
VGS 15° vertical G_F	.007	–.028	–.067	.229	**.245**	.103
VGS 20° vertical PE	–.098	.017	.015	.101	**–.267**	.052
VGS 25° vertical G_F	.059	.092	–.170	.151	**.161**	–.028
VGS 30° vertical G_F	.120	.116	–.103	.118	**.152**	–.099
MGS 2-step sequence skip errors	.001	.009	–.147	.004	**.186**	.172
MGS 3-step sequence skip errors	.030	.070	–.141	–.110	**.227**	.147
MGS Step 1 horizontal PE	.086	.019	.123	.122	**.172**	.044
MGS Step 1 vertical PE	.012	.046	–.189	–.001	**.221**	.201
MGS 3-step sequence vertical mean PE	.012	–.079	–.189	–.103	**.217**	–.025
SPEM pre-30°-gap SDRE	.085	.079	–.085	–.114	**–.148**	.105
Component 6: Processing Speed (PS)						
VGS 15° horizontal G_F	–.126	.134	.168	.036	.074	**.210**
VGS 20° horizontal G_P	–.122	.098	.152	.070	.030	**.164**
VGS 30° horizontal G_F	.019	.034	–.161	.131	–.021	**.296**
MGS Step 1 horizontal G_P	–.019	.146	–.123	.145	.053	**–.286**
MGS Step 3 horizontal PE	.161	.039	.108	.089	.147	**–.171**
MGS 3-step sequence ATI	–.148	–.041	.138	.052	–.075	**–.286**
SPEM post-60°-gap phase error	.048	.081	.058	–.024	–.241	**.242**

Note. n = 18. Bold text indicates largest component loading. VGS = visually-guided saccades; PE = position error; MGS = memory-guided saccade sequences; SPEM = predictive smooth pursuit eye-movement; RMSE = root mean square error; SDTE = standard deviation of tangential error; G_F = gain of the final eye position; G_P = gain of the eye position after the primary saccade; SDRE = standard deviation of radial error; ATI = absolute time index.

Table 9

Eye-Tracking Component Scores Between Groups

PC	HC (n = 8)		mTBI (n = 9)		$F(1,12)$	p	$FDR_{.05}$	f	β	b	SE	99% CI for b	
	M	SD	M	SD								LL	UL
PM	52.81	31.88	47.50	41.52	0.04	.838	.042	.060	0.05	3.71	17.77	–50.57	57.99
CF	51.34	26.73	48.81	36.27	0.00	.950	.050	.019	–0.02	–1.05	16.20	–50.53	48.44
AT	51.83	29.67	48.38	29.90	0.15	.707	.033	.111	–0.11	–5.90	15.33	–52.74	40.93
WM	**61.95**	**12.39**	**42.28**	**26.69**	**5.20**	**.042**	**.008**	**.658**	**–0.53**	**–23.79**	**10.43**	**–55.66**	**8.08**
GI	55.73	26.11	44.91	20.62	0.66	.434	.017	.234	–0.23	–10.40	12.83	–49.60	28.80
PS	48.55	15.87	51.29	25.84	0.30	.596	.025	.157	0.15	6.22	11.42	–28.66	41.10

Note. All component scores are represented as standardized T-scores (M = 50, SD = 10). Bold text indicates large effect sizes. Effect sizes are interpreted as small, medium, and large when Cohen's $f \geq .10$, .25, and .40, respectively (Cohen, 1988). HC = healthy control; mTBI = mild traumatic brain injury; PC = principal component. PM = psychomotor speed; CF = cognitive flexibility; AT = attention; WM = working memory; GI = general intelligence; PS = processing speed.

Table 10

White Matter Tract Integrity Between Groups

Tract	HC (*n* = 10)		mTBI (*n* = 11)		*F*(1,16)	*p*	$FDR_{.05}$	*f*	β	*b*	*SE*	99% CI for *b*	
	M	*SD*	*M*	*SD*								*LL*	*UL*
Quantitative Anisotropy													
FMa	**.263**	**.054**	**.310**	**.052**	**5.09**	**.038**	**.029**	**.564**	**0.48**	**.053**	**.024**	**–.016**	**.122**
Left IFO	**.200**	**.031**	**.221**	**.033**	**3.31**	**.088**	**.043**	**.455**	**0.39**	**.000**	**.001**	**–.002**	**.002**
Right IFO	**.183**	**.031**	**.208**	**.031**	**5.23**	**.036**	**.021**	**.572**	**0.46**	**.030**	**.013**	**–.008**	**.067**
Left MdLF	**.181**	**.036**	**.203**	**.039**	**2.14**	**.162**	**.050**	**.366**	**0.39**	**.025**	**.017**	**–.025**	**.075**
Right MdLF	**.163**	**.033**	**.186**	**.033**	**4.14**	**.059**	**.036**	**.509**	**0.43**	**.029**	**.014**	**–.013**	**.070**
Left SLF	**.178**	**.028**	**.207**	**.036**	**5.69**	**.030**	**.007**	**.597**	**0.49**	**.033**	**.014**	**–.007**	**.074**
Right SLF	**.174**	**.028**	**.203**	**.034**	**5.26**	**.036**	**.014**	**.573**	**0.49**	**.032**	**.014**	**–.009**	**.073**
Restricted Diffusion Imaging													
FMa	**.266**	**.055**	**.304**	**.046**	**4.26**	**.056**	**.043**	**.516**	**0.44**	**.045**	**.022**	**–.019**	**.109**
Left IFO	**.243**	**.042**	**.275**	**.041**	**4.35**	**.053**	**.036**	**.522**	**0.44**	**.037**	**.018**	**–.015**	**.090**
Right IFO	**.230**	**.042**	**.265**	**.038**	**5.16**	**.031**	**.007**	**.592**	**0.48**	**.040**	**.017**	**–.009**	**.089**
Left MdLF	**.253**	**.045**	**.285**	**.046**	**3.44**	**.082**	**.050**	**.463**	**0.41**	**.038**	**.020**	**–.022**	**.097**
Right MdLF	**.233**	**.044**	**.268**	**.041**	**4.82**	**.043**	**.021**	**.549**	**0.46**	**.041**	**.019**	**–.013**	**.095**
Left SLF	**.274**	**.051**	**.314**	**.051**	**4.57**	**.048**	**.029**	**.534**	**0.44**	**.046**	**.022**	**–.017**	**.109**
Right SLF	**.253**	**.048**	**.291**	**.046**	**5.09**	**.038**	**.014**	**.564**	**0.45**	**.044**	**.020**	**–.013**	**.102**
Generalized Fractional Anisotropy													
FMa	.165	.004	.166	.006	0.31	.583	.021	.140	0.14	.001	.002	–.006	.009
Left IFO	**.133**	**.007**	**.129**	**.004**	**1.60**	**.224**	**.007**	**.316**	**–0.30**	**–.003**	**.003**	**–.011**	**.004**
Right IFO	.131	.004	.129	.004	0.87	.364	.014	.233	–0.23	–.002	.002	–.007	.004
Left MdLF	.119	.004	.118	.006	0.07	.798	.036	.065	–0.07	–.001	.003	–.009	.007
Right MdLF	.118	.005	.118	.006	0.03	.867	.043	.043	0.04	.000	.002	–.007	.008
Left SLF	.112	.004	.112	.004	0.01	.905	.050	.030	0.03	.000	.002	–.006	.006
Right SLF	.117	.005	.117	.005	0.31	.586	.029	.139	–0.13	–.001	.002	–.007	.005
Tract Spread													
FMa	.016	.004	.015	.002	0.29	.597	.036	.135	–0.14	–.001	.001	–.005	.004
Left IFO	.030	.006	.029	.004	0.02	.894	.043	.034	–0.04	.000	.003	–.008	.007
Right IFO	.035	.004	.035	.004	0.01	.910	.050	.029	–0.03	.000	.002	–.005	.005
Left MdLF	**.011**	**.003**	**.010**	**.003**	**1.46**	**.244**	**.014**	**.303**	**–0.30**	**–.002**	**.001**	**–.006**	**.002**
Right MdLF	**.013**	**.003**	**.012**	**.002**	**1.48**	**.241**	**.007**	**.304**	**–0.29**	**–.001**	**.001**	**–.005**	**.002**
Left SLF	.016	.007	.014	.005	0.46	.505	.021	.170	–0.16	–.002	.003	–.009	.006
Right SLF	.024	.005	.026	.009	0.40	.538	.029	.157	0.12	.002	.003	–.006	.010

Note. FDR corrections were applied separately for each metric (7 comparisons each). Bold text indicates medium-to-large effect sizes.

Effect sizes are interpreted as small, medium, and large when Cohen's $f \geq .10$, .25, and .40, respectively (Cohen, 1988). HC = healthy

control; mTBI = mild traumatic brain injury; FMa = forceps major; IFO = inferior fronto-occipital fasciculus; MdLF = middle longitudinal fasciculus; SLF = superior longitudinal fasciculus.

Table 11

Partial Correlations Between Tract Integrity and Cognitive Function in Mild Traumatic Brain Injury

Tract	Neuropsychological Domain						Eye-tracking Component					
	PS		AT		WM		PS		AT		WM	
	$r_{ab.c}$	$r^2_{a(b.c)}$	$r_{ab.c}$	$r^2_{a(b.c)}$	$r_{ab.c}$	$r^2_{a(b.c)}$	$r_{ab.c}$	$r^2_{a(b.c)}$	$r_{ab.c}$	$r^2_{a(b.c)}$	$r_{ab.c}$	$r^2_{a(b.c)}$
Quantitative Anisotropy												
FMa	.08	.01	–.16	.02	–.19	.03	**–.48**	**.16**	**–.53**	**.28**	**–.58**	**.21**
Left IFO	–.02	.00	–.05	.00	–.32	.09	**–.51**	**.17**	**–.59**	**.34**	**–.63**	**.25**
Right IFO	.04	.00	–.06	.00	–.28	.07	**–.51**	**.18**	**–.57**	**.32**	**–.63**	**.26**
Left MdLF	.04	.00	–.01	.00	–.22	.04	**–.47**	**.15**	**–.58**	**.34**	**–.63**	**.25**
Right MdLF	.02	.00	–.07	.00	–.27	.07	**–.53**	**.19**	**–.48**	**.23**	**–.63**	**.25**
Left SLF	–.05	.00	–.22	.04	–.26	.06	–.40	.11	**–.60**	**.36**	**–.62**	**.25**
Right SLF	.10	.01	–.11	.01	–.13	.01	–.41	.12	**–.63**	**.40**	**–.54**	**.19**
Restricted Diffusion Imaging												
FMa	.13	.01	–.09	.01	–.15	.02	**–.46**	**.15**	**–.53**	**.28**	**–.55**	**.20**
Left IFO	.11	.01	.05	.00	–.18	.03	**–.48**	**.16**	**–.58**	**.34**	**–.60**	**.23**
Right IFO	.06	.00	–.05	.00	–.23	.05	–.42	.12	**–.51**	**.25**	**–.66**	**.28**
Left MdLF	.15	.02	.02	.00	–.16	.02	**–.47**	**.15**	**–.51**	**.26**	**–.61**	**.24**
Right MdLF	.13	.01	–.06	.00	–.18	.03	**–.48**	**.15**	**–.49**	**.24**	**–.60**	**.23**
Left SLF	.03	.00	–.13	.01	–.27	.06	**–.45**	**.14**	**–.48**	**.23**	**–.64**	**.26**
Right SLF	.05	.00	–.12	.01	–.20	.04	–.42	.12	**–.50**	**.25**	**–.64**	**.27**
Generalized Fractional Anisotropy												
FMa	–.37	.11	**–.66**	**.40**	**–.47**	**.20**	**–.50**	**.17**	–.29	.08	**–.77**	**.38**
Left IFO	**–.79**	**.51**	**–.67**	**.40**	**–.77**	**.51**	–.37	.09	–.28	.08	**–.64**	**.26**
Right IFO	–.25	.05	–.22	.04	–.43	.16	**–.55**	**.21**	**–.53**	**.28**	–.15	.02
Left MdLF	–.31	.08	–.29	.08	–.36	.11	–.39	.10	**–.50**	**.25**	**–.58**	**.22**
Right MdLF	–.36	.11	–.14	.02	**–.40**	**.14**	**–.45**	**.14**	–.16	.02	**–.50**	**.16**
Left SLF	–.22	.04	**–.45**	**.19**	–.03	.00	–.07	.00	**–.62**	**.38**	–.18	.02
Right SLF	.35	.10	.09	.01	.36	.11	–.13	.01	**–.90**	**.80**	.32	.07
Tract Spread												
FMa	–.24	.05	–.30	.08	–.15	.02	.05	.00	**.77**	**.59**	.25	.04
Left IFO	–.17	.02	.25	.06	–.08	.01	.01	.00	**–.72**	**.52**	.08	.00
Right IFO	.16	.02	.37	.12	.23	.05	.18	.02	**–.67**	**.44**	**.68**	**.30**
Left MdLF	–.22	.04	–.37	.12	–.38	.12	**–.75**	**.38**	–.21	.04	**–.46**	**.14**
Right MdLF	**–.47**	**.18**	**–.70**	**.44**	**–.51**	**.22**	–.24	.04	**.56**	**.31**	–.43	.12
Left SLF	**.90**	**.67**	**.62**	**.35**	**.64**	**.36**	–.29	.06	**–.47**	**.22**	.37	.09
Right SLF	.03	.00	.23	.05	.34	.10	**.60**	**.24**	**–.46**	**.21**	–.10	.01

Note. Bold text indicates medium-to-large effect sizes. Squared semi-partial correlations are interpreted as small, medium, and large effect sizes when $r^2_{a(b.c)}$ = .02, .13, and .26, respectively (Cohen, 1988). PS = processing speed; AT = attention; WM = working

memory; FMa = forceps major; IFO = inferior fronto-occipital fasciculus; MdLF = middle longitudinal fasciculus; SLF = superior longitudinal fasciculus.

Table 12

Prediction of Frequency and Severity of Post-Concussive Symptoms by Cognitive Function

Cognitive Function	Frequency		Severity	
	β	$r^2_{a(b.c)}$	β	$r^2_{a(b.c)}$
	Neuropsychological Domain Score			
PS	0.24	.05	0.02	.00
AT	**0.42**	**.16**	**0.44**	**.17**
WM	0.05	.00	–0.14	.02
	Eye-tracking Component Score			
PS	–0.12	.01	0.08	.00
AT	–0.20	.04	–0.16	.03
WM	**0.76**	**.37**	**0.45**	**.13**

Note. Bold text indicates a medium-to-large effect size. Squared semi-partial correlations are interpreted as small, medium, and large effect sizes when $r^2_{a(b.c)}$ = .02, .13, and .26, respectively (Cohen, 1988). PCS = post-concussive symptom; PS = processing speed; AT = attention; WM = working memory.

Table 13

Prediction of Frequency and Severity of Post-Concussive Symptoms by Tract Integrity

Tract	Frequency		Severity	
	β	$r^2_{a(b.c)}$	β	$r^2_{a(b.c)}$
		Quantitative Anisotropy		
FMa	–0.34	.10	–0.29	.07
Left IFO	–0.23	.04	–0.09	.01
Right IFO	–0.22	.04	–0.14	.02
Left MdLF	–0.32	.10	–0.18	.03
Right MdLF	–0.31	.08	–0.16	.02
Left SLF	–0.41	.12	–0.34	.08
Right SLF	–0.34	.11	–0.31	.08
		Restricted Diffusion Imaging		
FMa	–0.32	.09	–0.26	.06
Left IFO	–0.27	.06	–0.14	.02
Right IFO	–0.33	.10	–0.21	.04
Left MdLF	–0.29	.07	–0.19	.03
Right MdLF	–0.28	.07	–0.22	.04
Left SLF	–0.33	.09	–0.23	.04
Right SLF	**–0.41**	**.14**	–0.31	.08
		Generalized Fractional Anisotropy		
FMa	**–0.63**	**.28**	**–0.57**	**.23**
Left IFO	0.19	.02	0.16	.02
Right IFO	**0.64**	**.26**	0.39	.09
Left MdLF	**–0.45**	**.19**	–0.26	.07
Right MdLF	–0.30	.06	0.05	.00
Left SLF	–0.28	.05	**–0.52**	**.17**
Right SLF	0.16	.02	–0.12	.02
		Tract Spread		
FMa	–0.05	.00	0.08	.00
Left IFO	0.14	.01	0.31	.07
Right IFO	**0.66**	**.26**	**0.54**	**.18**
Left MdLF	–0.29	.07	–0.16	.02
Right MdLF	**–0.43**	**.16**	–0.27	.07
Left SLF	0.33	.08	0.07	.00
Right SLF	**–0.95**	**.32**	**–0.66**	**.15**

Note. Bold text indicates a medium-to-large effect size. Squared semi-partial correlations are interpreted as small, medium, and large effect sizes when $r^2_{a(b.c)}$ = .02, .13, and .26, respectively (Cohen, 1988). FMa = forceps major; IFO = inferior fronto-occipital fasciculus; MdLF = middle longitudinal fasciculus; SLF = superior longitudinal fasciculus.

Figure 1

Spatial Relationships of White Matter Pathways Involved in Processing Speed, Attention, and Working Memory

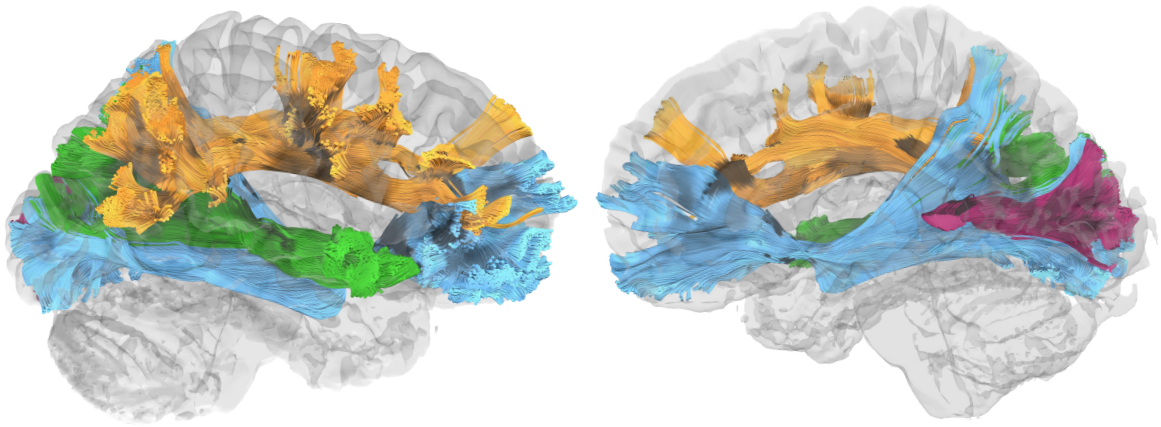

Note. Tract renderings of the forceps major (magenta), inferior fronto-occipital fasciculus (blue), middle longitudinal fasciculus (green), and superior longitudinal fasciculus (yellow) are shown from the lateral (left) and medial (right) surfaces in the right hemisphere of a healthy, 54-year-old, female. For the purposes of this figure, only the right half of the forceps major is shown. The tracts are overlaid by a cortical isosurface rendered from the subject's skull-stripped T1-weighted image.

Figure 2

Advantages of the Orientation Distribution Function (ODF) Over the Diffusion Ellipsoid When Mapping Complicated Fiber Trajectories

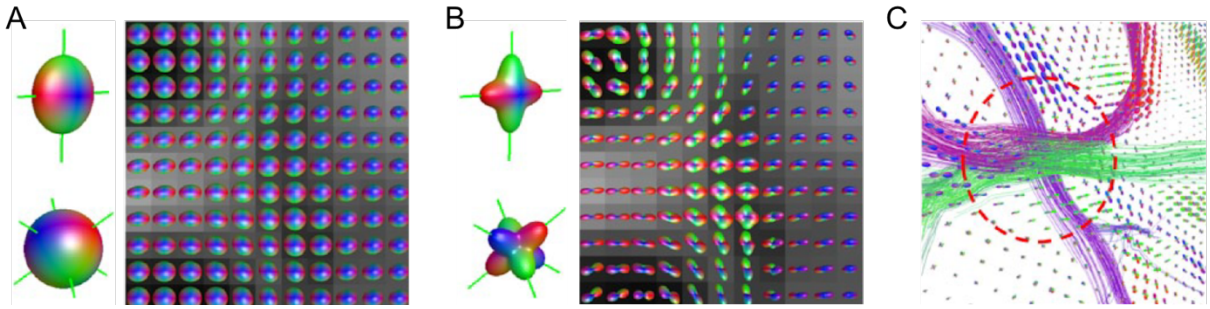

Note. (A) Diffusion ellipsoids for two- and three-fiber crossing configurations (left) and diffusion ellipsoid maps (right) with limited estimations of directionality. (B) ODF for two- and three-fiber crossing configurations (left) and ODF maps (right) indicating voxels with multiple fiber components. (C) Fiber trajectories in fiber crossing area constructed from ODF directional information. Adapted with permission from "Working memory: How important is white matter?" by M. Lazar, 2007, *The Neuroscientist, 23*(2), p. 202.

Figure 3

Possible Target Locations for the Saccade Paradigms

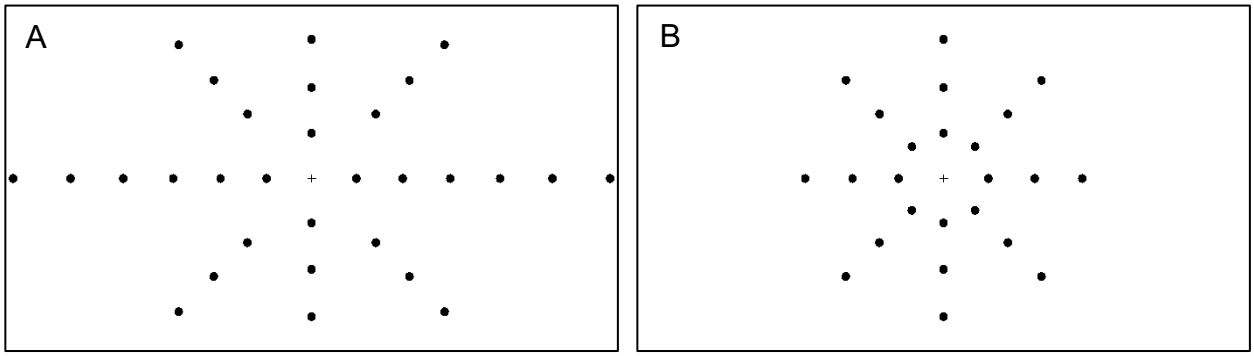

Note. The left panel (A) demonstrates a central fixation cross from which the 30 possible target locations may appear between 5° and 30° of visual angle during the visually-guided saccade task. The right panel (B) demonstrates a central fixation cross from which the 24 possible target locations may appear between 5° and 15° of visual angle during the memory-guided saccade sequences task (images are shown to scale).

Figure 4

Schematic of the Visually-Guided Saccade Task

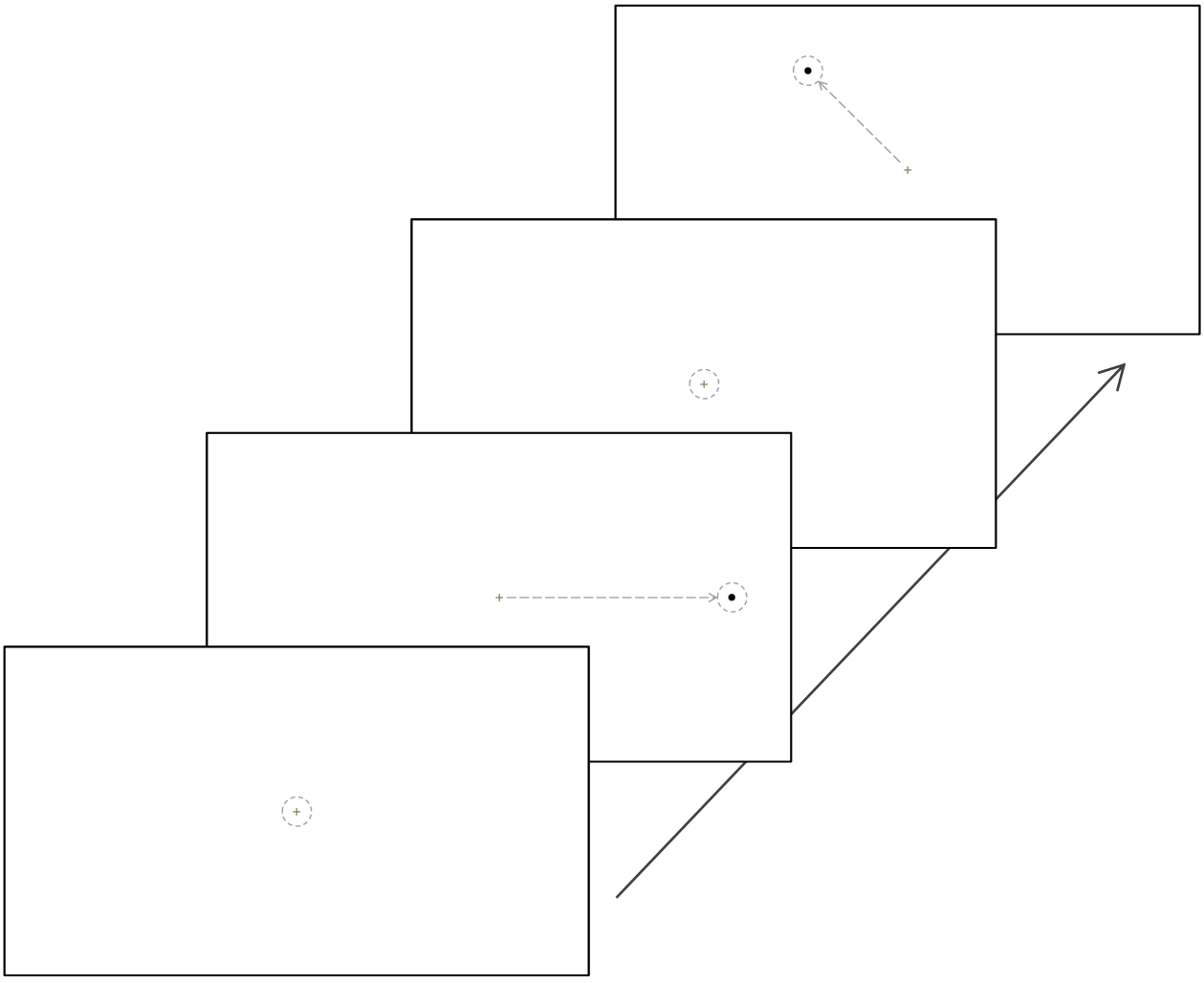

Note. The dashed gray circle represents the gaze location, and the dashed gray arrow represents trajectory of gaze upon presentation of the target stimuli (image is shown to scale).

Figure 5

Schematic of the Memory-Guided Saccade Sequences Task

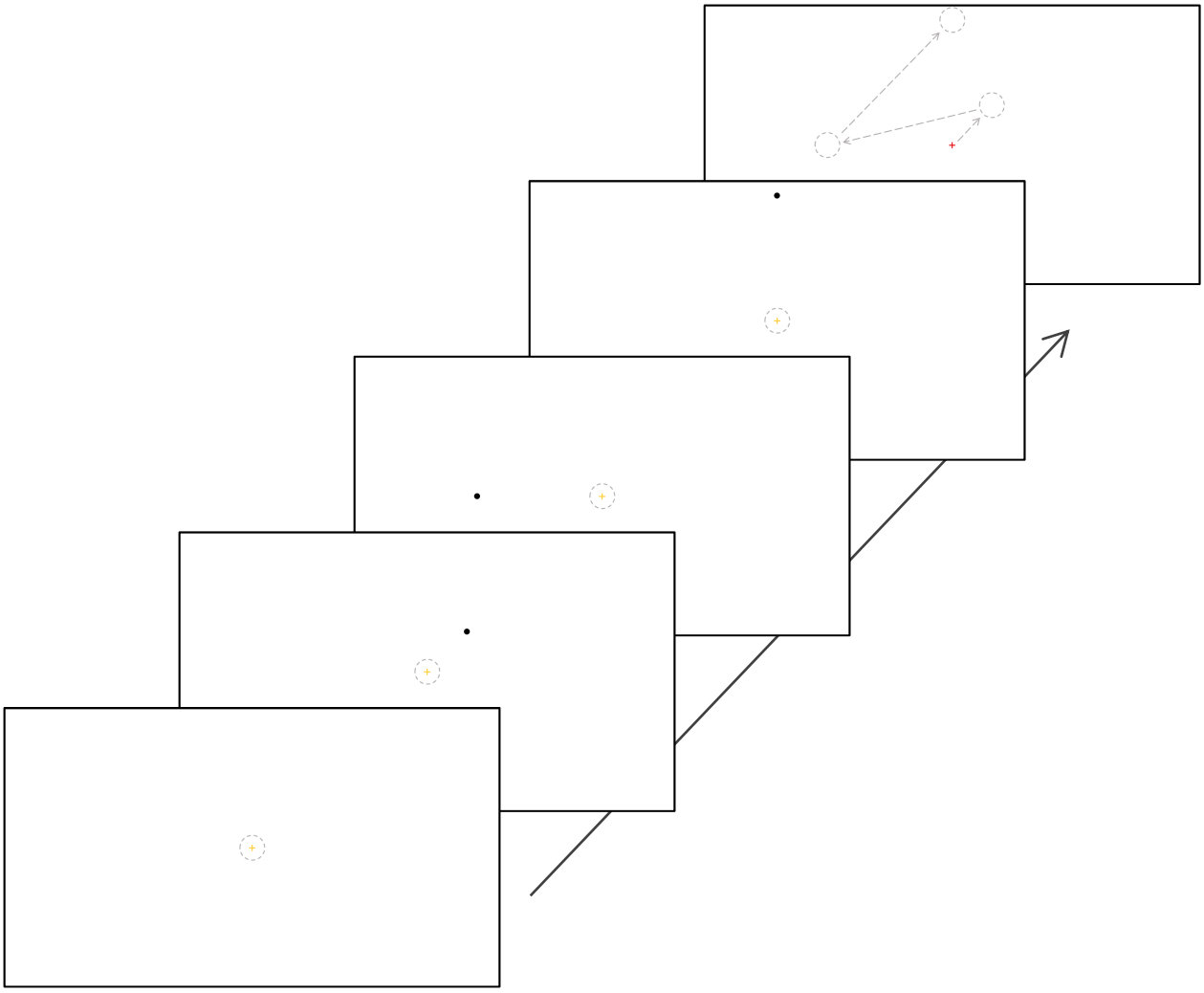

Note. The dashed gray circle represents the gaze location, and the dashed gray arrows represent the trajectory of gaze after the stimuli has been presented in a 3-step condition (image is shown to scale).

Figure 6

Illustration of the Predictive Smooth Pursuit Eye-Movement Task

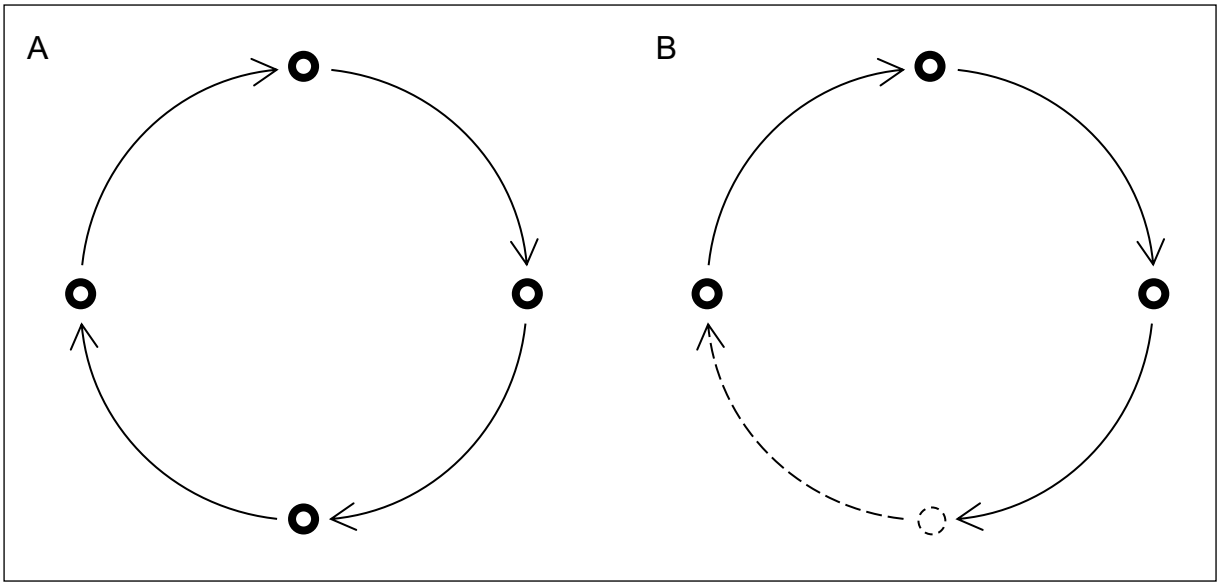

Note. The solid arrows represent the clockwise target trajectory of the target stimulus during (A) the continuous condition, where the target is visible throughout the entire cycle, and the (B) gap condition, where the target disappears (dashed gray target and arrow) and then reappears during the cycle (image is shown to scale).

Figure 7

Diagram Illustrating the Calculation of Predictive Smooth Pursuit Outcome Measures

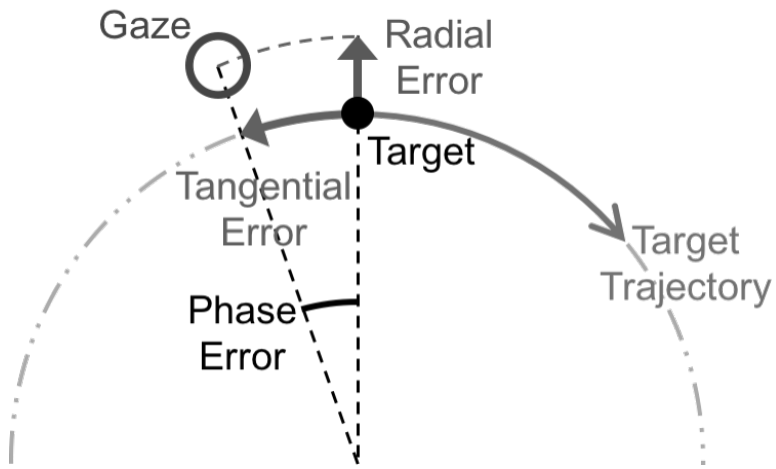

Figure 8

High-Definition Fiber Tractography of the FMa, IFO, MdLF, and SLF

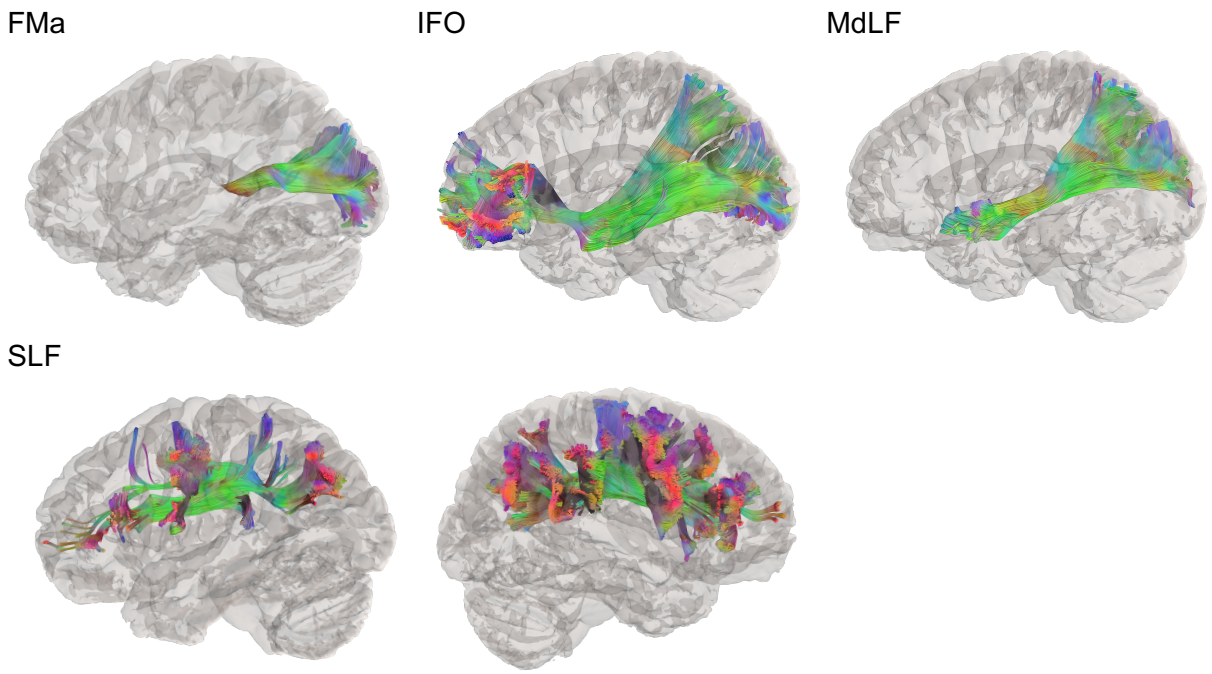

Note. The forceps major (FMa), inferior fronto-occipital fasciculus (IFO), and middle longitudinal fasciculus (MdLF) are shown in the left hemisphere only, as these tracts typically demonstrate bilateral symmetry. Due to the hemispheric asymmetry typically demonstrated by the superior longitudinal fasciculus (SLF), separate renderings of the left and right SLF are provided. Each tract is overlaid by a cortical isosurface rendered from the subject's skull-stripped T1-weighted image.

Figure 9

Three-Dimensional Rendering of the Cortical Isosurface Overlaid on Whole-Brain White Matter

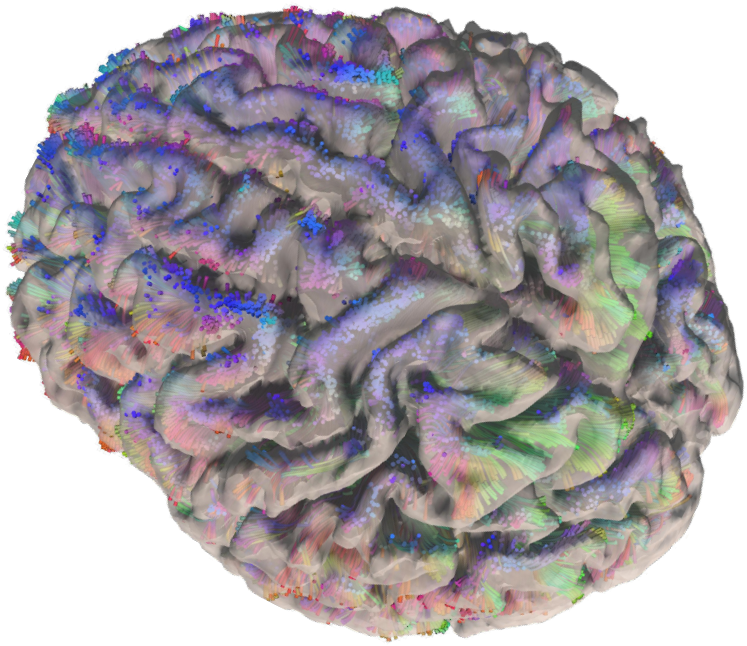

Note. A 3D isosurface was rendered from each subjects' skull-stripped T1-weighted images following linear registration to diffusion-weighted images. High-definition fiber tractography results in the close agreement of fiber terminations with and the gyral folding of the cortical surface, and the cortical isosurface is therefore very useful when used as a tract overlay to guide the manual tractography procedures.

Figure 10

ROC Curves Illustrating the Relative Sensitivity and Specificity of Neuropsychological Domain Versus Eye-Tracking Component Scores of Working Memory for mTBI Classification

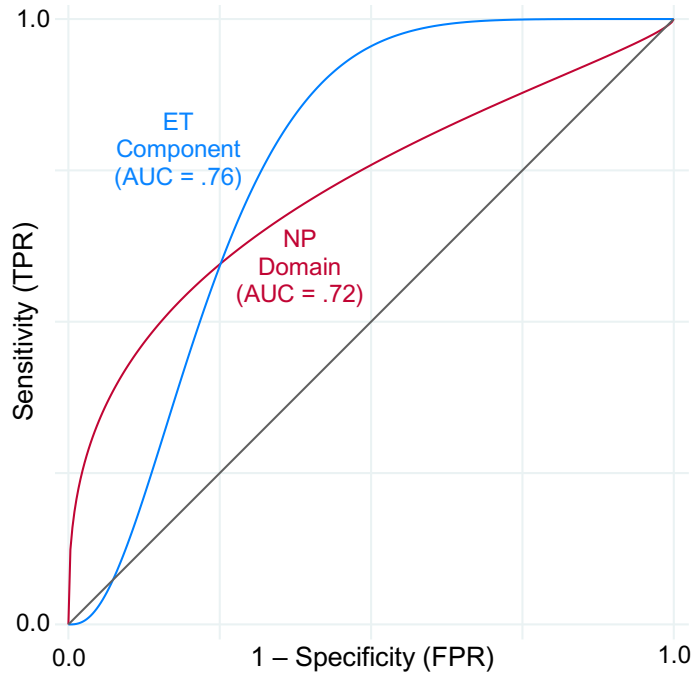

Note. Receiver operating characteristic (ROC) curves were estimated using parametric probit models fit by maximum likelihood estimation. mTBI = mild traumatic brain injury; ET = eye-tracking; NP = neuropsychological; AUC = area under the ROC curve; TPR = true-positive rate; FPR = false-positive rate.

Figure 11

Local Tract Indexes of QA and RDI in Healthy Adults Versus Those with Mild Traumatic Brain Injury

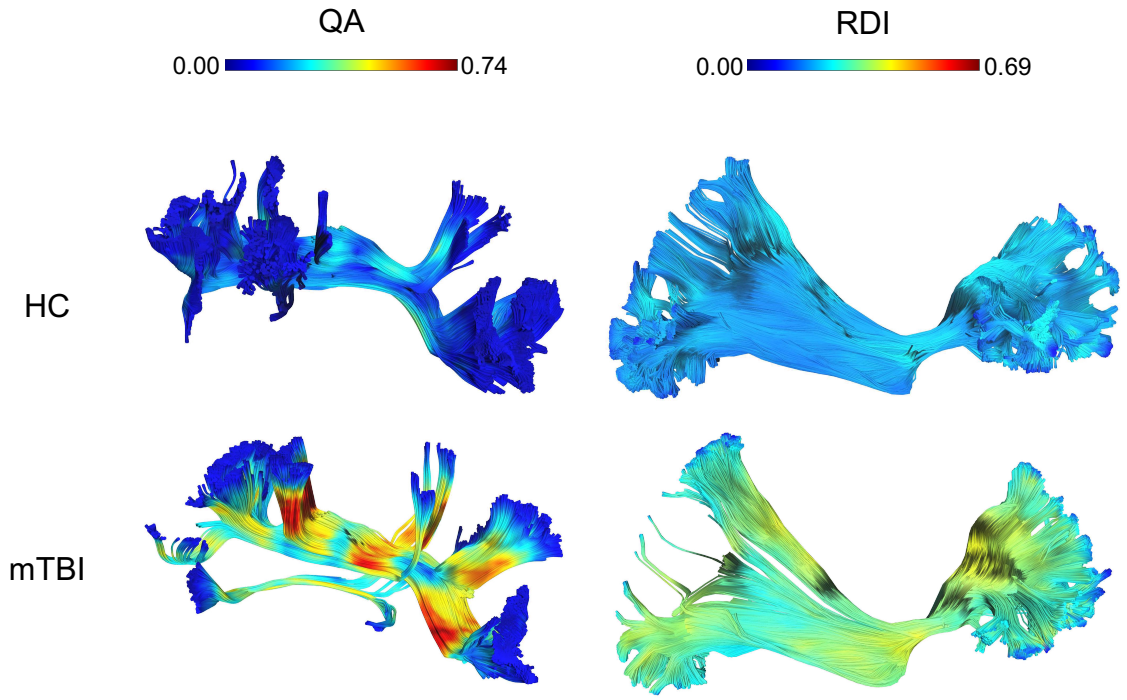

Note. Lower quantitative anisotropy (QA) and restricted diffusion imaging (RDI) values are indicated by dark blue hues while higher QA and RDI values are indicated by yellow and red (highest) hues. Local index of QA is shown in the left superior longitudinal fasciculus of a healthy control (HC) participant (top left) compared to that of a participant with mild traumatic brain injury (mTBI; bottom left). Local RDI index is shown in the right inferior fronto-occipital fasciculus of a HC participant (bottom left) compared to that of a participant with mTBI (bottom right).

Figure 12

Example of Inconsistency Across Associations Between Tract Spread and Performance on Cognitive Tasks

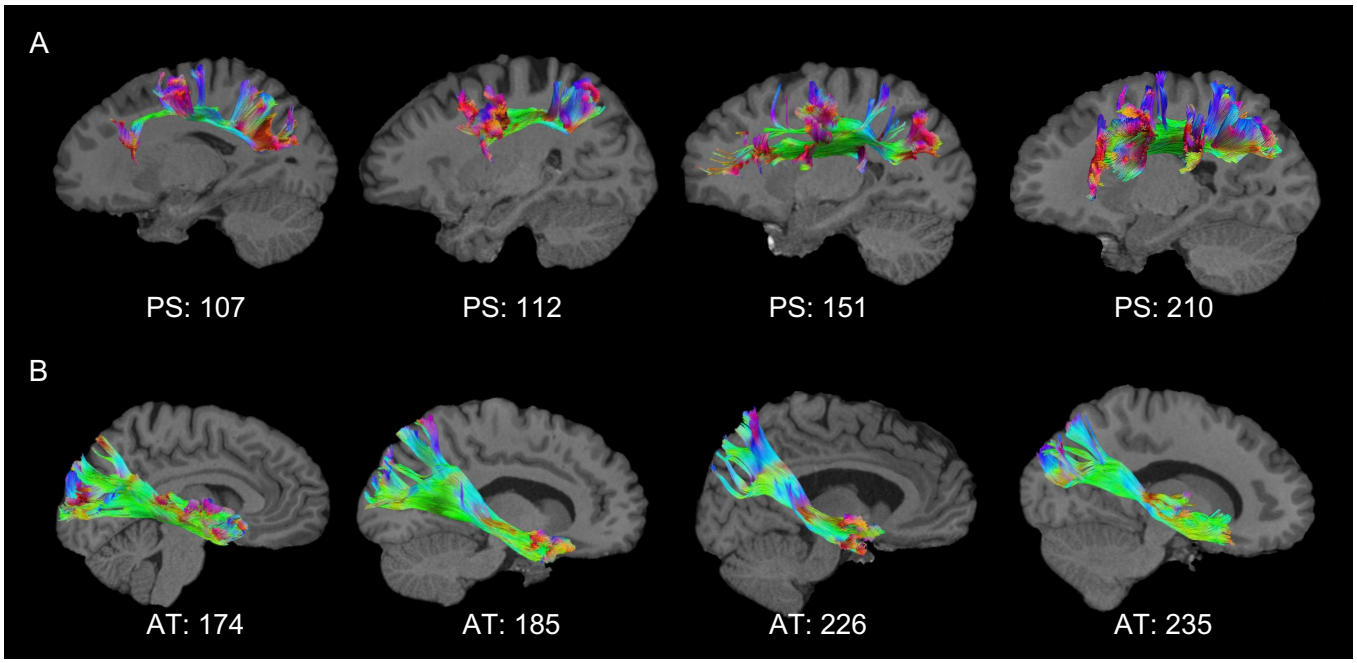

Note. Panel A demonstrates the positive association between increased tract spread of the left superior longitudinal fasciculus and increased performance on neuropsychological tasks of processing speed (PS). Panel B demonstrates the negative association between decreased tract spread of the right middle longitudinal fasciculus and improved performance on neuropsychological tasks of attention (AT).

Figure 13

Distribution of Persistent Post-Concussive Symptoms Experienced in Chronic mTBI

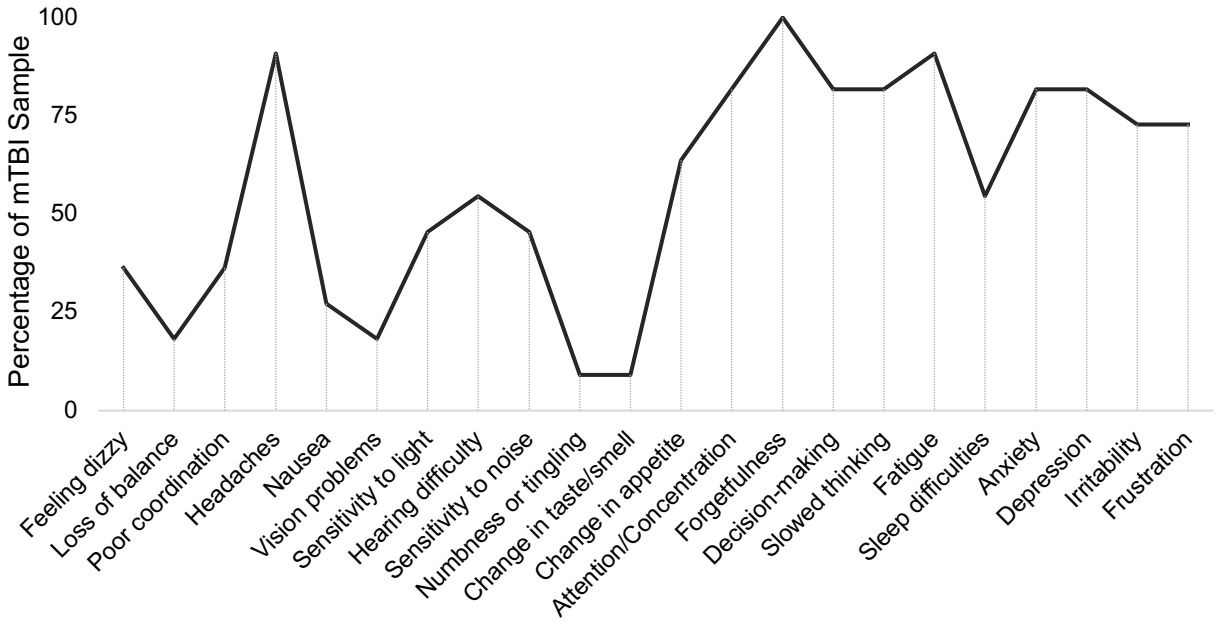

Note. The solid black line indicate the percentage of individuals with mild traumatic brain injury who rated individual post-concussive symptoms as being at least a mild problem (Neurobehavioral Symptom Inventory item score ≥ 1).